

**Exploring the influence of B cell receptor  
signaling components on the development and  
homeostasis of B cells**

Inaugural-Dissertation  
zur  
Erlangung des Doktorgrades  
Dr.nat.med  
Der Medizinischen Fakultät  
und  
der Mathematisch-Naturwissenschaftlichen Fakultät  
der Universität zu Köln

vorgelegt von  
Jian Song  
aus Heilongjiang, China

Köln 2007

Berichterstatter: Prof. Sigrun Korsching  
Prof. Hinrich Abken

Tag der mündlichen Prüfung:     Juni 2007

Für 靳慧明 und 宋希萌

<b>ABBREVIATIONS</b>	<b>8</b>
<b>1 INTRODUCTION</b>	<b>11</b>
<b>1.1 B Cell Development</b>	<b>11</b>
1.1.1 Regulation of B Cell Development by the Pre-BCR (positive selection)	12
1.1.2 Regulation of B Cell Development by the BCR (Negative Selection)	12
<b>1.2 The B Cell Receptor Complex</b>	<b>13</b>
1.2.1 IgM versus IgG1 B Cell Receptor	13
1.2.2 Ig $\alpha$ and Ig $\beta$	14
1.2.3 B Cell Response and B Cell Receptor Signaling	15
1.2.4 Aim of the Project	15
<b>1.3 Smad7</b>	<b>16</b>
1.3.1 Smad7 Works as an Inhibitor of TGF- $\beta$ Signaling	16
1.3.2 TGF- $\beta$ -associated Diseases by Aberrant Expressions of Smad7	17
1.3.3 TGF- $\beta$ and B Lymphocytes	18
1.3.4 Aim of the Project	19
<b>1.4 NF-<math>\kappa</math>B inducing kinase (NIK)</b>	<b>19</b>
1.4.1 The NF- $\kappa$ B Family Members and Their Regulation	19
1.4.2 <i>NIK</i> Deficient Model	20
1.4.3 Aim of the Project	21
<b>1.5 BAC Strategy for Gene Targeting</b>	<b>21</b>
1.5.1 BAC (bacterial artificial chromosome)	21
1.5.2 RED/ET Cloning	21
<b>2 MATERIALS AND METHODS</b>	<b>23</b>
<b>2.1 Chemicals and Biological Material</b>	<b>23</b>
<b>2.2 Molecular biology</b>	<b>25</b>
2.2.1 Competent Cells and Isolation of Plasmid DNA	25
2.2.2 Preparation of BAC DNA	25
2.2.2.1 Mini Preparation of BAC DNA	25
2.2.2.2 Maxi Preparation of BAC DNA	25
2.2.3 Preparation of Genomic DNA	26
2.2.3.1 DNA Extraction from Mouse Tail Biopsies	26
2.2.3.2 DNA Extraction from ES Cells (96-well micro titer plates)	26
2.2.4 Preparation of RNA	27
2.2.4.1 RNA Extraction by using TRIzol Reagent	27
2.2.5 cDNA Synthesis	27
2.2.6 Agarose Gel Electrophoresis and DNA Gel Extraction	28
2.2.7 DNA Sequencing	28
2.2.8 Polymerase Chain Reaction (PCR)	28
2.2.9 Southern Blot	28
2.2.9.1 Preparation and Transfer of the DNA Samples	29
2.2.9.2 Hybridization	29
2.2.10 Red/ET Cloning	30
2.2.10.1 Transformation of pSC101-BAD-gbaA into the <i>E. coli</i> Strain Carrying the BAC	31
2.2.10.2 Cloning of a PCR Product with Homology Arms into a BAC by Red/ET	31
<b>2.3 Cell Culture</b>	<b>32</b>
2.3.1 Reagents and Media for Cell Culture	32
2.3.2 Equipment	33
2.3.2.1 Dishes and Plastic Ware	33
2.3.2.2 Devices	34
2.3.3 Maintenance of Cells	34
2.3.4 Freezing and Thawing of Cells	34
2.3.5 Determination of Cell Numbers	35
2.3.6 Murine Embryonic Feeder Cells	35

2.3.6.1	Embryonic Feeder Cell Preparation	35
2.3.6.2	Mitomycin C Treatment	36
2.3.7	Murine Embryonic Stem Cells	36
2.3.7.1	Transfection of ES Cells	37
2.3.7.2	Selection for Targeted Clones in Culture	37
2.3.7.3	ES Cell Screening in 96-well Microtiter Plates	38
2.3.8	HTNC Treatment	38
2.3.8.1	Preparation of Targeted ES Cell Clones for Blastocyst Injection	39
2.3.8.2	Blastocyst Injections and Transfers	39
2.3.9	Preparation of Single Cell Suspensions From Lymphoid Organs	40
2.3.10	Preparation of Peripheral Cells from Mouse Blood	40
2.3.11	Flow Cytometry	41
2.3.12	Magnetic Cell Sorting and FACS Sorting	42
2.3.13	B Cell Receptor Internalization	42
2.3.14	Calcium flux	42
2.3.15	Culture of <i>ex vivo</i> Splenocytes and Lymphocytes	42
2.3.16	CFSE Labeling and <i>in vitro</i> B cell Activation	43
2.3.17	Induced Class Switch Recombination	43
2.3.18	Histological Analysis and Immunohistochemistry	43
2.3.19	Preparation and Immunostaining of Cytospins	44
2.3.20	Protein Extract Preparations	44
2.3.21	Western Blot	44
<b>2.4</b>	<b>Mouse Experiments</b>	<b>45</b>
2.4.1	Mice	45
2.4.2	NP-CG Immunization	46
2.4.3	ELISA	46
<b>3</b>	<b>Results</b>	<b>48</b>
<b>3.1</b>	<b>Generation of IgG1i mice</b>	<b>48</b>
<b>3.2</b>	<b>Generation of Ig<math>\alpha_{\Delta c}</math>/IgG1i, Ig<math>\beta_{\Delta c}</math>/IgG1i and Ig<math>\alpha_{\Delta c}</math>/Ig<math>\beta_{\Delta c}</math>/IgG1i mice</b>	<b>48</b>
3.2.1	IgG1 affects B cell compartments distinctly and diversely when in combination with intact or mutant Ig $\alpha$ and Ig $\beta$ BCR subunits	50
3.2.2	IgG1 expression compromises B cell development in the BM.	51
3.2.3	Competition of IgG1 and IgM during B cell development	53
<b>3.3</b>	<b>IgG1 signal in supporting B cells survival and proliferation</b>	<b>55</b>
3.3.1	Ig $\alpha_{\Delta c}$ or Ig $\beta_{\Delta c}$ B cells are sensitive to apoptosis	55
3.3.2	Proliferation capacity of IgG1i, Ig $\alpha_{\Delta c}$ IgG1i and Ig $\beta_{\Delta c}$ IgG1i B cells	57
<b>3.4</b>	<b>IgG1 derived BCR signaling</b>	<b>58</b>
3.4.1	IgG1 expression increases B cell activation in response to BCR engagement	58
3.4.2	BCR internalization and signaling of IgG1i, Ig $\alpha_{\Delta c}$ IgG1i and Ig $\beta_{\Delta c}$ IgG1i B cells	59
<b>3.5</b>	<b>IgG1 expression promotes the B cell maturation</b>	<b>63</b>
<b>3.6</b>	<b>B-1 B cells in the peritoneal cavity of IgG1 expressing mice</b>	<b>64</b>
<b>3.7</b>	<b>Serum IgG1 level in the IgG1 expressing mice</b>	<b>64</b>
<b>3.8</b>	<b>IgG1 B cells in Ig<math>\alpha</math>/Ig<math>\beta</math> double mutant mice</b>	<b>65</b>
<b>3.9</b>	<b>Deficiency of Smad7 in B cells enhanced IgA class switch</b>	<b>67</b>
3.9.1	Generation of Smad7 <sup>FL/FL</sup> mice	67
3.9.2	Generation of CD19Cre Smad7 <sup>FL/FL</sup> mice	68
3.9.3	B cell homeostasis in the BM and Spleen of CD19Cre Smad7 <sup>FL/FL</sup> mice	69
3.9.4	Smad7 mediates TGF- $\beta$ -controlled class switch	70
<b>3.10</b>	<b>Targeting NIK gene by BAC strategy</b>	<b>73</b>
3.10.1	Gene targeting of <i>NIK</i>	73
3.10.2	Generation of the Modified NIKBAC	75
3.10.3	Generation of the ES Cell Line NIK <sup>fllox</sup>	76

<b>4</b>	<b>DISCUSSION</b>	<b>79</b>
<b>4.1</b>	<b>IgG1 B cell receptors play distinct roles when in combination with Ig<math>\alpha</math>/Ig<math>\beta</math> mutation</b>	<b>79</b>
4.1.1	$\gamma$ 1 signals support the B cells survival	80
4.1.2	$\gamma$ 1 signals in the BCR signaling	82
4.1.3	$\gamma$ 1 in combination with mutation of both Ig $\alpha$ and Ig $\beta$	83
<b>4.2</b>	<b>Signals of Smad7 in the B cells immunity</b>	<b>83</b>
<b>4.3</b>	<b>BAC strategy for the gene targeting</b>	<b>86</b>
<b>5</b>	<b>Summary</b>	<b>88</b>
<b>6</b>	<b>Zusammenfassung</b>	<b>89</b>
<b>7</b>	<b>References</b>	<b>90</b>
<b>8</b>	<b>Acknowledgements</b>	<b>98</b>
<b>9</b>	<b>VERSICHERUNG</b>	<b>99</b>
<b>10</b>	<b>LEBENS LAUF</b>	<b>100</b>

## ABBREVIATIONS

A	adenosine
Amp	ampicillin
APC	allophycocyanin
BCR	B cell receptor
$\beta$ -me	$\beta$ -mercaptoethanol
bp	base pair
B4	Bruce-4
BSA	bovine serum albumin
C	cytosine
$^{\circ}$ C	temperature in degrees Celsius
CD	cluster of differentiation
cDNA	complementary DNA
cpm	counts per minute
Cre	site-specific recombinase
C region	constant region
Cyc	cychrome
dNTP	deoxyribonucleotide-triphosphate
DMEM	Dulbecco's modified Eagle medium
DMSO	Dimethyl sulfoxide
DNA	deoxyribonucleic acid
ds	double-stranded
DTT	1,4-Dithio- DL-threitol
<i>E. coli</i>	<i>Escherichia coli</i>
EDTA	ethylene-diaminetetraacetic acid
EF	embryonic fibroblasts
ES	embryonic stem
EtBr	ethidium bromide
FACS	fluorescence activated cell sorting
FCS	foetal calf serum
FITC	fluorescein-isothiocyanate
Flp	site-specific recombinase, product of yeast <i>FLP1</i> -gene
FRT	Flp recombination target



---

g	gram
GANC	ganciclovir
G418	geneticin sulfate
h	hour/s
HEPES	N-2-hydroxyethylpiperazine-N <sup>'</sup> -2-ethanesulfonic acid
Ig	immunoglobulin
i.p.	intraperitoneally
ITAM	immunoreceptor tyrosine-based activation motifs
kb	kilobase pairs
kD/ kDa	kilodalton
L	liter
LA	long arm of homology
LB	Luria-Bertani medium
LIF	leukaemia inhibitory facto
loxP	recognition sequence for Cre
M	molar
MHC	major histocompatibility locus
min	minute
ml	milliliter
mM	millimolar
μl	microliter
μM	micromolar
MCS	multiple cloning site
MMC	mitomycin C
NaCl	sodium chloride
NaOH	sodium hydroxide
neo	neomycin resistance gene
OD	optical density
PBS	phosphate buffered saline
PCR	polymerase chain reaction
PE	phycoerythrine
PIPES	Piperazine-N,N <sup>'</sup> -bis(2-ethanesulfonic acid)
RNA	ribonucleic acid
rpm	revolutions per minute

---

RT	room temperature
RU	relative units
s	second
SA	short arm of homology
SDS	sodium dodecyl sulfate
ss	single-stranded
SSC	sodium chloride/ sodium citrate buffer
TAE	Tris-acetic acid-EDTA buffer
Taq Pol	polymerase from <i>Thermus aquaticus</i>
TCR	T cell receptor
TE	Tris-EDTA buffer
Tris	2-amino-2-(hydroxymethyl)-1,3-propanediol
TWEEN	polyoxyethylene-sorbitan-monolaureate
U	units
UV	ultraviolet
V	volts
V region	variable region
v/v	volume per volume
w/v	weight per volume
wt	wild type
X-Gal	5-Bromo-4-chloro-3-indolyl- $\beta$ -galactopyranoside
5'	five prime end of DNA sequences
3'	three prime end of DNA sequences

# 1 INTRODUCTION

B cells are an important component of adaptive immunity. They produce and secrete millions of different antibody molecules, each of which recognizes a different (foreign) antigen. The fact that B lymphocytes express a very large repertoire of antibodies is due to the complex mechanism of V(D)J recombination of immunoglobulin (Ig) genes as well as other processes including somatic hypermutation, gene conversion and class switch recombination. On the other hand, these development processes are tightly controlled, where over 75% of the developing cells become apoptotic because of inappropriate immunoglobulin gene rearrangements resulting in recognition of self antigens or lack of signal transduction through newly formed BCR. (Ollila and Vihinen, 2005)

## 1.1 B Cell Development

B-lymphocytes follow a highly ordered program of development in the bone marrow (BM) (Fig.1), beginning with the commitment of lymphoid progenitors to the B lineage and the somatic recombination of heavy chain (HC) Ig alleles. After an initial rearrangement of diversity (DH) to joining (JH) gene segments, pro-B cells rearrange one of many upstream variable (VH) region segments to the D-JH segment, creating the V(D)J joint. Cells with a productive protein-encoding HC rearrangement express the HC together with the invariant surrogate Ig light chains VpreB and  $\lambda 5$  to form a pre-B cell receptor (Pre-BCR). Upon expression of the pre-BCR, cells undergo clonal expansion before initiation of rearrangements at the light chain (LC) loci (Espeli et al., 2006; Jung et al., 2006). A productive LC rearrangement results in the cell surface expression of IgM, defining entry into the immature B cell stage. A major selection event befalls these immature B cells in the BM where they interact with self-Ag. Self-reactive B cells are extinguished by three well-characterized mechanisms: receptor editing, apoptosis, and anergy. Throughout this process, appropriate BCR signals are required for B cell development and survival (Edry and Melamed, 2004). The B cells with aberrant BCR signals are deleted during positive and negative selection, which ensures the generation of a functionally competent, non-autoimmune repertoire.

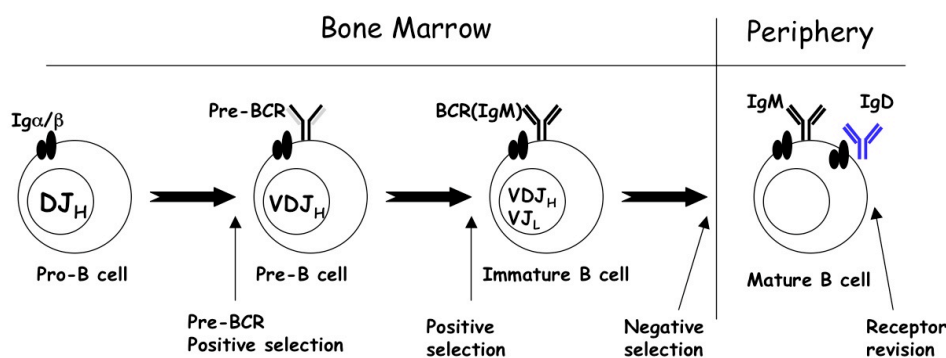


**Fig.1** Receptor editing is activated throughout B lymphopoiesis. Selection checkpoints mediated by the pre-BCR or the BCR are specified in the schematic. B cells that fail to fulfill appropriate receptor requirements stimulate receptor editing and undergo secondary recombination (Edry and Melamed, 2004).

### 1.1.1 Regulation of B Cell Development by the Pre-BCR (positive selection)

$V_H$  to  $D_HJ_H$  rearrangement is initiated in the transition from pre-B I to large pre-B II cells (Rolink et al., 2001). When an in-frame  $V_H D_H J_H$  rearrangement occurs, the subsequently expressed  $\mu_H$  chain protein can pair with the surrogate light chain (SL) components  $\lambda_5$  and VpreB. Upon association with the signal-transducing  $Ig\alpha$  and  $Ig\beta$  subunits, the pre-BCR complex is formed and can be active at the cell surface.

About 10% of pre-B I cells in the bone marrow express  $\mu_H$  chain in the cytoplasm. Not all of these  $\mu_H$  chains, however, are capable of forming a pre-BCR (Martensson et al., 2002). At the transition from pre-B I to pre-B II, those cells expressing a  $\mu_H$  chain capable of forming a pre-BCR are positively selected and enter into cellular division and expansion. (Melchers, 2005; Zhang et al., 2004).

### 1.1.2 Regulation of B Cell Development by the BCR (Negative Selection)

The next checkpoint in B cell development occurs during progression from immature to mature B cell stages, where encountering antigen capable of cross-linking BCR typically leads to one of three results in immature B cells: (a) cells are eliminated (clonal deletion); (b) cells are rendered non-responsive and short lived (anergic); or (c) cells revise their BCR to eliminate self-reactivity (editing) (Hardy and Hayakawa, 2001). High-affinity interactions with membrane-bound antigen result in deletion, whereas lower-affinity interactions and soluble antigens will result in editing or anergy (Benschop et al., 1999; Lang et al., 1996).

Immature B cells, which have not been negatively selected in the BM after exposure to self antigen, may migrate from the BM and through the terminal branches of central arterioles into the spleen. These splenic immature B cells, which will only survive for 4 days,

differentiate into mature B cells with a lifespan of around 15 weeks (Rolink et al., 1998). In the BM, however, 90% of the immature B cells will be negatively selected and lost before migration to the spleen.

As pre-BCR signaling results in a transient down-regulation of recombination activating gene (RAG) expression (Grawunder et al., 1995), production of a BCR appears critical in final cessation of *Rag* expression, as well as in Ig light chain rearrangement. Hence, productive B cell development requires expression of a light chain that can efficiently pair with a particular HC to form a cell surface BCR. However, the resulting BCR must not signal above some critical threshold (Lang et al., 1996). Otherwise, it appears that *Rag* expression continues, allowing further light chain kappaV genes to rearrange and produce alternative light chains to effectively pair with HC. In order to successfully generate a non-autoreactive BCR, this light chain editing process can continue on both kappa alleles and eventually proceed to the second light chain locus, resulting in lambda light chain expression (Tiegs et al., 1993).

## 1.2 The B Cell Receptor Complex

The B cell antigen receptor (BCR) is a hetero-oligomeric structure composed of antigen binding membrane immunoglobulin, and transducer-transporter substructures. The transducer-transporter substructure is composed of disulfide-linked dimers of immunoglobulin (Ig) $\alpha$  and Ig $\beta$  subunits. Naive B cells express BCRs that contain H chains of  $\mu$  and  $\delta$  (IgM and IgD) as antigen receptors, but after contact with antigen they can switch and use the membrane forms of  $\gamma$ ,  $\epsilon$ , and  $\alpha$  (IgG, IgA, or IgE).

### 1.2.1 IgM versus IgG1 B Cell Receptor

While the Ig heavy (H) chains of the classes  $\gamma$ ,  $\epsilon$  and  $\alpha$  carry evolutionarily conserved cytoplasmic tails of 14 to 28 amino acids, such structures are lacking in  $\mu$  and  $\delta$  chains (Geisberger et al., 2003; Neuberger et al., 1989; Reth, 1994). As the latter are expressed in developing and mature naïve B cells, the signaling function of the B cell antigen receptor (BCR) on those cells is thought to rely entirely on the cytoplasmic tails of the BCR-associated Ig $\alpha$ / $\beta$  heterodimer. However, in the generation of B cell memory, most of the antigen-activated B cells participating in the response switch to the expression of other antibody isotypes, and the BCR on these cells acquire the cytoplasmic tail of the newly expressed IgH chain as an additional signaling module. The functional importance of this module has become apparent in experiments in which the gene segments encoding the cytoplasmic tails of the constant (C) regions of the  $\gamma$ 1 and  $\epsilon$  chain, respectively, were deleted in the mouse germ-

line and a profound deficiency in the development of IgG1 or IgE expressing memory B cells was observed (Achatz et al., 1997; Kaisho et al., 1997). These results were complemented and supported by a study in which transgenic expression of  $\gamma 1$  or  $\mu/\gamma$  hybrid chains conferring a particular antigenic specificity in combination with a transgenic  $\kappa$  light chain led to an enhanced generation of memory and plasma cell progeny upon antigenic challenge, due to reduced cellular attrition (Martin and Goodnow, 2002).

### 1.2.2 Ig $\alpha$ and Ig $\beta$

The Ig $\alpha/\beta$  heterodimer is expressed on the surface of B cells as part of the BCR complex. On the other hand, it is also integral to the pre-BCR. A functional pre-BCR is required for pre-B cell expansion and the down-regulation of further HC rearrangement. The importance of the Ig $\alpha/\beta$  heterodimer in the pre-BCR is evidenced by the fact that only pro-B cells were detectable in mice containing truncations of both Ig $\alpha$  and Ig $\beta$  (Reichlin et al., 2001). Conversely, in mice containing either a truncated Ig $\alpha$  or a truncated Ig $\beta$ , the B lineage cells proceed through this checkpoint, undergo V<sub>H</sub> to DJ<sub>H</sub> rearrangement and establish a pre-B cell population. In mice containing the Ig $\beta$  truncation and therefore expressing a pre-BCR containing only functional Ig $\alpha$ , normal numbers of pre-B cells were generated, indicating substantial pre-B expansion (Reichlin et al., 2001). In contrast, in mice containing the Ig $\alpha$  truncation and therefore expressing a pre-BCR containing only Ig $\beta$ , reduced numbers of pre-B cells were observed (Torres et al., 1996). Thus signals downstream of Ig $\alpha$  appear more efficient at supporting the pro-B to pre-B transition or expanding pre-B cells.

Pre-B cells undergo rearrangement at the LC locus and those that express a functional BCR make the transition to immature B cells. Mice containing the Ig $\beta$  truncation exhibited normal levels of immature B cells (Reichlin et al., 2001). On the contrary, in mice containing a truncated Ig $\alpha$ , reduced levels of pre-B cells were matched by an equivalent reduction in immature B cell numbers (Torres et al., 1996). This suggests the possibility that the transition from pre-B to immature B cell is supported either by Ig $\alpha$  or Ig $\beta$  with equal efficiency.

After productive light chain rearrangement resulting in immature B cells, subsequent maturation generated a pool of mature recirculating B cells. The transition from immature to mature B cells is strikingly reduced in mice containing either the Ig $\alpha$  or Ig $\beta$  truncation, with most immature B cells undergoing programmed cell death (Torres et al., 1996). Consequently, while expression of the cytoplasmic domains of either Ig $\alpha$  or Ig $\beta$  is sufficient to support B lineage development to the immature B cell stage, albeit with differing efficiencies, the cytoplasmic domains of both Ig $\alpha$  and Ig $\beta$  are required for the efficient establishment of a mature B cell pool.

### 1.2.3 B Cell Response and B Cell Receptor Signaling

Antigen recognition by the BCR leads to a multitude of cellular responses in mature B cells. These responses include antigen internalization, T cell-independent B cell proliferation, and antibody production, as well as antigen presentation and the T cell-dependent antibody response. Experiments in cell lines and mice have provided insights into the proximal signaling requirements of the events after BCR engagement.

Aggregation of the BCR results in the phosphorylation of the immunoreceptor tyrosine-based activation motif (ITAM) tyrosine residues on Ig $\alpha$  and Ig $\beta$  by binding and activating spleen tyrosine kinase (Syk) and Lyn tyrosine kinase (Lyn) (Kurosaki, 1999), which are the first protein tyrosine kinases to be activated. Lyn stimulates receptor internalization and consequently negatively regulates aspects of BCR-dependent signaling (Ma et al., 2001). Moreover, Lyn and Syk phosphorylated a specific set of proximal BCR signaling molecules such as Bruton's tyrosine kinase (Btk), phospholipase C $\gamma$ 2 (PLC $\gamma$ 2) (Fruman et al., 2000), which subsequently form a supramolecular complex upon BCR crosslinking, nucleated by the tyrosine phosphorylated form of the adaptor B cell linker protein (BLNK) (Chiu et al., 2002; Fu et al., 1998; Wienands et al., 1998). This complex, also termed B cell signalosome, connects the BCR with pathways implicated in cellular activation and proliferation such as the calcium response and the nuclear factor  $\kappa$ B (NF- $\kappa$ B) and mitogen-activated protein (MAP) kinase pathways (Gugasyan et al., 2000; Ishiai et al., 1999; Kurosaki, 1999; Tan et al., 2001). Less is known about signaling requirements downstream of the BCR for the induction of antigen presentation to T cells and the T cell-dependent antibody response, although Syk may play a role in this respect (Lankar et al., 1998).

### 1.2.4 Aim of the Project

The conspicuous absence of the cytoplasmic tails in  $\mu$  and  $\delta$  chains could reflect peculiar signaling requirements in pre-B and immature B cells, predicting that expression of IgH chains with cytoplasmic tails would compromise B cell development. Indeed, while  $\delta$  chains alone can perfectly well mediate B cell development (Lutz et al., 1998; Roes and Rajewsky, 1991), transgenic expression of  $\gamma$  chains of various classes often seemed to disturb normal development (Roth et al., 1995), sometimes promoting the generation of cells co-expressing endogenous  $\mu$  and  $\delta$  chains (Chu et al., 2004). However, the physiological significance of these experiments remained uncertain, given the variations in transgene copy number and consequently expression levels inherent in the experimental approach. In order to investigate the physiological role of  $\gamma$ 1 chain containing BCRs, a new mouse model, termed

IgG1i, was generated in our laboratory using gene-targeting techniques. In this model the C $\gamma$ 1 gene segment in the mouse germ line replaced the C $\mu$ .

The signaling function of the B cell antigen receptor (BCR) on  $\mu$  and  $\delta$  cells is thought to rely entirely on the cytoplasmic tails of the BCR-associated Ig $\alpha$ / $\beta$  heterodimer. It remains to be answered whether the role of the  $\gamma$ 1 chain in keeping B cells compartment is dependent on, or independent of, the Ig $\alpha$  or Ig $\beta$  chain. Therefore, mice homozygous for the Ig $\alpha$  truncation mutation and homo- or heterozygous for IgG1i (Ig $\alpha_{\Delta c}$ IgG1i or Ig $\alpha_{\Delta c}$ IgG1i/+) or homozygous for the Ig $\beta$  truncation mutation and homo- or heterozygous for IgG1i (Ig $\beta_{\Delta c}$ IgG1i or Ig $\beta_{\Delta c}$ IgG1i/+) were generated. We also generated the triple mutant mice that are homozygous for the Ig $\alpha$  truncation mutation and homozygous for the Ig $\beta$  truncation mutation as well as  $\gamma$ 1 insertion (Ig $\alpha_{\Delta c}$ Ig $\beta_{\Delta c}$ IgG1i). In those mouse models, we dissected the interaction among the IgG1, Ig $\alpha$  and Ig $\beta$  in each B cell developmental stage and evaluated B cell survival, proliferation and activation.

### 1.3 Smad7

While responding to pathogens the immune system maintains tolerance to self and harmless antigens. Multiple mechanisms operate to ensure this normal immunological function. Of those, transforming growth factor- $\beta$  (TGF- $\beta$ ) is a potent regulatory cytokine with diverse effects on haematopoietic cells. The pivotal function of TGF- $\beta$  in the immune system is to maintain tolerance via the regulation of lymphocyte proliferation, differentiation, and survival (Li et al., 2006a).

TGF- $\beta$  receptor complex consists of TGF $\beta$ RI (ALK5) and TGF $\beta$ RII (Fig.4). Active TGF- $\beta$  dimer binds to the tetrameric ALK5 and TGF $\beta$ RII receptor complex to initiate cell signaling. Activated ALK5 phosphorylates receptor-activated Smads (R-Smads), Smad2 and Smad3, which translocate into the nucleus in a complex with Smad4. The Smad complex binds to a target promoter in association with other transcription factors (TFs) and regulates gene expression via recruiting histone acetyltransferase (HAT) or histone deacetylase (HDAC). The regulatory activity of TGF- $\beta$  is modulated by the presence of inflammatory cytokines and costimulatory molecules and by the intracellular inhibitory Smad proteins (I-Smads) that include Smad6 and Smad7.

#### 1.3.1 Smad7 Works as an Inhibitor of TGF- $\beta$ Signaling

Smad7 regulates signaling of TGF- $\beta$  in several ways (Fig.2). It is originally shown to compete with R-Smads for binding to activated type I receptors and thus to inhibit the



phosphorylation of R-Smads. Subsequently, they were found to recruit E3-ubiquitin ligases, known as Smad ubiquitination regulatory factor 1 (Smurf1) and Smurf2, to the activated type I receptor, resulting in receptor ubiquitination, degradation and termination of signaling. Smad7 was also shown to recruit a complex of GADD34 (Growth Arrest and DNA Damage-Inducible Protein) and the catalytic subunit of protein phosphatase 1 to the activated TGF- $\beta$  type I receptor, resulting in receptor dephosphorylation and inactivation and termination of signaling.

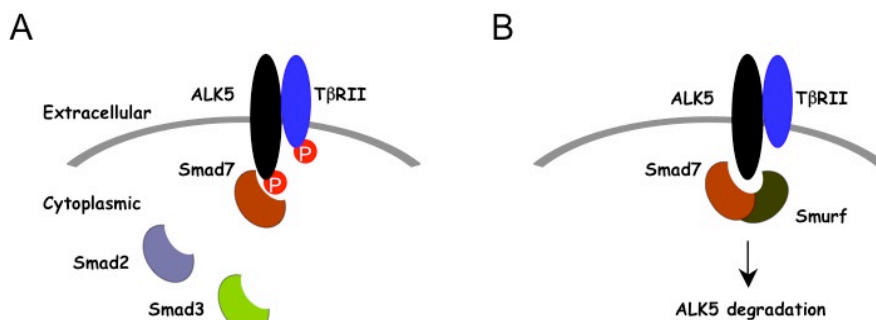


**Fig. 2 Smad7-dependent inhibition**

Smad7 down-regulates TGF- $\beta$  signaling (A) by competing with Smad2 and Smad3 for ALK5 binding and (B) by degrading ALK5 through recruiting Smurf-containing E3 ubiquitin ligase complexes (Li et al., 2006a).

### 1.3.2 TGF- $\beta$ -associated Diseases by Aberrant Expressions of Smad7

An excessive or deficient expression of Smad7 disrupts the balanced activity of TGF- $\beta$ . Abnormal expression of Smad7 is hypothesized to be one of the causes behind TGF- $\beta$ -associated diseases (Park, 2005). Blocking TGF- $\beta$  signaling by over-expression of Smad7 helps to maintain the chronic production of pro-inflammatory cytokines that drive the inflammatory process in IBD, and inhibition of Smad7 enables endogenous TGF- $\beta$  to down regulate this response (Monteleone et al., 2001). On the other hand, the deficient Smad7 expression plays a key role in hyperresponsiveness to TGF- $\beta$  in fibroblasts and development of the sclerotic skin diseases. The deficiency of Smad7 is presumably due to transcriptional inhibition of Smad7 gene or excessive degradation of Smad7 protein (Dong et al., 2002).

Aberrant expression of Smad7 is also observed in certain cancers. Recent study demonstrates that Smad7 plays an important role in the development of gastric carcinoma and that over-expression of Smad7 may be a significant independent prognostic indicator for clinical outcome in patients with gastric carcinoma (Kim et al., 2004). Smad7 overexpression is associated with poor outcome in gastric carcinomas, indicating that Smad7 expression may present one of the novel mechanisms for TGF- $\beta$  resistance in human gastric carcinoma.

Increased expression of Smad6 and Smad7 has been described in human pancreatic cancers (Kleeff et al., 1999;), but the mechanisms underlying these changes in Smad7 expression still remains unresolved.

### 1.3.3 TGF- $\beta$ and B Lymphocytes

It is known that TGF- $\beta$  induces apoptosis in immature B cells and resting B cells (Lomo et al., 1995). TGF- $\beta$  gives rise to NF- $\kappa$ B inhibitor I $\kappa$ B $\alpha$  and inhibits NF- $\kappa$ B activation (Arsura et al., 1996), which could lead to up-regulation of the BH3-only protein Bim, a proapoptotic member of the Bcl-2 family (Wildey et al., 2003). TGF- $\beta$  can also mediate apoptosis by down-regulating c-myc and inducing the expression of Id3 (inhibitor of DNA binding 3) (Kee et al., 2001). Interestingly, both c-myc and Id3 regulate B cell proliferation. Therefore, the anti-proliferation pathway and the apoptotic pathway of TGF- $\beta$  may overlap significantly. This is evidenced by the fact that TGF- $\beta$  induced apoptosis is associated with cell cycle blockade at G1/S because TGF- $\beta$  represses cyclin A expression and inactivates cyclin-dependent kinase 2 (cdk2), possibly via the up-regulation of the cyclin-dependent kinase inhibitor p27.

Other signaling pathways such as CD40 also modulate TGF- $\beta$  regulation of B cell proliferation. Engagement of CD40 can induce Smad7 expression and protects B cells from TGF- $\beta$ -induced growth inhibition (Patil et al., 2000).

TGF- $\beta$  promotes switching to IgA and IgG2b in mouse B cells *in vitro* (Kim and Kagnoff, 1990; McIntyre et al., 1993). In contrast, mice with a blockade of TGF- $\beta$  signaling in B cells showed that TGF- $\beta$  signaling is dispensable for IgG2b production. In these mice, serum IgA was absent whereas inactivation of TGF- $\beta$  signaling in B cells results in elevation of other serum Ig isotypes (Cazac and Roes, 2000). These *in vivo* studies reveal a general inhibitory function for TGF- $\beta$  on antibody production with the exception of IgA (Fig.3).

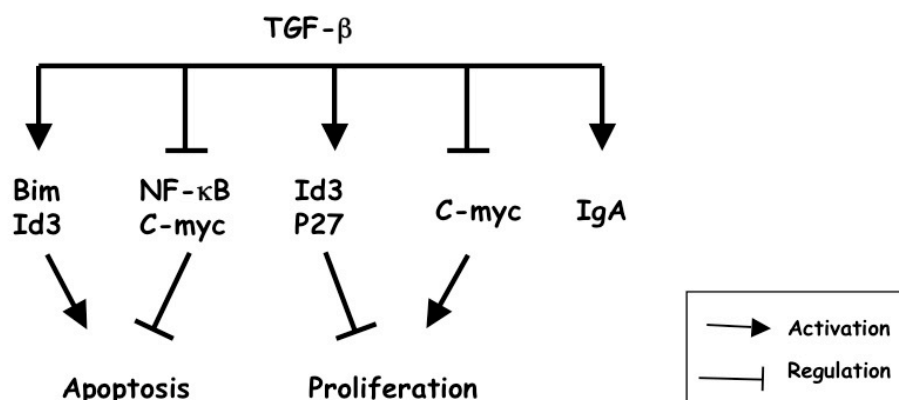


Fig. 3 TGF- $\beta$  regulation of B cell responses.

TGF- $\beta$  inhibits B cell proliferation through induction of Id3, p27, and p21 and inhibition of c-myc. TGF- $\beta$  promotes class switching to IgA through Smad3/4 and CBF $\alpha$ 3-mediated transactivation of germline  $\alpha$ -promoter. TGF- $\beta$  also induces apoptosis in immature and resting B cells through induction of Id3 and Bim, and inhibition of NF- $\kappa$ B and c-myc (Li et al., 2006a).

### 1.3.4 Aim of the Project

TGF- $\beta$  signaling is involved in the proliferation, differentiation, and survival of B-lymphocytes. In the mouse model, the absence of TGF- $\beta$ RII in B cells leads to a reduced life span of conventional B cells, expansion of peritoneal B-1 cells, and B cell hyperplasia in Peyer's patches, elevated serum immunoglobulin, and a virtually complete serum IgA deficiency. Therefore, it is interesting to evaluate the physiological role of Smad7, the TGF- $\beta$  signal inhibitor, in B cells proliferation, class switch, and survival and figure out the Smad7-regulated signaling pathway of TGF- $\beta$  receptor in the B cells. To disrupt the Smad7 selectively in B cells, Smad7<sup>flox</sup> mice were crossed to CD19-Cre mice, which induce efficient B lineage-specific deletion of *LoxP*-flanked target sequences. Using these mice, we analyzed the role of Smad7 in B cell activation and homeostasis.

## 1.4 NF- $\kappa$ B inducing kinase (NIK)

### 1.4.1 The NF- $\kappa$ B Family Members and Their Regulation

In mammals, NF- $\kappa$ B is composed of homo- or heterodimers of five proteins belonging to the Rel family, which are RelA, RelB, c-Rel and NF- $\kappa$ B1 (p105/p50) as well as NF- $\kappa$ B2 (p100/p52). (Li and Verma, 2002, Ghosh *et al.*, 1998) These Rel proteins form different NF- $\kappa$ B homo- and heterodimers, whose activation depends on two major NF- $\kappa$ B activation pathways: the canonical and the non-canonical pathway.

The canonical NF- $\kappa$ B activation pathway is the predominant pathway occurring in most cells. Dimer combinations of RelA, c-Rel and p50, which are kept inactive in the cytoplasm by their specific inhibitors, the I $\kappa$ B proteins (Ghosh and Karin, 2002), are activated by the canonical pathway. This pathway is essential for immune responses, inflammation and promoting cell survival.

The non-canonical pathway affects NF- $\kappa$ B2/p100, which preferentially dimerizes with RelB in the cytoplasm (Solan *et al.*, 2002). This pathway is triggered by certain members of the tumor necrosis factor (TNF) cytokine family (Senftleben *et al.*, 2001). Stimulation of a subset of receptors belonging to the TNFR super-family (such as BAFF-R, CD40, RANK, LT $\alpha$ R and LT $\beta$ R) leads to the recruitment of TRAF proteins like TRAF2, TRAF3 and TRAF6. This activates the NF- $\kappa$ B inducing kinase (*NIK*) through a currently unknown

mechanism. NIK then selectively phosphorylates and activates the IKK $\alpha$  catalytic subunit. Activated IKK $\alpha$  homodimers in turn phosphorylates the NF- $\kappa$ B precursor p100. p100 is subsequently polyubiquitinated and then processed to the mature subunit p52 by the proteasome (Massoumi et al., 2006). p52 and its binding partner RelB then enter the nucleus to turn on the transcription of target genes (Sun and Chen, 2004)(Fig.4).

This pathway is important for secondary lymphoid organogenesis, maturation of B cells, adaptive humoral immunity and optimal promotion of cell survival (Zarnegar *et al.*, 2004).

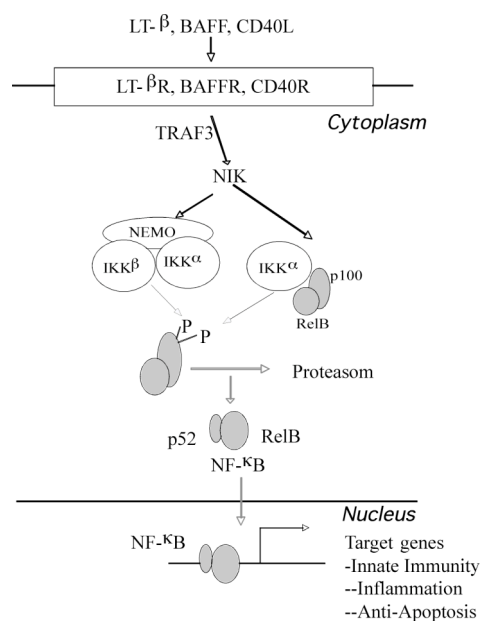


**Fig. 4: Schematic overview of the Non-Canonical Pathway of NF- $\kappa$ B activation**

Proteins are depicted by name and by oval symbols. Receptors are symbolized by boxed names. Arrows indicate activation processes. P stands for phospho-groups, and Ub for ubiquitin.

### 1.4.2 NIK Deficient Model

Alymphoplasia (*aly*) mice, which carry a spontaneous point mutation in the *NIK* gene, are characterized by the systemic absence of lymph nodes and Peyer's patches, disorganized splenic and thymic architectures, and immunodeficiency (Miyawaki et al., 1994). Another unique feature of *aly/aly* mice is that they exhibit increased numbers of B1 B cells in the peritoneal cavity compared to *aly/+* mice. Transfer experiments of peritoneal lymphocytes from *aly/aly* mice into RAG-2 mice revealed that B and T cells fail to migrate to lymphoid tissues, particularly to the gut-associated lymphatic tissue system (Fagarasan et al., 2000). The migration defect of *aly/aly* lymphocytes was due to impaired signal transduction downstream of the receptors, indicating that NIK is involved in the chemokine-signaling pathway.

NIK knockout mice (NIK<sup>-/-</sup>) displayed similar abnormalities in both lymphoid tissue development and antibody responses that observed in *aly* mice (Yin et al., 2001). In addition, a phenotype of immuno-suppression mediated by CD25<sup>+</sup>Foxp3<sup>-</sup> memory CD4<sup>+</sup> cells were observed in the mice deficient for NIK (Ishimaru et al., 2006). Biochemical studies of those

cells indicated an involvement of a cell-intrinsic mechanism in which NF- $\kappa$ B2 (p100) limits nuclear translocation of NF- $\kappa$ B1–RelA and thereby functions as a regulatory ‘brake’ for the activation of naive T cells. Moreover, analyses of NIK<sup>-/-</sup> mice showed that although NIK is essential for B and T cell activation, it is dispensable for activation of dendritic cells (DCs) (Garceau et al., 2000).

### 1.4.3 Aim of the Project

Deficiency of NIK (*aly/aly*) causes defects in the formation of secondary lymphoid organs in embryonic development in mice (Miyawaki et al., 1994) but the role of NIK in postnatal maturation of lymph nodes and Peyer’s patches remains unclear. Further, NIK knockout mice exhibit various phenotypes in different lineages. Due to the complex interaction between lineages such as B and T cells, the importance of NIK in cellular lineage and development stage are not known. To identify the physiological functions of NIK, we disrupted the NIK locus using conditional gene targeting, an established genetic method to investigate the gene function solely in the specific tissues and/or cell types.

## 1.5 BAC Strategy for Gene Targeting

### 1.5.1 BAC (bacterial artificial chromosome)

BACs can be used to clone DNA fragments of up to 300kb. The vectors are based on the naturally occurring large *E. coli* plasmid called the *F-factor*. This plasmid contains two genes, *parA* and *parB*, which maintain the copy number of the *F-factor* at 1-2 per cell. Recombinant BACs containing large DNA fragments are produced as in standard plasmid vector cloning. BACs are introduced into *E. coli* cells by electroporation. Large DNA fragments cloned into BACs have been found to be stable through hundreds of generations (Shizuya *et al.*, 1992). Recently, huge BAC libraries have been generated and were used for shotgun sequencing of several genomes. BAC stocks are available from the Children’s Hospital of Oakland Research Institute (CHORI).

### 1.5.2 RED/ET Cloning

All targeting techniques described so far require the production of complicated targeting constructs. This is often a limitation, since the availability of unique restriction sites on targeting vectors and genomic DNA is restricted and also the capacity with respect to insert size of the usual cloning vectors is limited. Development of efficient phage-based homologous recombination systems in the past five years has made it possible to engineer large segments of genomic DNA very easily (Murphy, 1998; Zhang *et al.*, 1998, Yu *et al.*

2000, Muyrers *et al*, 1999). With this new technique it is possible to engineer bacterial artificial chromosomes (BACs) in a way that they can be used as targeting vectors later on.

Red/ET recombination relies on homologous recombination *in vivo* in *E.coli*. It allows a wide range of modifications of DNA molecules at any chosen position. Homologous recombination allows the exchange of genetic information between two DNA molecules in a precise, specific and faithful manner (Copeland *et al.*, 2001; Liu *et al.*, 2003). These qualities are optimal for engineering a DNA molecule regardless of its size. Therefore Red/ET cloning is a valuable tool to generate targeting vectors with very long stretches of homology to the target gene. (Fig.5)

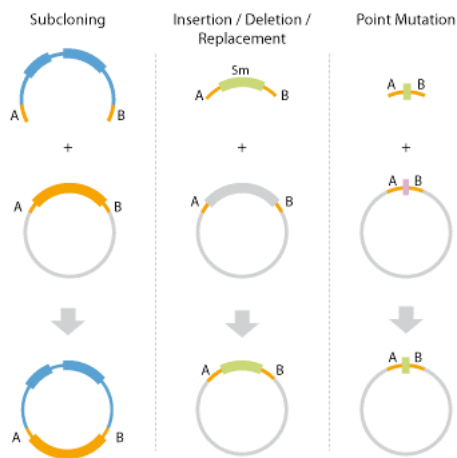


**Fig.5 Applications of Red/ET (genebridges)**

Red/ET allows every type of DNA engineering possible regardless of target size or type of modification.

## 2 MATERIALS AND METHODS

### 2.1 Chemicals and Biological Material

Chemicals were purchased from Sigma-Aldrich (Steinheim), Fluka Chemie (Deisenhofen), Merck (Darmstadt) or AppliChem (Darmstadt) unless stated otherwise. Solutions were prepared with double distilled water (ddH<sub>2</sub>O). Bacterial media were autoclaved prior to use.

Sterility of solutions and chemicals used in cell culture was maintained by working under a sterile hood (Heraeus, Germany).

Name of chemical	Supplier
β-Mercaptoethanol (β-ME)	Fluka Chemie GmbH, Switzerland
Acetone	Merck, Darmstadt
Agar	Gibco Life Technologies GmbH, Karlsruhe
Agarose, electrophoresis grade	AppliChem, Darmstadt
Ampicillin	Sigma-Aldrich, Steinheim
L-Arabinose	Sigma-Aldrich, Steinheim
Bovine serum albumin (BSA)	Sigma-Aldrich, Steinheim
Calcium chloride	Sigma-Aldrich, Steinheim
Chloroform	Merck, Darmstadt
Citric acid	Fluka Chemie GmbH, Switzerland
2'-Deoxyguanosine Monohydrate	AppliChem, Darmstadt
Diethylpyrocarbonate (DEPC)	AppliChem, Darmstadt
Dextran sulfate	AppliChem, Darmstadt
Dextrose	Merck, Darmstadt
Dithiothreitol (DTT)	Boehringer Mannheim GmbH, Mannheim
Dimethylsulfoxide (DMSO)	Merck, Darmstadt

dNTPs	Pharmacia Biotech, USA
Ethylendiamine tetraacetate (EDTA)	Fluka Chemie GmbH, Switzerland
Ethanol, abs.	AppliChem, Darmstadt
Ethidium bromide	Sigma-Aldrich, Steinheim
Fetal calf serum (FCS)	Boehringer Mannheim GmbH, Mannheim
Ficoll 400	Amersham Pharmacia, Freiburg
Glacial acetic acid	Fluka Chemie GmbH, Switzerland
Hydrochloric acid (37 %)	Merck, Darmstadt
Isopropanol	AppliChem, Darmstadt
Magnesium chloride	Sigma-Aldrich, Steinheim
Magnesium chloride (for PCR)	Gibco Life Technologies GmbH, Karlsruhe
Mineral oil	Sigma-Aldrich, Steinheim
Orange G	Chroma Gesellschaft Schmidt & Co, Stuttgart
Phenol	Sigma-Aldrich, Steinheim
Potassium acetate	Fluka Chemie GmbH, Switzerland
Potassium chloride	Merck, Darmstadt
Proteinase K	Roche, Switzerland
Salmon sperm DNA	Biomol, Hamburg
Sodium azide	Fluka Chemie GmbH, Switzerland
Sodium chloride	AppliChem, Darmstadt
Sodium citrate	Fluka Chemie GmbH, Switzerland
Sodium dodecyl sulfate	AppliChem, Darmstadt
Sodium hydrogencarbonate	Fluka Chemie GmbH, Switzerland
Sodium hydroxide	Fluka Chemie GmbH, Switzerland
Tris base	Fluka Chemie GmbH, Switzerland
Tris/ HCl	AppliChem, Darmstadt

**Table 1: Chemicals**



## **2.2 Molecular biology**

Standard methods of molecular biology were performed – if not otherwise stated- according to protocols described in Sambrook et al. (1989).

### **2.2.1 Competent Cells and Isolation of Plasmid DNA**

Competent *Escherichia coli* DH5 $\alpha$  or M1 or Topo 10 cells were prepared according to the protocol of Inoue et al. (Inoue et al., 1990) and used in heat shock transformations of plasmid DNA. DNA ligation was performed with the NEB DNA ligase according to the manufacturer's instructions. Plasmid DNA was isolated from transformed *Escherichia coli* bacteria with an alkaline lysis method (QIAGEN, Hilden, Germany). The procedure was performed according to the protocol of (Zhou et al., 1990). Mini or Maxi Plasmid DNA of higher purity was obtained with QIAGEN columns (QIAGEN, Hilden, Germany) following the supplier's instruction.

### **2.2.2 Preparation of BAC DNA**

Preparation of BAC DNA is very similar to preparation of plasmid DNA. Some precautions must be taken in order to maintain the integrity of the BAC. Vortexing or shaking should be left out, because this may lead to shearing of the BAC.

#### **2.2.2.1 Mini Preparation of BAC DNA**

BAC DNA was prepared from a 5 ml overnight culture. Four ml of this culture were used for every lysis. Cells were centrifuged at 13000 rpm for 3 min. The pellet was dissolved in 200  $\mu$ l of buffer P1. 220  $\mu$ l P2 were added followed by gentle shaking of the tubes. The solution was incubated for a maximum of 5 min at room temperature. Subsequently, 220  $\mu$ l of P3 were added. After 5 min incubation the solution was centrifuged for 10 min at 13000 rpm, the cleared supernatant was transferred into a fresh 1.5 ml tube. BAC DNA was precipitated with 550  $\mu$ l of isopropanol and washed with 70 % (v/v) ethanol. The DNA pellet was directly resuspended in a restriction digest mix to avoid any shearing of the BAC DNA.

#### **2.2.2.2 Maxi Preparation of BAC DNA**

BAC DNA was prepared from a 200 ml overnight grown culture. Cells were pelleted at 4700 rpm for 15 min. DNA extraction was performed using the Nucleobond AX 500 kit (Macherey + Nagel, Düren) following the manufacturer's instruction. After clearance of genomic DNA and cell debris by centrifugation, the protocol was modified. The cleared lysate was filtered through a sterile nylon mesh. Afterwards the DNA was precipitated with an equal

amount of isopropanol (centrifugation: 4700 rpm, 25 min, 4°C). The DNA was washed twice with 5 ml of 70 % (v/v) ethanol (centrifugation: 4700 rpm, 10 min, room temperature) and resuspended in 200 µl of TE buffer. Prior to use in transfection of ES cells, the DNA was purified following the phenol/chloroform extraction protocol. To prevent shearing of the DNA, the solution was not vortexed, but gently shaken.

### **2.2.3 Preparation of Genomic DNA**

Genomic DNA was prepared using a simplified protocol that allows the turnover of many samples at the same time (Laird *et al.*, 1991). DNA from either mouse-tail biopsies or ES cells was extracted.

#### **2.2.3.1 DNA Extraction from Mouse Tail Biopsies**

Cells were lysed over night at 56°C in lysis buffer (10 mM Tris-HCl, pH 8; 10 mM EDTA; 150 mM NaCl; 0.2% (w/v) SDS; 400 mg/ml proteinase K). Subsequently, DNA was precipitated from the solution by the addition of an equal volume of isopropanol. DNA was pelleted by centrifugation, washed in 70% (v/v) EtOH and resuspended in TE-buffer (10 mM Tris-HCl, pH 8; 1 mM EDTA).

#### **2.2.3.2 DNA Extraction from ES Cells (96-well micro titer plates)**

After washing ES cells twice with 100 µl PBS, 50 µl of ES cell lysis buffer was added to each well. The plates were transferred into a pre-warmed humidified box in which digestion of cellular proteins proceeded overnight at 56°C. After lysis and denaturation, samples were cooled to room temperature for 1 h. ES cell derived genomic DNA was precipitated with absolute ethanol for an additional hour at room temperature. DNA strands were visible under the microscope. To remove the ethanol the plates were inverted and the wells carefully drained on paper towels. DNA usually remained attached to the plastic surface. Every well was washed three times with 70 % (v/v) ethanol. DNA was air-dried and ready for further processing, e.g. restriction digests.

#### **ES cell lysis buffer**

10 mM Tris/HCl pH 7.5

10 mM EDTA

0.5 % (w/v) sarcosyl (sodium lauryl sarcosinate)

10 mM NaCl

0.4 mg/ml proteinase K (added prior to lysis)

## 2.2.4 Preparation of RNA

### 2.2.4.1 RNA Extraction by using TRIzol Reagent

Cells were washed off the culture plate inserts with 500  $\mu$ l of PBS. Cells were collected by centrifugation (3500 rpm, 5 min) and resuspended in 1 ml of TRIzol Reagent (GibcoBRL, USA). RNA was either prepared directly afterwards or the cells were stored at  $-80^{\circ}\text{C}$  for storage. All the following steps were performed at a separate workbench, using filtered tips, a separate set of pipettes, and keeping the tubes on ice at all times. The TRIzol Reagent, a monophasic solution of phenol and guanidine isothiocyanate, is an improvement of the single-step RNA isolation method developed by Chomczynski and Sacchi (Chomczynski, P., and Sacchi, N. 1987). Cells were lysed by pipetting up and down several times. The homogenized cells were incubated at room temperature for 5 min to allow the complete dissociation of nucleoprotein complexes. Chloroform (0.2 ml) was added to each tube and the tubes were shaken vigorously for 15 sec and then incubated for 3 min at room temperature. Tubes were centrifuged at 13000 rpm for 15 min at  $4^{\circ}\text{C}$ . The mixture separates into an upper aqueous phase containing the RNA, an interphase with proteins, and a lower phenol-chloroform phase. The upper phase was transferred into a fresh tube and the RNA was precipitated with 0.5 ml isopropanol. The samples were incubated for 10 min at room temperature and the RNA was collected by centrifugation (13000 rpm, 10 min,  $4^{\circ}\text{C}$ ). The supernatant was removed carefully and the RNA was washed with 1 ml 70 % (v/v) ethanol prepared with DEPC treated water (6000 rpm, 5 min,  $4^{\circ}\text{C}$ ). Diethylpyrocarbonate (DEPC; AppliChem, Darmstadt) inactivates RNases. The ethanol was completely removed and the RNA was dried for a maximum of 10 min at room temperature. Afterwards the RNA was dissolved in 30  $\mu$ l of DEPC-water for 10 min at  $55^{\circ}\text{C}$ . It was stored at  $-20^{\circ}\text{C}$  for later preparation of cDNA.

### 2.2.5 cDNA Synthesis

8  $\mu$ l of total RNA were mixed with 2  $\mu$ l of 10 mM dNTP mix, 2  $\mu$ l of oligo (dT<sub>12-18</sub>) (0.5  $\mu$ g/ $\mu$ l) and 18  $\mu$ l of DEPC treated water. The mixture was incubated at  $65^{\circ}\text{C}$  for 5 min. After a 2 min incubation on ice, 4  $\mu$ l of 10 x RT buffer, 8  $\mu$ l of 25 mM MgCl<sub>2</sub>, and 4  $\mu$ l of 0.1 M DTT were added and incubated for 2 min at  $42^{\circ}\text{C}$ . At this point, 1  $\mu$ l of Superscript II reverse transcriptase was added. All reagents were purchased from Invitrogen, USA. cDNA synthesis was performed at  $42^{\circ}\text{C}$  for 50 min. The reverse transcriptase was inactivated at  $70^{\circ}\text{C}$  for 15 min. The cDNA was stored at  $-20^{\circ}\text{C}$  for further analysis.

### 2.2.6 Agarose Gel Electrophoresis and DNA Gel Extraction

Separation of DNA fragments by size was achieved by electrophoresis in agarose gels (0.8% - 2% (w/v); 1x TAE (Sambrook, 1989); 0.5 mg/ml ethidium bromide). DNA fragments were recovered from agarose gel slices with either the QIAEX II or the QIAquick Gel Extraction Kit (QIAGEN, Hilden, Germany) following the manufacturer's instructions.

### 2.2.7 DNA Sequencing

DNA was sequenced using the 'Big Dye termination Cycle Sequencing Kit' (Applied Biosystems, Foster City, USA), which is a PCR-based modification of the original Sanger protocol (Sanger et al., 1977). The fluorescently labeled DNA fragments were separated and analysed with the ABI373A and ABI377 systems (Applied Biosystems, Foster City, USA).

### 2.2.8 Polymerase Chain Reaction (PCR)

The polymerase chain reaction is a rapid procedure for *in vitro* enzymatic amplification of a specific segment of DNA (Saiki *et al.*, 1985; Saiki *et al.*, 1988). The first step of PCR simply entails mixing template DNA, two appropriate oligonucleotide primers (18-75 nucleotides), *Taq* or another thermostable polymerases, deoxyribonucleoside triphosphates (dNTPs), and a buffer. Once assembled, the mixture is cycled many times (usually 25-40) through temperatures that permit denaturation (94-95°C), annealing (54-61°C) and DNA synthesis (68-72°C) to exponentially amplify a product of specific size and sequence (Mullis *et al.*, 1986; Mullis, 1990). The *Taq* polymerase synthesizes the complementary strand starting from the 3' end of the primer. PCR reactions were performed with the PTC-200 PCR cycler (MJ Research) or Biometra Trio Thermoblock (Biometra).

To amplify cDNA fragments for cloning or sequencing, the High Fidelity Master Kit with proofreading activity was used. (Roche, Mannheim, Germany)

### 2.2.9 Southern Blot

Southern blotting is the transfer of DNA fragments from an electrophoresis gel to a membrane. The transfer results in immobilization of the DNA fragments, so the membrane carries a semi-permanent reproduction of the banding pattern of the gel. After immobilization, the DNA can be hybridized with radioactively labeled probes and visualized by autoradiography (Southern, 1975).

Genomic DNA was digested with restriction endonucleases, and the resulting fragments were separated according to size by agarose gel electrophoresis on a 0.7 % (w/v) agarose gel.

The DNA was denatured *in situ* and transferred onto a positively charged nylon membrane. Blotted DNA was fixed by incubation at 80°C for 20 min. The DNA was hybridized to a <sup>32</sup>P-radioactively labeled DNA probe specific for the desired genomic region. Autoradiography was used to locate the positions of bands to which the probe hybridized.

### 2.2.9.1 Preparation and Transfer of the DNA Samples

Southern blot analysis was used to identify the targeted allele in the genome of ES cells, for typing of genetically modified mice and to identify targeted BACs.

The digested DNA and a DNA size marker were separated on a 0.7 % agarose gel overnight (40V, 16 h). The gel was photographed under UV light with a ruler aligned to the 1 kb DNA size marker and its bands were marked with a yellow tip. Afterwards the gel was gently shaken in 0.25 M HCl for 15-20 min that leads to partial depurination of the DNA, which in turn leads to strand cleavage. The HCl was exchanged with a 0.4 M NaOH solution which functions as a denaturation agent, to obtain single-stranded DNA. The DNA is ready to be transferred onto a positively charged nylon membrane (Hybond N<sup>+</sup>, Amersham Biosciences, UK). The DNA was transferred using downward capillary transfer with an alkaline transfer buffer. Transfer was performed for 4-16 h.

After completion of the transfer, the membrane was marked with a pencil corresponding to the previously marked size marker. Afterwards the membrane was baked for 20 min at 80°C to immobilize the DNA on the membrane.

Depurination buffer	Denaturation buffer	Transfer buffer
0.25 M HCl	0.4 M NaOH	0.4 M NaOH
		0.6 M NaCl

### 2.2.9.2 Hybridization

After baking of the membrane, it was moistened with 2 x SSC and thereafter incubated in a rotating oven for at least 2 h at 65°C with prehybridization solution. In the meantime, the DNA probe was labeled with <sup>32</sup>P.

30-100 ng of DNA (probe) were mixed with 2 µl of random primers (TaKaRa labeling kit) and filled up with water to a final volume of 10 µl. The solution was boiled for 5 min, to get single stranded DNA. After 5 min incubation on ice, 2.5 µl of Bca buffer, 2.5 µl of dNTPs, 6.5 µl of H<sub>2</sub>O, 1.0 µl of Bca BEST polymerase (all components part of the TaKaRa labeling kit) and 25 µCi <sup>32</sup>P-CTP were added. The mix was incubated at 55°C for 1 h. The labeling reaction was stopped by adding 100 µl of H<sub>2</sub>O. The labelled probe was purified from

non-incorporated nucleotides on a Micro Spin S 200 HR column (Amersham Bioscience, UK). The purified probe was boiled for 5 min, incubated on ice for 3 min and finally added to the prehybridization solution. Hybridization was performed by rotating the membrane in the solution overnight at 65°C. To avoid background labeling, the membrane was washed the next day with 2 x SSC/ 0.1 % SDS and 1 x SSC/ 0.1 % SDS until the counts decreased to 40-100 cpm. Afterwards, the membrane was sealed in a plastic bag. The blot was analyzed by phosphoimaging. The sizes of the bands were estimated using their electrophoretic mobility relative to the previously photographed gel or per overlay with the marked bands of the size ladder on the blot.

**Prehybridization solution**

1 M NaCl

50 mM Tris pH 7.5

10 % (w/v) dextrane sulfate

1 % (w/v) SDS

250 µg/ml salmon sperm DNA (sonicated)

**20 x SSC**

3 M NaCl

300 mM sodium citrate

adjust to pH 7.0 w/ NaOH

**2.2.10 Red/ET Cloning**

The Plasmid pSC101-BAD-gbaA-tetra (available from GeneBridges, Dresden) carries the  $\lambda$  phage *red* $\gamma\beta\alpha$  operon expressed under the control of the arabinose-inducible pBAD promoter (Guzman *et al.* 1995) and confers tetracycline resistance. The pBAD promoter is both positively and negatively regulated by the product of the *araC* gene (Schleif, 1992). AraC is a transcriptional regulator that forms a complex with L-arabinose. Arabinose binds to AraC and allows transcription to begin. In the absence of arabinose transcription is blocked by the AraC dimer. To minimize toxic side effects of the red  $\gamma$  gene, expression is tightly controlled. The plasmid is a derivative of a thermo sensitive pSC101 replicon which is a low copy number plasmid depending on the oriR101. The RepA protein encoded by plasmid pSC101 is required for plasmid DNA replication and the partitioning of plasmids to daughter cells at division (Miller *et al.*, 1995). Since a temperature sensitive (Ts) RepA protein is expressed cells have to be cultured at 30°C, pSC101 derivatives are easily curable at 37°C to 43°C. The temperature-sensitivity of the RepA proteins leads to a rapid loss of the plasmid in the absence of continued selection pressure.

We used the system of GeneBridges, Dresden.

### **2.2.10.1 Transformation of pSC101-BAD-gbaA into the *E. coli* Strain Carrying the BAC**

Ten colonies carrying the BAC were picked and inoculated in an Eppendorf tube containing 1.0 ml LB medium supplemented with 15 µg/ml chloramphenicol. The lid was punctured for ventilation. The tubes were cultured overnight at 37°C shaking at 300 rpm. The next day, a fresh Eppendorf tube containing 1.4 ml LB medium conditioned with chloramphenicol was inoculated with 30 µl of the overnight culture. Cells were cultured for three hours at 37°C shaking at 1000 rpm. All the following steps were performed on ice in a cold room. The cells were centrifuged (11000 rpm, 30 sec, 4°C). The pellet was placed on ice and resuspended in 1 ml ice-cold dH<sub>2</sub>O. After centrifugation, cells were resuspended and centrifuged a second time. The supernatant was removed leaving 20 to 30 µl in the tube. One µl of pSC101-BAD-gbaA were added to the cell slurry. The mixture was transferred into a chilled electroporation tube (BioRad, 1 mm). Electroporation was performed at 1800 V, 25 µF, 200 Ω with the Eppendorf Electroporator 2510. The electroporated cells were resuspended in 1 ml LB medium and incubated at 30°C for 60-80 min shaking at 1000 rpm. 100 µl of those cells were plated on LB agar plates containing tetracycline (3 µg/ml) and chloramphenicol (15 µg/ml). The plates were incubated at room temperature for at least 24 h.

### **2.2.10.2 Cloning of a PCR Product with Homology Arms into a BAC by Red/ET**

At least ten colonies from the previous transformation were picked and inoculated together in a ventilated tube containing LB medium conditioned with tetracycline and chloramphenicol. Tubes were incubated at 30°C shaking overnight at 300 rpm. The next day, two new tubes containing 1.4 ml fresh medium were inoculated with 30 µl of overnight culture. The tubes were incubated shaking at 30°C at 1100 rpm for 2 hours (OD<sub>600</sub> ~ 0.2). 20 µl of 10 % (w/v) L-arabinose were added to one of the tubes to induce the expression of the Red/ET recombination proteins. Cells were incubated at 37°C shaking at 1100 rpm for 40 min (cells should not grow further than OD<sub>600</sub> ~ 0.4). The following steps were performed as described above in section 1.2.10.1. Instead of the pSC101-BAD-gbaA, 1 µl of the PCR product with homology arms was added to the cell slurry. After electroporation, the cells were resuspended in 1 ml of LB medium and incubated at 37°C for 70 min. During this period, recombination occurs. 100 µl of the cells were plated on LB agar plates conditioned with 15 µg/ml chloramphenicol and 50 µg/ml kanamycin. The plates were incubated at 37°C overnight. Individual clones were analyzed with PCR and Southern blotting as described before.

## 2.3 Cell Culture

Cells were kept in incubators at 37°C in a humidified atmosphere (5 % (v/v) H<sub>2</sub>O) and a constant CO<sub>2</sub> concentration of 10 % (v/v). All procedures requiring sterility were carried out under a laminar flow sterile hood (Heraeus). Media and solutions were prepared in sterile bottles, with sterile glass or plastic pipettes and filter-sterilized if necessary.

Material and devices were cleaned with either 70 % (v/v) ethanol or Bacillol (Bode Chemie, Hamburg) prior to use. Gloves were worn at all times. Glass pipettes were flamed additionally to autoclaving prior to use.

The described techniques are modified according to Torres and Kühn (Torres and Kühn, 1997).

### 2.3.1 Reagents and Media for Cell Culture

**Embryonic feeder cell (EF) medium** (also used for CV-1 5B cells)

500 ml DMEM w/ Glutamax (Gibco/BRL)

60 ml EF FCS (Gibco/BRL)

6 ml 100 x sodium pyruvate (Gibco/BRL)

**Embryonic stem cell (ES) medium**

500 ml DMEM (Gibco/BRL)

75 ml ES FCS (Gibco/BRL)

6 ml 100 x sodium pyruvate (Gibco/BRL)

6 ml 100 x L-glutamine (Gibco/BRL)

6 ml 100 x non-essential amino acids (Gibco/BRL)

0.6 ml Leukemia inhibitory factor (LIF)

0.6 ml 0.1 M β-mercaptoethanol (Sigma)

**PBS** (phosphate buffered saline)

Dulbecco's phosphate buffered saline w/o calcium and magnesium (PAA laboratories)

**1 x trypsin/EDTA**

10 ml 10 x trypsin/EDTA (Gibco/BRL)

90 ml PBS

**Mitomycin C (MMC)**



2 mg MMC (Sigma) were dissolved in 2 ml EF medium; filter sterilized and diluted 1:100 in 200 ml EF medium (final concentration: 10  $\mu\text{g/ml}$ ). 7 ml aliquots were stored at  $-20^{\circ}\text{C}$ .

### **0.1 % gelatine (w/v)**

10 ml of a 2 % gelatine stock solution (Sigma) were heated to  $37^{\circ}\text{C}$  and diluted 1:20 in 190 ml of PBS.

### **Transfection buffer**

RPMI w/o phenol red (Gibco/BRL)

### **Geneticin (G418 sulfate, Gibco/BRL)**

Five g G418 sulfate were dissolved in 28 ml of PBS for a 600 x stock solution. 1 ml of this stock was added to one bottle of ES medium, resulting in a concentration of 300  $\mu\text{g/ml}$ . Since the G418 batch used has a relative activity of 71 %, the final effective working concentration was reduced to 225 $\mu\text{g/ml}$ .

### **Ganciclovir (Ganc, Hoffmann-La Roche, Switzerland)**

Ganc was purchased as Cymeven i.v. 4.3 mg of Ganc were dissolved in 80  $\mu\text{l}$  of  $\text{H}_2\text{O}$ . 10  $\mu\text{l}$  of this stock were diluted 1:100 in ES medium, filter sterilized and diluted 1:1000 in ES medium, resulting in a final concentration of 2  $\mu\text{M}$ .

## **2.3.2 Equipment**

### **2.3.2.1 Dishes and Plastic Ware**

15 cm plates	TPP, Switzerland
10 cm plates	Greiner Bio-One, Germany
6 well plates	Becton-Dickinson, USA
12 well plates	Becton-Dickinson, USA
24 well plates	Corning Incorporated, USA
48 well plates	Corning Incorporated, USA
96 well plates (round and flat bottom)	Costar, USA
250 ml tissue culture flask	Greiner Bio-One, Germany
Plastic pipettes (1, 5, 10 and 25 ml)	Corning Incorporated, USA
Pipette tips Tip-One	Starlab, Finland

Cryogenic vials	Nunc, Denmark
15 ml polystyrene tubes	Corning Incorporated, USA
50 ml polystyrene tubes	Greiner Bio-One, Germany
Medium reservoir 50 ml	Corning Incorporated, USA
Filter unit 250 ml	Nalgene, USA
0.22 $\mu$ m filter	Millipore, Ireland

### 2.3.2.2 Devices

Heraeus HA 2448 sterile hood	Heraeus, Germany
Heraeus incubator	Heraeus, Germany
Gene pulser electroporator	Bio Rad, Germany
Centrifuge	Heraeus, Germany
Counting chamber	Neubauer, Germany

### 2.3.3 Maintenance of Cells

All cell types were monitored on a daily basis with an inverse phase contrast microscope. Fibroblast cell lines like the EF cells or the CV-1 5B cells were passaged when they reached confluence. ES cells were not grown to full confluence to avoid differentiation of the colonies. Prior to passaging the cells were washed with PBS and trypsinized with 1 x trypsin at 37°C for 3-6 min depending on the cell type. The cell suspension was washed off the plate, transferred into a conical tube and centrifuged at 1200 rpm for 5 min at 4°C. After removing the supernatant, the cells were resuspended in their respective medium and plated on fresh plates.

### 2.3.4 Freezing and Thawing of Cells

Filter sterilized freezing medium (70 % medium, 20 % FCS, 10 % DMSO) was added to trypsinized cells which were then aliquoted into cryogenic vials on ice and slowly frozen at -80°C. 24-72 hrs later the cryotubes were transferred into the liquid nitrogen tank for long term storage (Ure *et al.*, 1992). Cells can also be frozen in plates, e.g. 96 well plates. Single cell suspensions were mixed with freezing medium to a final DMSO-concentration of 10 %. The plates were slowly frozen at -80°C.

Frozen cells were defrosted in a water bath at 37°C and rapidly transferred into 10 ml of medium. The cell suspension was centrifuged at 1200 rpm for 5 min. The supernatant was discarded. cells were resuspended in their respective medium and plated on the appropriate

amount of plates. Frozen plates were placed on saran wrap and gently shaken in a water bath at 37°C. The cell suspension was transferred into a new well and fresh medium was added until the well was completely full to compensate for the toxic effects of DMSO.

### **2.3.5 Determination of Cell Numbers**

Cell numbers were determined using Neubauer counting chambers. 10 µl of cell suspension was pipetted under the coverslip of a counting chamber. Four of the nine big quadrants were counted. One big quadrant has a total volume of 0.1 µl. The average cell number per quadrant was multiplied by 10<sup>4</sup> giving the amount of cells present in 1 ml of suspension. Total cell numbers were calculated by including the dilution factor and the total volume.

To distinguish between viable and non-viable cells, trypan blue was mixed 1:1 with the cell suspension. Trypan blue enters dead cells through the punctured membrane and stains the cell blue. Only viable cells were counted.

### **2.3.6 Murine Embryonic Feeder Cells**

ES cells have to be kept under conditions that prevent differentiation. For that reason, ES cell culture was carried out on mitotically inactivated embryonic feeder cells in ES cell medium supplemented with LIF (leukemia inhibitory factor).

#### **2.3.6.1 Embryonic Feeder Cell Preparation**

For ES cell transfection experiments neomycin resistant embryonic feeder cells are required. A male mouse from the transgenic mouse line IL-4 which carries a neomycin resistance gene (pEP. IL4:neo, Müller *et al.*, 1991) was crossed to a female C57BL/6 mouse. The day after, female mice were checked for a vaginal plug. Plug positive mice were sacrificed 13 days later. Embryos were isolated from the opened uterus under sterile conditions. After washing them with PBS, embryonic liver, heart and head were removed and the remaining material transferred to a PBS containing petri dish. The tissue was digested with 50 ml 1 x Trypsin/EDTA for 30 min at 37°C. Afterwards, EF medium was added and the cells were collected by centrifugation. The resuspended cells were counted and 2.5x10<sup>6</sup> cells were plated on a 15 cm tissue culture plate. Cells were grown until they reached confluency and frozen in aliquots of approximately 5x10<sup>6</sup> cells according to the procedure described previously.

For ES cell culture three generations of feeder cells were used. According to their passage stage they are called EF<sub>1</sub>, EF<sub>2</sub> and EF<sub>3</sub>. Freshly isolated EF cells are designated EF<sub>0</sub> cells. For targeting experiments only EF<sub>1</sub> or EF<sub>2</sub> were used.

### **2.3.6.2 Mitomycin C Treatment**

In order to use EF cells to support ES cell growth they had to be mitotically inactivated. Mitosis was inhibited by treating the EF cells with mitomycin C (MMC)(10 µg/ml, Sigma) for 2-5 hours. Afterwards, cells were washed twice with PBS to remove residual MMC and trypsinized. The single cell suspension was plated on the desired plates with fresh EF medium. Usually the plates were gelatinized beforehand. MMC treated feeder cells were used as basal layer for ES culture.

### **2.3.7 Murine Embryonic Stem Cells**

ES cells are derived from the inner cell mass of a three and a half day old mouse embryo, the blastocyst and maintained in culture (Evans and Kaufmann, 1981; Martin, 1981). ES cells are pluripotent giving them the potential to develop into all cell types or even produce a whole animal.

Murine ES cells are accessible for experimental genetic manipulation *in vitro* (Gossler *et al.*, 1986; Robertson *et al.*, 1986) and can be re injected afterwards into blastocysts. The injected blastocysts are then transferred into pseudo pregnant recipient mothers. The manipulated ES cells can contribute to the embryo formation resulting in the generation of chimeric mice. Chimeric founders possess a mixed coat color pattern because usually blastocysts and ES cells are derived from mouse strains with different coat color. The chimeric mice are used as an indicator for the contribution of the modified ES cells in embryogenesis. To achieve a high rate of chimerism and germline transmission, the culture conditions must guarantee the undifferentiated state of the ES cells (Smith, 1992). This is obtained by culturing the cells on a layer of mitotically inactive murine fibroblasts (feeder cells) and the addition of the cytokine LIF (leukemia inhibitory factor) to the ES cell medium (Smith *et al.*, 1988). LIF specifically suppresses differentiation of pluripotent ES cells without compromising their developmental potential.

The ES cells form colonies with a defined shape which have to be checked by microscopy on a daily basis to avoid differentiation. Before the colonies lose their blank borders and touch each other they have to be passaged onto a new feeder layer. The success of germline transmission is highly dependent on the quality of cell culture.

### 2.3.7.1 Transfection of ES Cells

The cloned targeting vector was linearized via endonuclease digestion and after protein contaminations were removed with a phenol-chloroform extraction the DNA was stored in 70 % (v/v) ethanol to guarantee sterility. Approximately 40 µg of DNA were used to transfect  $1 \times 10^7$  ES cells.

Four days prior to transfection ES cells were thawed. The cells were passaged two days later. Four hours before transfection, the medium was replaced by fresh ES cell medium. The cells were trypsinized and counted.  $1 \times 10^7$  cells were sedimented and resuspended in 400 µl of transfection buffer. The linearized targeting vector was dissolved in 400 µl of transfection buffer and added to the ES cells. The mix was transferred to an ice-cold electroporation cuvette (Gene Pulser cuvettes, 4 mm, BioRad, Germany). Electroporation was performed with a GenePulser Electroporator (BioRad, Germany) at 240 V and 500 µF. Afterwards, the cells were incubated at room temperature for 10 min, resuspended in ES medium and plated on 4-6 MMC-treated EF cell covered 10 cm plates.

### 2.3.7.2 Selection for Targeted Clones in Culture

After transfection of the ES cells with a targeting construct, one has to select for cells which have incorporated the linearized vector by use of a positive selection marker. The targeting vectors contain the neomycin resistance gene ( $neo^R$ ) that allows the isolation of all ES cell clones that stably incorporated the construct into their genome. Positive selection was performed by drug selection with the neomycin analogon G418. Positive selection was started at day 2 after transfection by feeding the cells with medium supplemented with G418 (225 µg/ml active concentration, Gibco/BRL). The cells were kept under G418 selection throughout the whole screening procedure.

Since integration of the targeting construct can either be random or homologous, the targeting construct often also contains a negative selection cassette at its 3' end. During homologous recombination this cassette is lost whereas random integrants usually integrate it into the genome (Folger *et al.*, 1982). The targeting vector contains the thymidine kinase gene from the *Herpes simplex* virus (HSV-TK). Starting at day 5 after transfection the negative selection drug ganciclovir (GANC) is added to the G418-containing ES medium (final concentration of GANC 2µM). After intracellular expression, the thymidine kinase phosphorylates GANC to GANC-monophosphate that is further phosphorylated to GANC-triphosphate by cellular enzymes. GANC-triphosphate is incorporated into newly synthesized DNA during replication that finally leads to cell death. Therefore, application of GANC

represents an approach to select against random integration events, whereas homologous recombinants will not be affected by the drug since they have lost the HSV-TK gene.

### **2.3.7.3 ES Cell Screening in 96-well Microtiter Plates**

Screening the targeted ES cells in 96-well plates is a very efficient approach to screen large numbers of transfected cells.

After 8-10 days of drug selection the surviving colonies need to be analyzed for proper integration of the targeting construct into the genome. To this end, colonies had to be isolated, one colony per well of a 96-well plate, and grown for later analysis.

The cells were washed twice with 10 ml 1 x PBS. Plates were covered with 10 ml 1 x PBS and single colonies were picked with a pipette in a volume of 20  $\mu$ l. Only colonies with a round shape and bright color were chosen. Each clone was placed in a well of a round-bottom 96-well plate together with 50  $\mu$ l of 1 x trypsin. After 20 -30 min of picking colonies, the 96-well plate was incubated for 3- 4 min at 37°C. Afterwards 80  $\mu$ l of ES cell medium was added per well to stop the trypsinization of the cells. After picking is finished, the 150  $\mu$ l of cell suspension in each well were distributed onto three wells of gelatinized EF-covered 96-well flat-bottom plates. ES medium was added to a final volume of 200  $\mu$ l per well. The plates were placed in an incubator and grown for 3- 4 days with daily exchange of medium. Cell growth was monitored daily to ensure optimal growing conditions.

Two plates were frozen as a backup storage for subsequent recovery of positive clones. For this purpose the plates were washed twice with 100  $\mu$ l of PBS per well and then trypsinized in 50  $\mu$ l of 1 x trypsin for 3 min at 37°C. The reaction was stopped by adding 100  $\mu$ l of ES cell medium. 100  $\mu$ l of ice-cold freezing medium (20 % DMSO (v/v) in ES-FCS) per well were added, the plates were sealed with parafilm and slowly frozen at – 80°C.

The third plate was grown to confluency, washed with PBS, trypsinized and split onto three gelatinized 96-well flat-bottom plates. These plates were grown to confluency and used to prepare ES cell DNA for Southern blot analysis. After removal of the ES medium and washing with 100  $\mu$ l PBS per well, two of the three plates were frozen at - 20°C. ES cells of the third plate were used for DNA isolation as described previously. The air-dried DNA was digested in a volume of 35  $\mu$ l per well, electrophoretically separated and analyzed by Southern blot hybridization as described previously.

### **2.3.8 HTNC Treatment**

$2 \times 10^5$  ES cells were plated in a well of a 6-well culture dish with MEFs, 5 h prior to HTNC treatment. The medium was removed and replaced with DMEM without FCS/PBS,

1:1, 4-0.25  $\mu\text{M}$  HTNC from a 50% (v/v) glycerol stock solution of 180  $\mu\text{M}$  HTNC for 20 h (Peitz et al., 2002; M. Peitz, unpublished). Thereafter, the cells were cultured as described above. The deletion efficiency at 2  $\mu\text{M}$  HTNC was usually 97%.

### 2.3.8.1 Preparation of Targeted ES Cell Clones for Blastocyst Injection

Five days prior to injection a vial of ES cell clones was thawed on a EF cell covered 10 cm plate. After two days the cells were split according to cell numbers on 10 cm plates. On the day of injection the best-looking plate was prepared. The ES cells were washed twice PBS and trypsinized. The single cell suspension was centrifuged for 5 min at 1200 rpm at 4°C. The supernatant was removed and the pellet resuspended in 10 ml of ES medium. The cells were plated on a gelatinized 10 cm plate and incubated for 30- 40 min at 37°C. The majority of the ES cells stay in the supernatant whereas the EF cells attach to the plastic. Different fractions were taken after the incubation:

The supernatant containing the ES cells was pipetted into a 15 ml tube (fraction 1). Afterwards the plate was washed with 10 ml ES medium and the resulting cell suspension was transferred into a second 15 ml tube (fraction 2). Samples of both fractions were checked under the microscope for purity and amount of cells. The cell fractions were centrifuged at 1200 rpm for 5 min at 4°C. The supernatant was discarded. the pellet resuspended in 500  $\mu\text{l}$  of ice-cold injection buffer and kept on ice (Torres and Kühn, 1997; Stewart, 1993).

#### Blastocyst Medium

250 ml DMEM (Gibco/BRL)  
 45 ml EF-FCS (Gibco/BRL)  
 3 ml sodium pyruvate (Gibco/BRL)  
 3 ml non- essential amino acids (Gibco/BRL)  
 3 ml penicillin/ streptomycin (Gibco/BRL)  
 3 ml L- glutamine (Gibco/BRL)  
 8.35 ml HEPES (Gibco/BRL)

#### Injection Medium

250 ml blastocyst medium  
 0.0375 g DNase A  
 stored in 5 ml aliquots at  $-20^{\circ}\text{C}$

### 2.3.8.2 Blastocyst Injections and Transfers

The prepared ES cells were microinjected with a Leica micromanipulator into precultured blastocysts derived from CB20 mice. The injection of 129/OLA ES cells into CB20 mice with white coat color resulted in offspring with brown-white coat color

chimerism. The injection of Bruce-4 ES cells derived from black-colored C57BL/6 mice into CB20 mice will result in offspring with black-white coat color chimerism.

10- 15 ES cells were injected in each of the blastocysts and cultured in blastocyst medium prior to transferring them into recipient foster mice. These mice are pseudopregnant CB20 mice that were previously mated with vasectomized male mice.

### **2.3.9 Preparation of Single Cell Suspensions From Lymphoid Organs**

Mice were killed and the organs of interest were taken and placed in ice-cold PBS. Single cell suspensions were prepared by passing the organs through a mesh or sieve. Cells were stored in ice-cold PBS-BSA-azide (PBA). It is important to keep the cells in PBA to prevent capping of the antibodies during the staining procedure. The azide shuts down the cell metabolism which prevents the metabolization of the antibody. Cells from spleen were pelleted (5 min, 1200 rpm, 4°C) and resuspended in 1 ml red blood cell lysis buffer to lyse erythrocytes. After a three minute incubation at room temperature, the reaction was stopped by diluting the lysis buffer with 10 ml ice-cold PBA. Cells were collected by centrifugation and resuspended in PBA. The cell numbers of the different single cell suspensions were determined.

#### **PBA**

PBS with  
1 % (w/v) BSA  
0.01 % (w/v) sodium azide  
Stored at 4°C

#### **Red Blood Cell Lysis Buffer**

1 volume of 8.3 g/l NH<sub>4</sub>Cl  
9 volumes of 20.59 g/l Tris/HCl pH 7.6

### **2.3.10 Preparation of Peripheral Cells from Mouse Blood**

In order to obtain approximately 100-200 µl mouse blood, the tail vein was cut with a razor blade. The blood was mixed directly with 10 µl of Heparin (Liquemin N500). 500 µl of room temperature Ficoll (7 %, v/v) were added to fresh tubes. The blood was carefully pipetted on top of the Ficoll layer followed by centrifugation (5 min at 4000 rpm, room temperature). The uppermost phase was transferred into a fresh tube together with 1 ml PBS. After another round of centrifugation (3500 rpm, 5 min at room temperature) the cells were ready to be stained for FACS analysis.



### 2.3.11 Flow Cytometry

Single cell suspensions were prepared from all tested organs. Red blood cells from LN and spleen were lysed in cell suspension with Tris-ammoniumchloride, pH 7.2. Cells ( $10^6$  per sample) were surface stained in 30  $\mu$ l PBS, 0.1% (w/v) BSA, 0.01% (w/v)  $\text{NaN}_3$  with combinations of fluoresceine isothiocyanate (FITC), phycoerythrine (PE) and Cy-Chrome<sup>TM</sup> (Cyc), APC or bio-conjugated mAbs for 20 min on ice. Stainings with biotinylated mAbs were followed by a secondary staining step with Streptavidin-Cychrome<sup>TM</sup> (Pharmingen). After staining, the samples were washed and resuspended in PBS-BSA- $\text{NaN}_3$ . Stained cells were analysed on a FACSCalibur and data were evaluated using CellQuest software (Becton Dickinson, Mountain View, USA). Dead cells were labeled with Topro-3 and excluded from the analysis. Monoclonal antibodies, listed in Table 1, were either homemade (C. Uthoff-Hachenberg, B. Hampel, Institute for Genetics, Cologne, Germany) or purchased from Pharmingen (San Diego, USA).

Specificity	Clone	Reference and Supplier
IgM	R33-24.12	(Gruetzmann, 1981), lab-made
IgD	G12-47/30	(Seemann et al., 1981), lab-made
B220/CD45R	RA3-6B2	(Leo et al., 1987), Pharmingen
CD4	GK.1.5/4	(Dialynas et al., 1983), Pharmingen
CD5	53-7.3	(Ledbetter and Herzenberg, 1979), Pharmingen
CD8	53-6.7	(Ledbetter and Herzenberg, 1979), Pharmingen
CD19	1D3	(Springer et al., 1979), Pharmingen
CD21/CD35	7G6	(Kinoshita et al., 1988), Pharmingen
CD22	Cy34.1	(Symington et al., 1982), Pharmingen
CD23	B3B4	(Rao et al., 1987), Pharmingen
CD24/HSA	M1/69	(Springer et al., 1979) Pharmingen
CD25 (IL2R $\alpha$ )	7D4	(Malek et al., 1983), Pharmingen
CD43	S7	(Gulley et al., 1988), Pharmingen
CD62L (L-Selectin)	MEL-14	(Gallatin et al., 2006), Pharmingen
CD69	H1.2F3	(Yokoyama et al., 1988), Pharmingen
CD86/B7.2	GL1	(Inaba et al., 1994), Pharmingen
CD90.2/Thy1.2	CFO-1	(Opitz et al., 1982), Pharmingen
CD95/Fas	Jo2	Pharmingen
AA4.1	AA4.1	Pharmingen
BP-1	BP-1	(Cooper et al., 1986), Pharmingen
c-Kit	c-Kit	Pharmingen

Fas	Fas	Pharmingen
MHC II	M5/114	(Bhattacharay et al., 1981), Pharmingen
IgG1	IgG1	Pharmingen
PNA	PNA	Pharmingen

Table 2: List of antibodies used for flow cytometry

### 2.3.12 Magnetic Cell Sorting and FACS Sorting

Specific cell populations were either sorted or depleted from a heterogenous cell suspension by magnetic cell sorting (MACS; Miltenyi Biotec, Bergisch Gladbach, Germany). Cell populations were labeled with antibody-coupled microbeads (10  $\mu$ l beads, 90  $\mu$ l PBS-BSA-N<sub>3</sub> per 10<sup>7</sup> cells) and separated on VS or CS MACS columns in a magnetic field (Miltenyi et al., 1990). For cell sorting, B cells were purified by MACS and then stained with antibodies against various cell surface markers. B cells of individual B cell subsets were then sorted using a dual laser FACStar (Becton Dickinson, Franklin Lakes, USA). The purity of isolated populations was subsequently tested by FACS analysis: MACS-isolated B cells were normally >80% pure and sorted B cell subpopulations were 95% pure.

### 2.3.13 B Cell Receptor Internalization

To measure endocytosis, splenocytes were preequilibrated at 4°C in RPMI 0.5% FBS and incubated with either biotin goat anti-mouse IgM Fab' or goat anti-mouse IgM (Fab')<sub>2</sub>. Cells were then either fixed in 0.5% paraformaldehyde in PBS (T<sub>0</sub>) or incubated at 37°C for the indicated times (T<sub>n</sub>) before termination with 0.5% paraformaldehyde in PBS. Fixed cells were stained with PE-B220 and streptavidin Red 670 (Invitrogen), and surface BCR expression was determined by flow cytometry. Percent internalization was calculated by the formula  $[\text{MFI sIgM}(T_0) - \text{MFI sIgM}(T_n)] / \text{MFI IgM}(T_0) \times 100$ .

### 2.3.14 Calcium flux

Splenic cells were labeled with Fluro 3 (Molecular Probes), and calcium flux of B cells resuspended in 10<sup>6</sup> cell/ml RPMI 2% FCS was assayed by measurement of emission of FL1 channel in the BD Calibur.

### 2.3.15 Culture of *ex vivo* Splenocytes and Lymphocytes

The spleens were aseptically removed from mice and then pressed through a sterile sieve. Erythrocytes were lysed for 2 min by NH<sub>4</sub>Cl (140 mM NH<sub>4</sub>Cl, 17 mM Tris-HCl pH 7.65). Splenocytes were kept in DMEM supplemented with 10% (v/v) FCS, 1 mM sodium pyruvate, 2 mM L-glutamine, 1x non-essential amino acids, 0.1 mM 2- $\beta$ -mercaptoethanol

supplemented with various activation compounds (LPS; ConA; PMA; BAFF) for no longer than four days.

### **2.3.16 CFSE Labeling and *in vitro* B cell Activation**

B cells were purified using MACS (as described above). For activation marker studies 1.5 to  $4 \times 10^6$  cells were plated in a 24-well plate and analysed after 24 h. Supernatants were collected for cytokine analysis. For proliferation analysis, B cells were resuspended in 1 ml per  $10^7$  cells 2.5  $\mu$ M CFSE (5mM stock in DMSO, Molecular probes) in PBS at RT for 6 min ((Lyons and Parish, 1994)). The labeling reaction was stopped by addition of 10 ml DMEM/10% (v/v) FCS medium. The cells were then washed once in medium. Labeled B cells were plated at  $0.5 \times 10^6$  cells per well in round bottom 96-well plates. The cells were incubated in DMEM medium plus 10% (v/v) FCS, untreated or treated with 5  $\mu$ g/ml anti-CD40, anti-IgM (5  $\mu$ g/ml), LPS (2  $\mu$ g/ml) and LPS plus IL-4 (5 ng/ml) with or without BAFF (100 ng/ml). Labeled cells were analysed after various time points.

### **2.3.17 Induced Class Switch Recombination**

Using the MACS system, B cells were isolated from various mice.  $4 \times 10^6$  B cells were incubated in 24-well plates for 5 days in the presence of 10  $\mu$ g/ml LPS plus 20 ng/ml IL-4 or 2 ng/ml TGF- $\beta$ . Thereafter, the B cells were analysed for the expression of IgG1 or IgA by flow cytometry.

### **2.3.18 Histological Analysis and Immunohistochemistry**

Shock frozen tissues were sectioned in 5-8  $\mu$ m slices, fixed in ice cold acetone for 10 min and air dried for 10 min. Using a Pap pen, the tissue was outlined on the glass slide, placed in a wet chamber, and TBS was added for 5 min at RT. Slides were then incubated with quenching buffer containing 0.3% (v/v)  $H_2O_2$  for 30 min and washed once with TBS. The sections were incubated with avidin solution and biotin solution for 15 min each and subsequently washed three times with TBS. The sections were then incubated with the primary antibodies for 60 min. After incubation, the sections were washed three times with TBS and incubated with secondary reagents Peroxidase-Streptavidin 1:500; Alkaline Phosphatase Goat anti-Rat 1:50 containing 5% (v/v) mouse serum for 60 min. Sections were washed three times with TBS. The slides were incubated with freshly prepared POX solution for 10 min and subsequently washed with TBS. The AP was developed using the Alkaline Phosphatase Substrate Kit III, washed three times with TBS and air dried before mounting with glycerol or crystal mount.

Dissected testes were fixed in Bouin solution for 24 h, processed, and paraffin-embedded using standard protocols. The initial morphology of testes was examined after hematoxylin and eosin staining of 5  $\mu\text{m}$  sections.

### **2.3.19 Preparation and Immunostaining of Cytospins**

In order to evaluate the expression levels of different proteins in B cells, cytopins were prepared. Therefore,  $2 \times 10^5$  B cells were centrifuged on glass cover slips (5 min at maximum speed) resulting in cell spots and stored at  $-80^\circ\text{C}$ .

Cytopins of purified B cells were fixed in acetone for 10 min at  $-20^\circ\text{C}$  and stained according to standard methods, using rabbit IgG antibody (Santa Cruz, Heidelberg, Germany). All incubation steps during the staining procedure were carried out at RT. The cytopins were counterstained with Hoechst 33258.

### **2.3.20 Protein Extract Preparations**

Protein lysates from mouse organs were prepared either freshly or from frozen tissue. Tissue was diced into small pieces using a clean razor blade. Then, RIPA buffer (1x PBS, 1% (v/v) NP-40) was added at 3 ml/g tissue supplemented with various protease inhibitors. Samples were centrifuged at 13,000 rpm for 5 min to separate supernatants from debris. Supernatants were transferred to fresh tubes and protein concentrations were determined in a photometer using Bradford assay (Ref). Protein extracts were diluted with RIPA buffer to 15 mg/ml before adding running buffer (3 x SDS sample buffer, NEB, Schwalbach, Germany) and DTT (30x DTT, NEB, Schwalbach, Germany) to 200  $\mu\text{g}$  of protein extracts. To separate the cytoplasmic protein fractions from the nuclear extracts, cells were resuspended at  $10^6/15 \mu\text{l}$  in hypotonic solution (10 mM Hepes [pH 7.9], 10 mM KCl, 2 mM  $\text{MgCl}_2$ , 0.5 mM DTT, 0.1 mM EDTA, supplemented with various protein inhibitors) and incubated at  $4^\circ\text{C}$  for 10 min. Then NP-40 was added to 1% (v/v) and the cells were centrifuged at 13,000 rpm for 1 min. The supernatant containing the cytoplasmic fraction was recovered from the nuclear pellet and the nuclear pellet was resuspended in  $10^6$  cells per 10  $\mu\text{l}$  of high salt buffer (20 mM Hepes [pH 7.9], 420 mM NaCl, 1.5 mM  $\text{MgCl}_2$ , 0.5 mM DTT, 0.2 mM EDTA and 10% (v/v) glycerol) and incubated on ice for 30 min. Nuclear extracts were recovered after centrifugation at 10,000 rpm for 10 min at  $4^\circ\text{C}$  and stored at  $-80^\circ\text{C}$ .

### **2.3.21 Western Blot**

Protein extracts were electrophoresed by SDS-PAGE (8-15% (v/v)) (Laemmli, 1970) and transferred to Immobilon-PVDF membranes (Millipore, Bedford, USA). The membranes were blocked with 5% (w/v) NF-milk/PBS or 5% (w/v) BSA/PBS for 1 h and probed using

primary antibodies. Membranes were then incubated with goat anti-rabbit IgG-horseradish peroxidase (HRP) conjugates (Vector, Burlingame, USA) as secondary antibody and developed using the ECL or ECL+ kit.

Specificity	Clone/Supplier
$\beta$ -Actin	(AC-40, Sigma)
Akt	(9272, Cell signaling)
PY99	(C-14; Santa Cruz)
Btk	(3532, Cell signaling)
pBtk	(3537, Cell signaling)
I $\kappa$ B $\alpha$	(C21, Santa Cruz)
p-I $\kappa$ B $\alpha$	(B9, Santa Cruz)
p38	(9212, Cell signaling)
p-p38	(9215, Cell signaling)
Jnk	(FL7, Santa Cruz)
p-Jnk	(G7, Santa Cruz)
Syk	(2712, Cell signaling)
p-Syk	(2711, Cell signaling)
Lyn	(2732, Cell signaling)
p-Lyn	(2731, Cell signaling)

**Table 3: List of antibodies used for Western Blotting**

## 2.4 Mouse Experiments

Tail bleeding as well as the general handling of mice was performed according to Hogan (Hogan *et al.*, 1987) and Silver (Silver, 1995).

### 2.4.1 Mice

C57BL/6 mice were obtained from Charles River or Jackson Laboratories. CD19-Cre mice (Rickert *et al.*, 1997) and Flp deleter mice ((Rodriguez *et al.*, 2000) were intercrossed with the *Smad7*<sup>FL/FL</sup> mouse strain in conventional facilities.

Name of primer	Sequence	Purpose
Luz6	CCT TCC TCC TAC CCT ACA AGC C	Used for typing of the IgM and IgG1 locus

Luz8	AGG ACG AGG GGG AAG ACA TTT G	Used for typing of the IgM and IgG1 locus
$\gamma$ 1-389	CAG ATG GGG GTG TCG TTT TGG CTA C	Used for typing of the IgM and IgG1 locus
4532-FOR	GCA GCA GGC GTC GGG	Used for typing of the Ig $\alpha$ locus
4815-wt-REV	AGG CAG GAT GCT GGA GT	Used for typing of the Ig $\alpha$ locus
2017-FOR	TTC CCC GAA GTA AAC AAG AAC	Used for typing of the Ig $\alpha$ locus
3026-REV	TGG AAG GAC AAA CCT TGG AA	Used for typing of the Ig $\alpha$ locus
INTRO-REV	CAG GGG TCA GAG AGG AGA CA	Used for typing of the Ig $\alpha$ locus
B29 I4-FW	GAG ACT CTG GCT ACT CAT CC	Used for typing of the Ig $\beta$ locus
B29 6R	CCT TCA GCA AGA GCT GGG GAC	Used for typing of the Ig $\beta$ locus
IRES-R	CGA CAT TCA ACA GAC CTT GC	Used for typing of the Ig $\beta$ locus
S7 FLOX5	GTC AGG TTG GAT CAC CAT GCC	Used for typing of Smad7 <sup>flox</sup> and Smad7 <sup>del</sup>
S7 FLOX3	GAC TGC CTG GAG AAG TGT GTC	Used for typing of Smad7 <sup>flox</sup>
S7 DEL3	TCT CCA TCC TAC CAC TGC CC	Used for typing of Smad7 <sup>del</sup>

**Table 4: Primer used for typing**

### 2.4.2 NP-CG Immunization

Primary T cell dependent responses were induced with alum precipitated NP-CG (4-hydroxy-3-nitrophenylacetyl chicken- $\gamma$ -globulin) (Weiss and Rajewsky, 1990). The antigen was prepared by mixing 1 volume of NP-CG (1 mg/ml in PBS) with 1 volume of 10% (w/v)  $\text{KA}_1(\text{SO}_4)_2$ . The solution was adjusted to pH 6.5 and kept 30 min on ice. Then, the precipitate was washed three times in PBS and resuspended in PBS. Mice were immunized by i.p. injections of 50  $\mu\text{g}$  NP<sub>17</sub>-CG in a volume of 200  $\mu\text{l}$ .

### 2.4.3 ELISA

Ig serum concentrations to NP were determined with ELISA as described previously (Roes and Rajewsky, 1993). Briefly, microtiter plates (Greiner, Frickenhausen, Germany) were coated with NP<sub>14</sub>-BSA at 4°C o/n, and subsequently blocked at RT for 30 min in 0.5% (w/v) BSA. Next, serially diluted sera samples were applied to the wells and incubated at 37°C for 1 h together with the standard. Secondary biotinylated antibody was then added for 1 h at 37°C. Detection of the biotinylated anti-sera was achieved with SA-conjugated alkaline phosphatase (AP, Boehringer: 30 min at RT) and p-nitrophenylphosphate as substrate (Boehringer). Following each incubation step, unbound antibodies or SA-conjugated AP were

removed by five washes with tap water. The OD<sub>405</sub> was measured with an ELISA-photometer (Anthos 2001, Anthos Labtech Instruments, Salzburg, Austria) and the relative antibody concentration were determined by calculating the association constant as described by Cumano and Rajewsky (Cumano and Rajewsky, 1986), following a method developed by Herzenberg et al. (Herzenberg et al., 1980).

Coating	Biotin-Conjugate	Specificity	Standard
R33-24.12	gam IgM (SBA)	IgM	B1-8 $\mu$
gam IgG1 (Sigma)	gam IgG1 (SBA)	IgG1	N1G9
ram IgG2aa (Nordic)	gam IgG2a (SBA)	IgG2aa	41.2-3
G12-47/30	G1247/30	IgG2ab	S43-10
R14-50	IgG2b (SBA)	IgG2b	D3-13F1
2E.6	IgG3 (SBA)	IgG3	S24/63/63
95.3	ram IgE (Pharmingen)	IgE	B1-8e
IgA gam (Sigma)	gam IgA (SBA)	IgA	233.1.3

**Table 5: Antibody combinations to determine serum antibody isotypes**

### 3 Results

#### 3.1 Generation of IgG1i mice

In the generation of B cell memory, most of the antigen-activated B cells participating in the response switch to the expression of IgH chains of the classes  $\gamma$ ,  $\epsilon$  and  $\alpha$ , and the BCR on these cells acquire the cytoplasmic tail of the newly expressed IgH chain as an additional signaling module (Geisberger et al., 2003; Neuberger et al., 1989; Reth, 1994). The functional importance of this module has been investigated in some of the transgenic mouse models expressing the  $\gamma$  chains (Lutz et al., 1998; Roes and Rajewsky, 1991). However, the physiological significance of these experiments remained uncertain, given the variations in transgene copy number and consequently expression levels inherent in the experimental setup. To investigate the physiological role of  $\gamma$ 1 chain containing B cell receptor (BCR), using the technique of gene targeting, a new mouse model, termed IgG1i, was generated in our laboratory. In this model the  $\gamma$ 1 constant region ( $C\gamma$ 1) gene segment replaced the  $\mu$  constant region ( $C\mu$ ) in the mouse germ line. This was achieved by constructing a mouse strain whose IgH constant region gene cluster is replaced by a *loxP*-flanked simplified locus containing a  $C\mu$  and a  $C\gamma$ 1 gene segment in opposite orientation (Fig. 6).

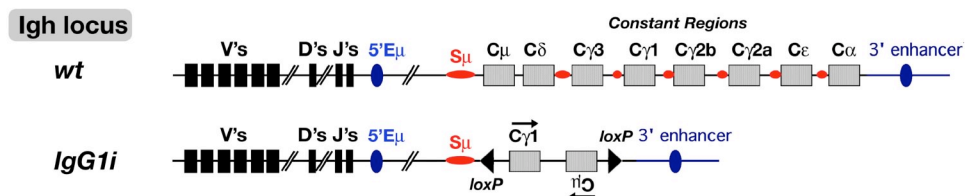


**Fig. 6 Genomic structure of the IgG1i locus.**

All IgH constant regions were replaced by the  $C\gamma$ 1 region followed by the  $C\mu$  region in opposite transcriptional orientation flanked by inverted *loxP* sites to generate the IgG1i allele. B cells carrying the IgG1i allele express exclusively a BCR of the IgG1 isotype. Cre recombinase activity can be employed to switch the *loxP*-flanked region towards the exclusive expression of a BCR of the IgM isotype (IgMi allele).

#### 3.2 Generation of Ig $\alpha_{\Delta c}$ /IgG1i, Ig $\beta_{\Delta c}$ /IgG1i and Ig $\alpha_{\Delta c}$ /Ig $\beta_{\Delta c}$ /IgG1i mice

The BCR consists of the membrane immunoglobulin (mIg), and a signaling subunit, a disulfide-linked heterodimer of the Ig $\alpha$  and Ig $\beta$  proteins that are non-covalently associated (Fig. 7). Ig $\alpha$  and Ig $\beta$  each contain a single immunoreceptor tyrosine-based activation motif (ITAM) within their cytoplasmic tail that initiates signal transduction following BCR aggregation (Flaswinkel and Reth, 1994).



The signaling of IgM expressing BCR is known to rely entirely on the cytoplasmic tail of Ig $\alpha$ /Ig $\beta$  (Reichlin et al., 2001). This is evidenced by the severely compromised B cell development in mice carrying a mutation in the cytoplasmic part of Ig $\alpha$  or Ig $\beta$  (Kraus et al., 1999; Reichlin et al., 2001). Both mouse strains generate less than one percent of mature B cells compared to WT mice. Mice with a truncated Ig $\alpha$  chain have a block in B cell development between the pro- and pre-B cell stages, whereas mice with truncated Ig $\beta$  co-receptor show a less severe block in B cell development, allowing the cells to develop to the immature stage. This unique biological function of Ig $\alpha$  and Ig $\beta$  might result from distinct signal transduction through their cytoplasmic tails. Since membrane-bound IgG1 also contains a cytoplasmic tail, it is of interest to assess whether the tail of Ig $\alpha$  or Ig $\beta$  is required for signal transduction of IgG1 BCR. Therefore, we bred mice homozygous for the Ig $\alpha$  mutation (Ig $\alpha_{\Delta c}$ ) while homo- or heterozygous for IgG1i (Ig $\alpha_{\Delta c}$ IgG1i). Likewise, mice homozygous for the Ig $\beta$  mutation (Ig $\beta_{\Delta c}$ ) and homo- or heterozygous for IgG1i (Ig $\beta_{\Delta c}$ IgG1i) were also bred. We also produced triple mutant mice (Ig $\alpha_{\Delta c}$ Ig $\beta_{\Delta c}$ IgG1i), which are homozygous for the Ig $\alpha$  truncation mutation and homozygous for the Ig $\beta$  truncation mutations in addition to the  $\gamma 1$  insertion. (Fig.7)

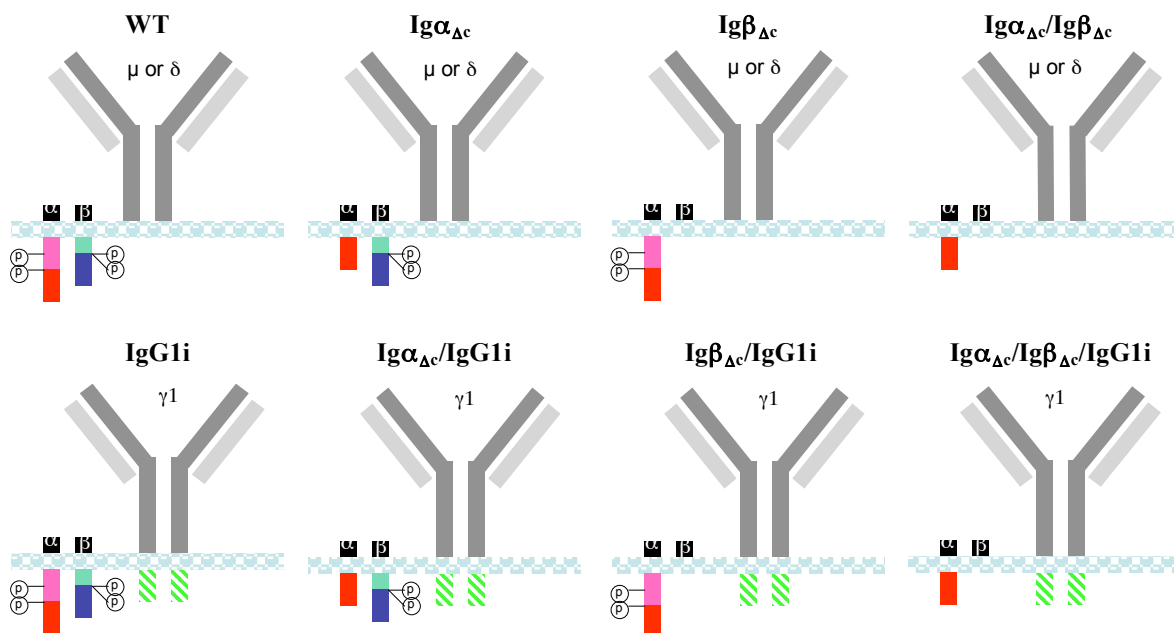


**Fig. 7 BCR/Ig $\alpha$ /Ig $\beta$  mutant mice**

The BCR consists of the membrane immunoglobulin (mIg), and a signaling subunit, a disulfide-linked heterodimer of the Ig $\alpha$  and Ig $\beta$  proteins. To investigate the interaction between immunoglobulin and Ig $\alpha$ /Ig $\beta$ , we crossed the IgG1i mice to Ig $\alpha_{\Delta c}$  or Ig $\beta_{\Delta c}$  mice to get IgG1i/Ig $\alpha_{\Delta c}$ , IgG1i/Ig $\beta_{\Delta c}$  and IgG1i/Ig $\alpha_{\Delta c}$ /Ig $\beta_{\Delta c}$  mice.

### 3.2.1 IgG1 affects B cell compartments distinctly and diversely when in combination with intact or mutant Ig $\alpha$ and Ig $\beta$ BCR subunits

All the above mutant mice are viable and do not demonstrate any differences in survival capacity compared to WT mice. However, the B cell compartments differ between the different mouse strains. We detected that IgG1i mice contain a decreased population of lymph node and splenic B cells compared to WT mice (IgG1i: 33% 34% WT: 40% 59%). In the Ig $\beta$  mutant mice in combination with the IgG1i allele (Ig $\beta_{\Delta c}$ IgG1i), a three-fold decrease of the B-lymphocyte proportion was detected compared to the Ig $\beta$  mutant mice (Ig $\beta_{\Delta c}$ ) (Ig $\beta_{\Delta c}$ IgG1i: 0.4% 0.3% Ig $\beta_{\Delta c}$ : 0.2% 0.1%). In contrast to the decreased B cell compartment in these two IgG1 expressing mouse strains, a four-fold increased population of B-lymphocytes was observed in the lymph nodes and spleen of the Ig $\alpha$  mutant mice in combination with IgG1i (Ig $\alpha_{\Delta c}$ IgG1i) compared to the Ig $\alpha$  mutant mice (Ig $\alpha_{\Delta c}$ ) (Ig $\alpha_{\Delta c}$ IgG1i: 3% 3.3% Ig $\alpha_{\Delta c}$ : 0.8% 0.8%). (Fig.8)

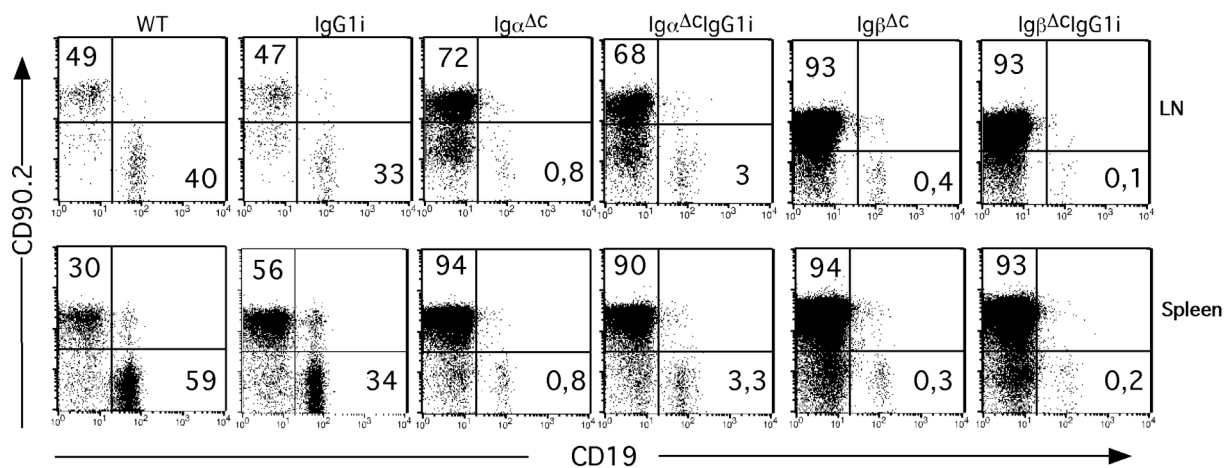


**Fig. 8 B cell compartments in the spleen and lymph nodes**

Flow cytometry of lymphocytes isolated from the depicted organs of mice with the indicated genotypes using B220 and CD90 antibodies. The numbers in the quadrants represent percentage of the gated population.

Next, we assessed whether the changed proportion of B cells in the mutant mice was consistent with the numbers of B cells. As seen in the Fig. 9, the B cell numbers matched the B cell proportions. As IgG1i mice contained a slightly reduced number of B cells compared to WT mice, Ig $\beta_{\Delta c}$ IgG1i mice exhibited a 1,5-fold decrease in the number of B cells compared to the Ig $\beta_{\Delta c}$  mice (Ig $\beta_{\Delta c}$ IgG1i:  $0.05 \pm 0.01$  Ig $\beta_{\Delta c}$ :  $0.07 \pm 0.02$ ). Consistent to the B cell proportion, we noticed the pronounced increase of B cells in the Ig $\alpha_{\Delta c}$ IgG1i mice compared to Ig $\alpha_{\Delta c}$  mice (Ig $\alpha_{\Delta c}$ IgG1i:  $3.18 \pm 0.7$  Ig $\alpha_{\Delta c}$ :  $0.21 \pm 0.02$ ). These results indicate that IgG1 signaling is able to partially restore splenic and lymph node B cell compartments in

genetically challenged mice lacking functional Ig $\alpha$  via compensatory signaling through the Ig $\beta$  subunit.

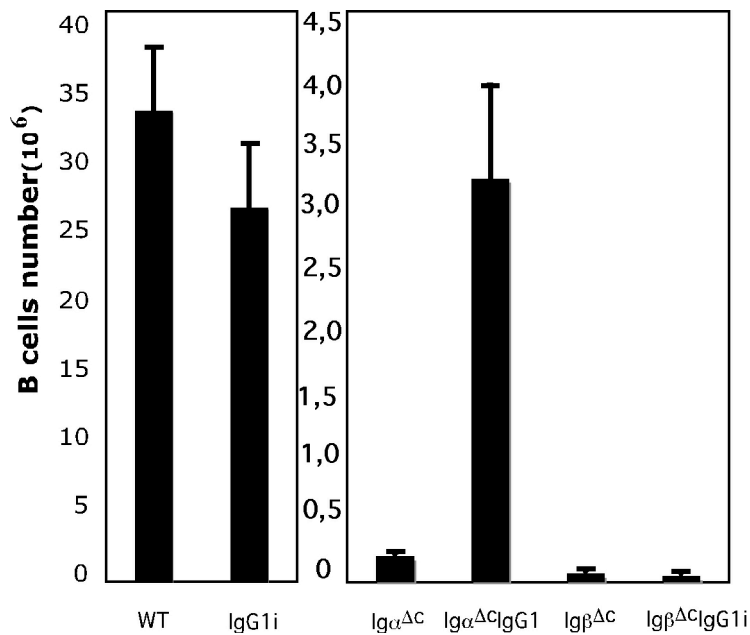


**Fig. 9 Total B cells number in the spleen**

Bar charts of total B cells numbers in spleen of indicated mice.

### 3.2.2 IgG1 expression compromises B cell development in the BM.

The BCR light chains are composed of protein expressed from two gene families, namely  $\kappa$  light chain and  $\lambda$  light chain. The majority of B cells express  $\kappa$  light chains and only a small population of B cells expresses an  $\lambda$  light chain. Previous studies reported that aberrant B cell development could result in increased usage of  $\lambda$  chain (Lang et al., 1996; Tiegs et al., 1993). In light of this finding, we opted to use increased lambda chain expression on B cells as a peripheral ‘readout’ for aberrant B cell development. We initially observed that IgG1i mice contain 12%  $\lambda^+$  B cells whereas WT mice exhibit normally five percent, indicating a compromised B cell development programme in the absence of IgM (Fig.10). Ig $\alpha$ -deficient mice (Ig $\alpha_{\Delta C}$ ) presented with an increased proportion of lambda-expressing B cells in the periphery when compared to WT controls. This increase was further aggravated in mice lacking only the Ig $\beta$  (Ig $\beta_{\Delta C}$ ), thus implicating a more important role for Ig $\beta$  signaling with IgM in determining the expression of lambda light chains. This trend was reproducible in IgG1i mice lacking Ig $\alpha$  and Ig $\beta$ . (Fig.10). These results indicate that untimely signaling through the Ig $\alpha$  or Ig $\beta$  subunit will result in an up-regulated expression of lambda light chains on the B cells. Thus, we proceeded to investigate the BM B cell development in those mice.

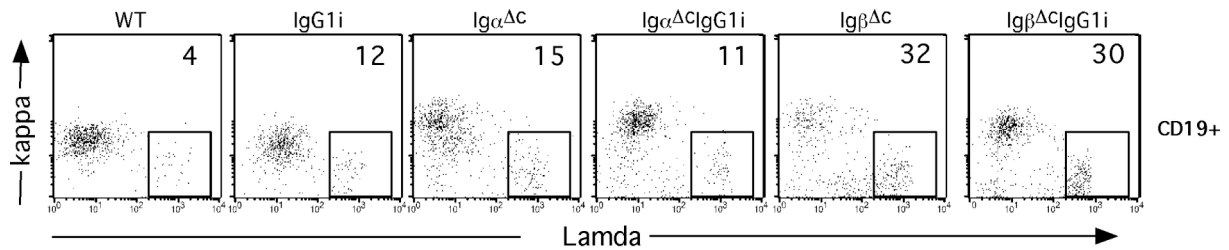


**Fig. 10 FACS analysis of B cell development in the spleen of IgG1i/mutant mice**

Splenic cells were gated on CD19<sup>+</sup> cells and stained for the expression of the cell surface markers  $\kappa$  and  $\lambda$ . The numbers refer to the percentages of the specific cells population gated on live lymphocytes.

B-lymphocytes follow a highly ordered program of development in the bone marrow (BM), beginning with the commitment of lymphoid progenitors to the B lineage and proceeding from pro-B cells to pre-B cells and finally to immature B cells that either undergo negative selection or enter peripheral organs (Edry and Melamed, 2004).

We detected an increase in the pro-B cell (c-Kit<sup>+</sup>) fraction of IgG1i mice compared to WT mice (Fig.11A). This increase was also observed in the Ig $\alpha$  or Ig $\beta$  truncated mice (Ig $\alpha_{\Delta C}$  65%, Ig $\beta_{\Delta C}$  40%), which appeared to be more severe in combination with the  $\gamma 1$  heavy chain (Ig $\alpha_{\Delta C}$ IgG1i 70% or Ig $\beta_{\Delta C}$ IgG1i 52%). Furthermore, we found that the increased populations of pro-B cells are paralleled with decreased proportions of pre-B cell in the all the IgG1 expressing mice (Table.6). Thus, the  $\gamma 1$  expression compromised the transition from pro- to pre-B cells and its combination with Ig $\alpha$  or Ig $\beta$  mutation consequently results in synergic developmental block in the Ig $\alpha_{\Delta C}$ IgG1i mice as well as in the Ig $\beta_{\Delta C}$ IgG1i mice (Fig.11A, Table.6).

To evaluate the transition from pre-B to immature B cells, BM cells were stained with B220, AA4.1 and CD43 as well as CD25 antibodies. As observed in Fig.11B, the proportions of immature B cell (B220<sup>+</sup>AA4.1<sup>+</sup>CD43<sup>-</sup>CD25<sup>-</sup>) are increased relative to their decreased pre-B cell population (B220<sup>+</sup>AA4.1<sup>+</sup>CD43<sup>-</sup>CD25<sup>+</sup>) in the IgG1 expressing mice. However, when the total cell numbers in all the six mouse strains were compared, we found that the actual numbers of immature B cells in the BM from IgG1 expressing mice were comparable and equal to those their wild type counterparts, indicating a true representation of altered BM subsets (Fig.11B, Table.6).

In summary, we observed that mice expressing IgG1 (IgG1i, Ig $\alpha_{\Delta C}$ IgG1i and Ig $\beta_{\Delta C}$ IgG1i) exhibit a more severe block at the transition from pro-B to pre-B cell stage compared to non-IgG1 expressing mice (WT, Ig $\alpha_{\Delta C}$  and Ig $\beta_{\Delta C}$ ). This was shown by the accumulation of pro-B cells and the reduction of pre-B cells in those mice expressing IgG1 (Table.6). However, in spite of the decreased population of pre-B cells, the immature B cells in the IgG1

expressing mice are comparable to non-IgG1 expressing mice (Table.6). This indicates that the increased number of peripheral B cells in the  $Ig\alpha_{\Delta C}IgG1i$  mice compared to  $Ig\beta_{\Delta C}IgG1i$  mice did not come from an advantage in the BM B cell development, but rather from a peripheral influence.

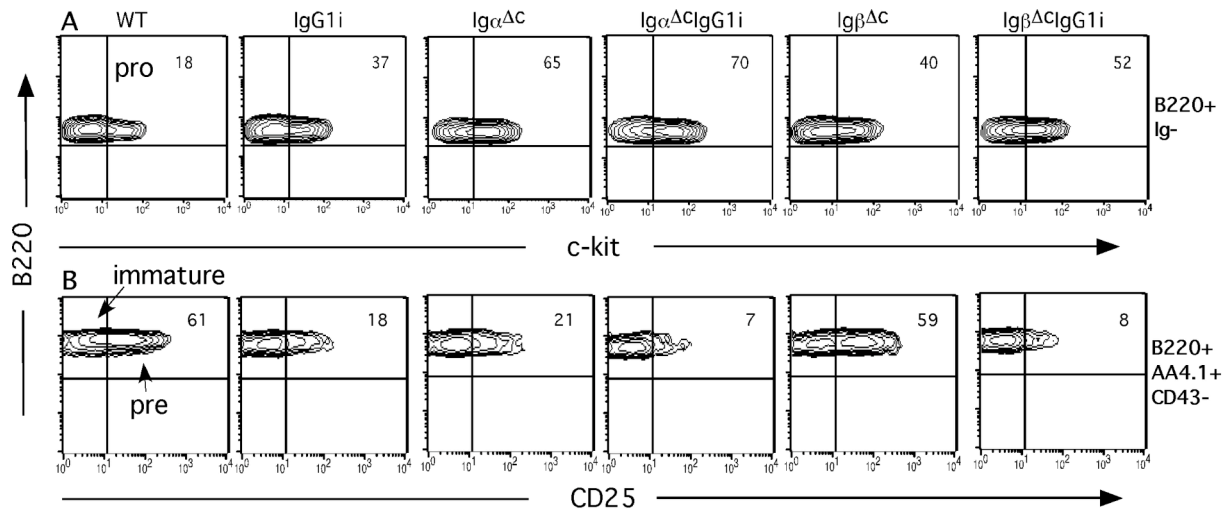


**Fig. 11 FACS analysis of B cell development in the BM of IgG1i/mutant mice**

BM lymphocytes were prepared from the indicated mice. (A) Cells were gated on  $B220^+Ig^-$  cells and stained with the pro-B cells marker c-kit. (B)  $B220^+AA4.1^+CD43^-$  cells were gated to analyze the ratio of  $CD25^+$  vs.  $CD25^-$  cells. The numbers in the quadrants refer to the percentages of the specific cells population gated on live lymphocytes.

Mice	No.	Percentage of all bone marrow cells			
		Pro-B (A-C)	Pre-B (D)	Immature (E)	Recirculating (F)
WT	N=4	3.52 ± 0.56	10.4 ± 1.79	6.67 ± 1.13	5.87 ± 1.10
IgG1i	N=4	5.80 ± 0.92	1.16 ± 0.20	5.29 ± 0.90	1.61 ± 0.28
Ig $\alpha_{\Delta C}$	N=4	19.8 ± 3.41	1.41 ± 0.24	5.30 ± 0.89	0.05 ± 0.01
Ig $\alpha_{\Delta C}IgG1i$	N=4	18.5 ± 2.94	0.41 ± 0.07	5.47 ± 0.93	0.16 ± 0.02
Ig $\beta_{\Delta C}$	N=4	9.76 ± 1.54	6.21 ± 1.07	4.31 ± 0.73	ND
Ig $\beta_{\Delta C}IgG1i$	N=4	13.8 ± 2.19	0.52 ± 0.09	6.01 ± 1.01	ND

**Table 6: B cell numbers in the BM**

The mean averages of B cell subset proportions in the indicated developmental are given (+/- SEM). ND stands for 'not detectable'.

### 3.2.3 Competition of IgG1 and IgM during B cell development

In order to assess whether IgG1 or IgM expression have an advantage during B cells development, we analyzed the mice heterozygous for IgG1i/WT associating with intact  $Ig\alpha/Ig\beta$  (IgG1i/WT), truncated  $Ig\alpha$  (IgG1i/WT;  $Ig\alpha_{\Delta C}$ ) or  $Ig\beta$  (IgG1i/WT;  $Ig\beta_{\Delta C}$ ). Since the

surface expression of the BCR appears at the stage of BM immature B cells, we analyzed the expression of IgG1 or IgM only in this stage and also in peripheral B cells.

In the periphery of the heterozygous IgG1i/WT mice with intact Ig $\alpha$ /Ig $\beta$  (IgG1i/WT), approximately 80% of peripheral B cells expressed IgM. This advantage of IgM expression is also observed in the heterozygous mice with truncated Ig $\beta$  (IgG1i/WT;Ig $\beta_{\Delta c}$ )(Fig.12). However, there are much fewer IgM B cells (9%) than IgG1 B cells (65%) in the heterozygous mice with truncated Ig $\alpha$  (IgG1i/WT;Ig $\alpha_{\Delta c}$ )(Fig.12). These results indicate and support our previous findings that forced Ig $\alpha$  signaling (Ig $\beta_{\Delta c}$ ) induces IgM expression, whereas Ig $\beta$  signaling (Ig $\alpha_{\Delta c}$ ) preferentially polarizes peripheral B cells to an increased expression of IgG1. Hence, it is reasonable to investigate whether this distinct competition originates from immature B cell stage in the BM.

In the BM of IgG1i/WT;Ig $\beta_{\Delta c}$  as well as IgG1i/WT, the competition of IgG1 vs. IgM on immature B cells matched the peripheral result that IgM takes the advantage over IgG1 in those mice (Fig.12). Surprisingly, in contrast to the dominance of IgG1 usage in the periphery, IgG1i/WT;Ig $\alpha_{\Delta c}$  mice exhibit less IgG1<sup>+</sup> than IgM<sup>+</sup> cells at the immature stage (Fig.12). Therefore, the increased  $\gamma 1$  expressing B cells in the IgG1i/WT;Ig $\alpha_{\Delta c}$  mice did not exist at the immature stage. We therefore wanted to investigate a potential increase in capacity for survival and proliferation in the periphery.

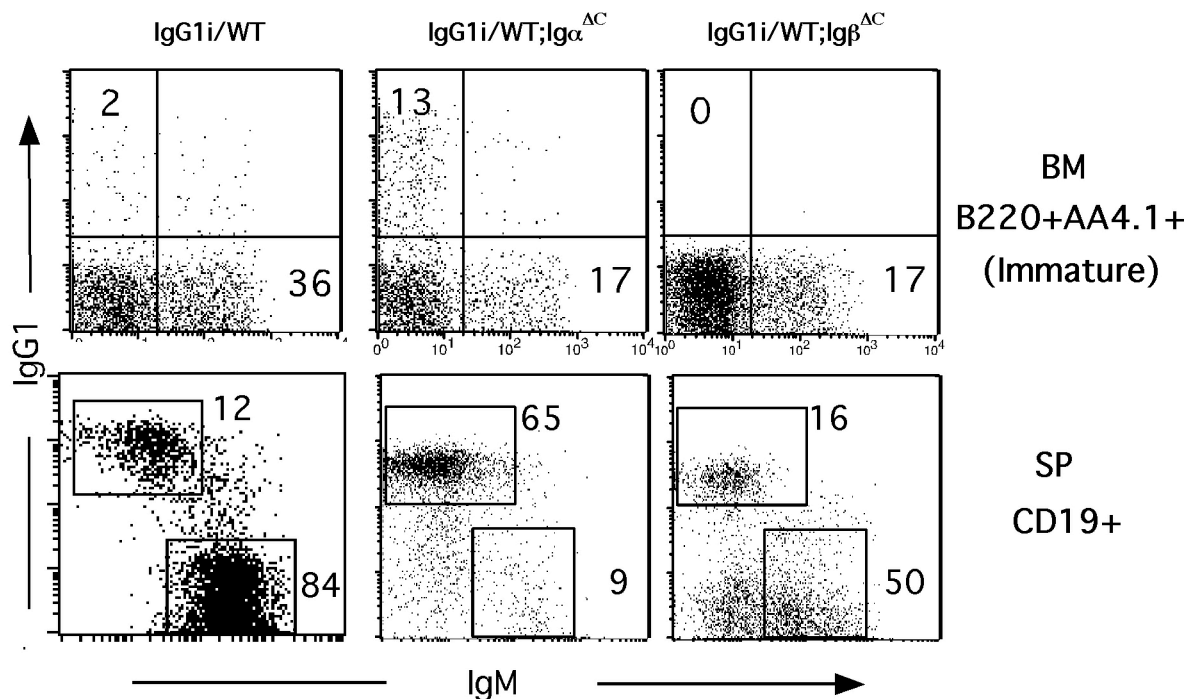


**Fig. 12 FACS analysis of competition of IgM<sup>+</sup> and IgG1<sup>+</sup> B cells in the heterozygous mice**

Splenic cells from indicated mice were gated on B220<sup>+</sup> cells and checked for the surface markers IgM and IgG1. BM lymphocytes were gated on B220<sup>+</sup>AA4.1<sup>+</sup> cells and check the surface marker of IgM and IgG1.

B220<sup>+</sup>AA4.1<sup>+</sup>Ig<sup>+</sup> indicates immature B cells. B220<sup>+</sup>AA4.1<sup>-</sup>Ig<sup>+</sup> indicates recirculating B cells. The numbers in the quadrants refer to the percentages of the specific cells population gated on live lymphocytes.

### 3.3 IgG1 signal in supporting B cells survival and proliferation

#### 3.3.1 Ig $\alpha_{\Delta c}$ or Ig $\beta_{\Delta c}$ B cells are sensitive to apoptosis

Ten times more B cells were detected in mice with a combination of Ig $\alpha$  mutation and IgG1 expression (Ig $\alpha_{\Delta c}$ IgG1i) compared to Ig $\alpha$  mutant mice (Ig $\alpha_{\Delta c}$ ). This relative enlargement of the mature B cell compartment might result from the increased signaling of Ig $\alpha_{\Delta c}$ IgG1i BCR in the periphery resulting in either sustained survival signals or increased proliferation.

To investigate the survival capacities, B cells from the six indicated mouse strains were MACS purified or sorted and cultured in enriched medium and monitored for survival by FACS analysis using the dead cell marker 7AAD. As shown in the Fig.13A, after 72 hours of culture there are more viable WT, IgG1i and Ig $\alpha_{\Delta c}$ IgG1i B cells compared to the other three genotypes, which seems to resemble the B cell populations in the mice. However, it was noticed that B cells from Ig $\alpha_{\Delta c}$ IgG1i mice survived even better than B cells from WT whereas the *ex vivo* experiment showed a 10-fold decrease of B cell numbers in these mice compared to WT (Fig. 13A).

BAFF, a member of the tumor necrosis factor (TNF) super-family, is known to signal through the BAFF receptor (BAFFR) and enhance B cell survival (Mecklenbrauker et al., 2004; Schneider and Tschopp, 2003). To elucidate the contradicted phenotype of Ig $\alpha_{\Delta c}$ IgG1i in B cell survival, we cultured B cells in medium supplemented with BAFF. As seen in Fig.8A, more viable WT and IgG1i B cells were detected in the medium with BAFF than without BAFF. However, the numbers of the Ig $\alpha$  or Ig $\beta$  mutant B cells, regardless of immunoglobulin expression (Ig $\alpha_{\Delta c}$ IgG1i and Ig $\beta_{\Delta c}$ IgG1i B cells), are not increased during culture with BAFF (Fig.13A). Interestingly, the viable B cell populations after culturing with BAFF strongly resemble the *ex vivo* peripheral B cell numbers shown previously (Fig.13A, Fig.8). Therefore, these data indicate that Ig $\alpha$  or Ig $\beta$  mutant B cells respond inefficiently to BAFF stimuli, thereby leading to the increased cell death compared to intact Ig $\alpha/\beta$ -bearing B cells (WT or IgG1i).

Furthermore, the surface levels of BAFF receptor were analyzed by FACS. In Fig.14B, we show that the Ig $\alpha$  or Ig $\beta$  mutant B cells expressed a much lower level of BAFFR on the surface compared to WT B cells, which explains the weak response of those B cells to the BAFF survival signal.

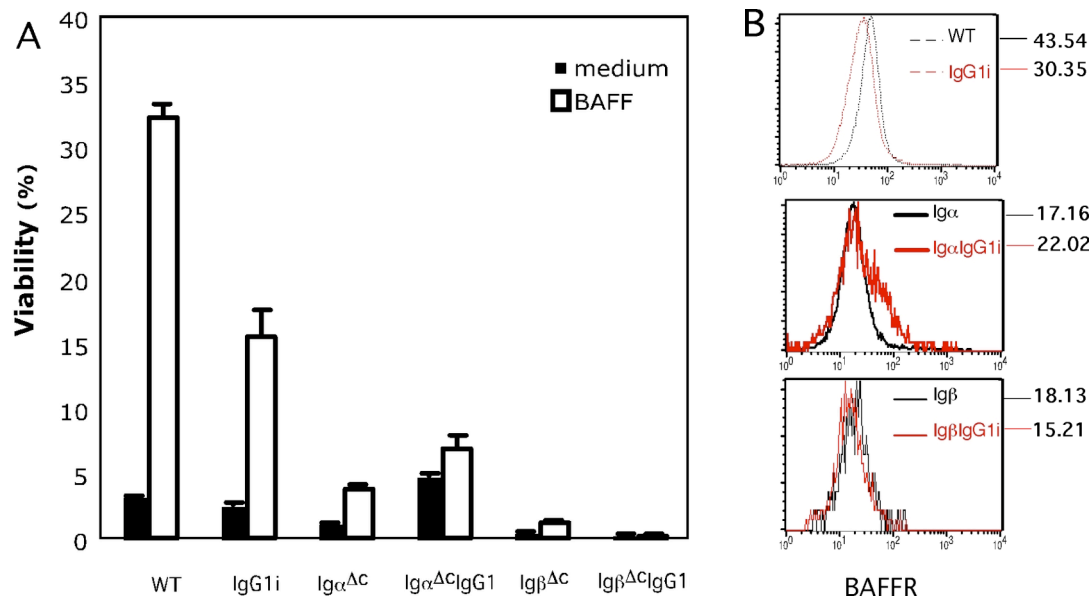


**Fig. 13 Viabilities of periphery B cells *in vitro* and BAFFR surface level of BCR/ Ig $\alpha$ /Ig $\beta$  mutant**

(A) Mature B cells were sorted based on CD19<sup>+</sup>CD23<sup>+</sup> expression and then cultured in the absence or presence of BAFF (100ng/ml) for 72 hours. Viable cells were determined by 7AAD staining. Bars indicate the live cells proportion.

(B) BAFFR surface level of B cells from BCR/ Ig $\alpha$ /Ig $\beta$  mutant mice

The defect in the survival capacity of Ig $\alpha$  or Ig $\beta$  mutant B cells might be attributed to the down-regulation of anti-apoptotic genes. To investigate the mechanism underlying the defective survival of the Ig $\alpha$  or Ig $\beta$  mutant B cells, we performed quantitative real time PCR to evaluate the copies of mRNA transcripts from *bcl2* and *bcl2-like1*, representing the proteins Bcl-2 and Bcl-X<sub>L</sub>, respectively. Both proteins play pivotal roles in anti-apoptotic regulation and processes of B cells survival.

Indeed, Ig $\alpha$  or Ig $\beta$  mutant B cells exhibited 5-10 fold decreased levels of gene transcription of Bcl-X<sub>L</sub> compared to WT B cells (Fig.14A). This reduction of Bcl-X<sub>L</sub> corresponds with the increased cell death of Ig $\alpha$  or Ig $\beta$  mutant B cells compared to WT and IgG1i B cells. Moreover, transcript levels of Bcl-X<sub>L</sub> in Ig $\alpha^{\Delta C}$ IgG1i B cells were relatively higher than Ig $\alpha$  mutant B cells (Ig $\alpha^{\Delta C}$ ) whereas B cells from Ig $\beta^{\Delta C}$ IgG1i display a decreased level of Bcl-X<sub>L</sub> compared to Ig $\beta$  mutant B cells (Ig $\beta^{\Delta C}$ ) (Fig.14A). These results are consistent with the viability in those B cells (Fig.13A) and suggest that the truncation of cytoplasmic tail of Ig $\alpha$  or Ig $\beta$  results in defective downstream expression of Bcl-X<sub>L</sub>, which consequently causes B cells to be sensitive to apoptosis.

Interestingly, while Bcl-2 was significantly decreased in the Ig $\beta$  mutant B cells (Ig $\beta^{\Delta C}$  and Ig $\beta^{\Delta C}$ IgG1i), it appears at an elevated level in the Ig $\alpha^{\Delta C}$  B cells (Ig $\alpha^{\Delta C}$  and Ig $\alpha^{\Delta C}$ IgG1i) compared to intact Ig $\alpha$ / $\beta$  B cells (WT and IgG1i) (Fig.14B). These results indicate a critical



role for Ig $\beta$  signaling in regulating Bcl-2 expression. Furthermore, the fact that Ig $\alpha$  mutation downregulated the transcript of Bcl-X<sub>L</sub> but not Bcl-2 suggests that distinct signals exist which regulate Bcl-2 and Bcl-X<sub>L</sub> separately in the inhibition of cell death.

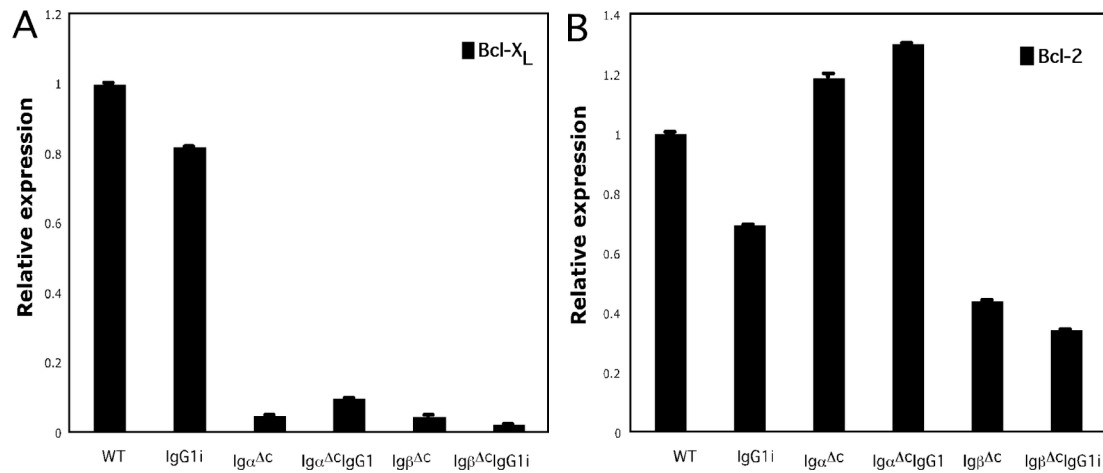


**Fig. 14** Transcript level of Bcl-2 and Bcl-x<sub>L</sub> gene in the BCR/ Ig $\alpha$ /Ig $\beta$  mutant mice

Periphery B cells were sorted based on CD19<sup>+</sup>CD23<sup>+</sup> and lysed for RNA according to the Trizol protocol.

Bars indicate the live cells proportion. (A) Bcl-X<sub>L</sub> (B) Bcl-2

### 3.3.2 Proliferation capacity of IgG1i, Ig $\alpha^{\Delta c}$ IgG1i and Ig $\beta^{\Delta c}$ IgG1i B cells

Since the truncations of Ig $\alpha$  or Ig $\beta$  result in decreased B cell compartments *in vivo*, it is of interest to make an inquiry as to whether Ig $\alpha$  or Ig $\beta$  mutation leads to hypoproliferation of B cells in response to stimulation or not. CFSE-labeled B cells were incubated with optimal concentrations of anti-IgM F(ab')<sub>2</sub> antibodies or were stimulated via toll like receptor (TLR) 4. As seen in Fig.15, in medium there was no difference detected in the proliferative capacity among B cells from the indicated mouse strains. Moreover, B cells from Ig $\alpha$  or Ig $\beta$  mutant mice responded similarly to the B cell activator lipopolysaccharide (LPS). However, BCR induced proliferation in B cells from the Ig $\alpha^{\Delta c}$ , Ig $\beta^{\Delta c}$  and Ig $\beta^{\Delta c}$ IgG1i mice was drastically decreased compared to WT B cells. Approximately half of the live B cells from those mouse strains kept the high intensity of CFSE labeling and did not proliferate. In contrast, the proliferation of Ig $\alpha^{\Delta c}$ IgG1i B cells in response to BCR cross-linker is increased compared to WT B cells (Fig.15). These results postulated that the impaired signaling through Ig $\alpha$  or Ig $\beta$  ablated not only the survival but also the proliferation capacity of B cells, but the combination of IgG1 and Ig $\alpha$  mutation (Ig $\alpha^{\Delta c}$ IgG1i) could replenish some of these survival signals.

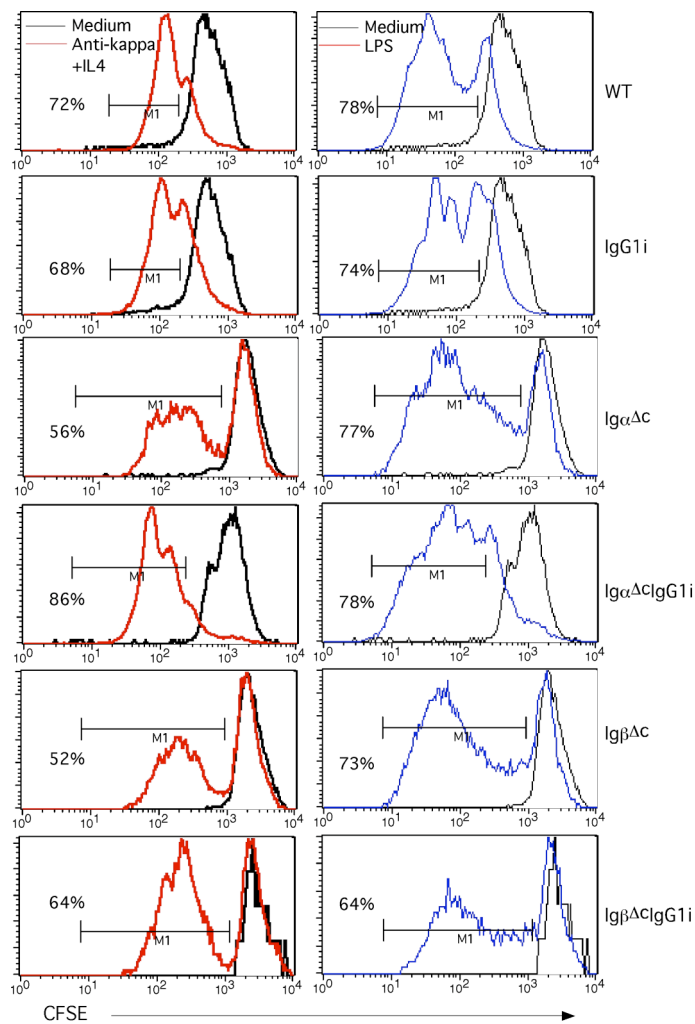


**Fig. 15 Proliferation of periphery B cells *in vitro***

Peripheral B cells were labeled with CFSE. Cells were co-cultured in the absence or presence of anti-kappa (10 $\mu$ g/ml) plus IL4 (2ng/ml) for four days. The proliferation is evidenced by the loss of CFSE signal shown in the histogram.

### 3.4 IgG1 derived BCR signaling

#### 3.4.1 IgG1 expression increases B cell activation in response to BCR engagement

Calcium mobilization is an indicator of B cell activation and is also involved in BCR signaling (Kraus et al., 1999). The sustain time and strength of calcium flux could determine the NF- $\kappa$ B and NFAT signals, respectively (Dal Porto et al., 2004). We have measured the calcium mobilization of Ig $\alpha_{\Delta c}$  or Ig $\beta_{\Delta c}$  B cells by kinetic analyses that define the change of calcium flux over time (Fig.16). B cells were enriched by negative depletion using MACS CD43 beads in order to get detectable density of B cells on the FACS and subsequently labeled with a calcium indicator, Fluo-3. After reaching 10,000 cells during a continuous acquisition, optimal concentrations of anti-kappa were injected into the acquisition tube.

As shown in Fig.16, BCR induced calcium flux of IgG1i B cells was observed to run in a similar kinetic compared to WT B cells. However, the calcium flux occurs over a shorter period in B cells with Ig $\alpha$  mutation in combination with IgG1 BCR (Ig $\alpha_{\Delta c}$ IgG1i) compared to Ig $\alpha$  mutant B cells (Ig $\alpha_{\Delta c}$ ). In contrast, the B cells with Ig $\beta$  mutation in combination with IgG1 (Ig $\beta_{\Delta c}$ IgG1i) exhibit a prolonged calcium influx in response to BCR engagement than in the Ig $\beta$  mutant B cells (Ig $\beta_{\Delta c}$ ). Actually, the calcium level in the Ig $\beta_{\Delta c}$ IgG1i B cells had not returned to the initial level ten minutes after triggering (Fig.16). These data suggested that the signal of IgG1 shifted the calcium influx mainly in a time dependent manner, shortening it in the B cells with Ig $\alpha$  mutation and extending it in the B cells with Ig $\beta$  mutation. This diverse calcium mobilization indicates a distinct role of Ig $\alpha$  and Ig $\beta$  in transducing the signal of IgG1 BCR-mediated calcium mobilization. Furthermore, the alteration of calcium flux implicated not only the abnormal upstream signal from B cell receptor but also the cascade changes on the downstream effectors.

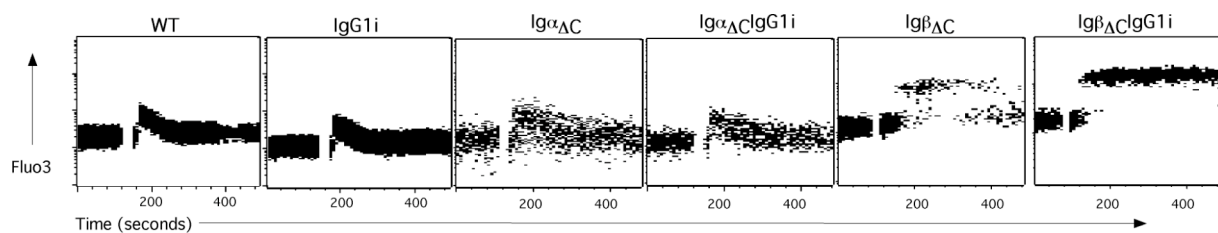


**Fig. 16 Calcium flux response**

B cells were dyed with the calcium indicator Fluo-3. Calcium flux was measured in response to BCR cross-linking with 10 $\mu$ g/ml anti-kappa in splenic B cells gated based on CD23<sup>+</sup> from Ig $\alpha_{\Delta c}$ , Ig $\alpha_{\Delta c}$ IgG1i, Ig $\beta_{\Delta c}$  and Ig $\beta_{\Delta c}$ IgG1i mice. Dot plots show the kinetics of Fluo-3 intensity (y axis) that indicates the calcium flux over 400 seconds (x axis).

### 3.4.2 BCR internalization and signaling of IgG1i, Ig $\alpha_{\Delta c}$ IgG1i and Ig $\beta_{\Delta c}$ IgG1i B cells

Altered BCR level is associated with changes of the BCR internalization in the Ig $\alpha$  or Ig $\beta$  mutant mice (Gazumyan et al., 2006). We also assessed whether IgG1 expression affects the surface level of BCR. As shown in Fig. 17A, where the surface level of BCR of IgG1 B cells is lower than WT B cells, Ig $\alpha_{\Delta c}$ IgG1i or Ig $\beta_{\Delta c}$ IgG1i B cells expressed BCR to a similar extent to Ig $\alpha_{\Delta c}$  or Ig $\beta_{\Delta c}$  B cells. In addition, BCR levels of both Ig $\alpha_{\Delta c}$  and Ig $\beta_{\Delta c}$  B cells were increased compared to WT (Fig. 17A). To determine whether these deviant cell surface levels of BCR in the Ig $\alpha_{\Delta c}$  or Ig $\beta_{\Delta c}$  mice were associated with the altered BCR internalization, we measured the ligand induced internalization by treating B cells with (Fab')<sub>2</sub> anti-Ig

antibody for the indicated times (Fig. 17B). The BCR internalizations of each time point were judged by down-regulation of the fluorescence intensity in response to BCR engagement.

Indeed,  $Ig\alpha_{\Delta C}$  and  $Ig\beta_{\Delta C}$  B cells were severely impaired in BCR internalization compared with WT B cells (Fig.17B). However,  $IgG1$  expressing B cells ( $IgG1i$ ,  $Ig\alpha_{\Delta C}IgG1i$  or  $Ig\beta_{\Delta C}IgG1i$ ) exhibit faster BCR endocytosis compared to WT B cells (Fig. 17B). Comparing these results with the respective BCR surface level, we observed that the slow internalization in the  $Ig\alpha_{\Delta C}$  or  $Ig\beta_{\Delta C}$  B cells is consistent with their high surface level of BCR. However, the fast internalization in the  $Ig\alpha_{\Delta C}IgG1i$  or  $Ig\beta_{\Delta C}IgG1i$  B cells is in contrast with their high BCR surface level. Therefore, other than altered BCR internalization, there might be some reasons remaining for the down-regulated surface levels of BCR in  $Ig\alpha_{\Delta C}IgG1i$  or  $Ig\beta_{\Delta C}IgG1i$  B cells. Nonetheless, it is clear that whereas truncation of cytoplasmic tail of  $Ig\alpha$  or  $Ig\beta$  impaired non- $IgG1$  BCR endocytosis, it did not influence  $IgG1$  BCR endocytosis, which indicated that the cytoplasmic signal of  $Ig\alpha$  or  $Ig\beta$  is not required for  $IgG1$  BCR internalization.

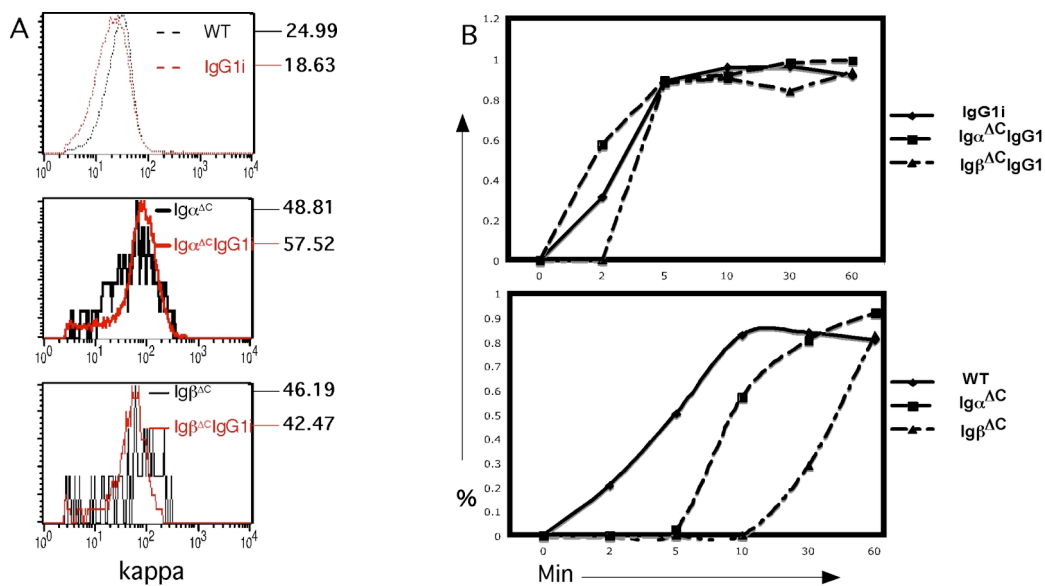


**Fig. 17 BCR surface level and ligand induced internalization assay**

(A) Peripheral B cells were stained with CD19 and kappa antibodies.  $CD19^+$  B cells were gated to measure the BCR surface level shown in the histogram.

(B) B cells were cultured with  $10\mu g/ml$  bio-(Fab')<sub>2</sub> anti-IgM+IgG1 on ice or in  $37^\circ C$  for the indicated time. PFA was used to fix the cells and stop the reaction. Surface level was evaluated according to fluorescence intensity and the percentage of internalization was calculated based on the formula described in *materials and methods*.

It was suggested that B cell receptor internalization is an important mechanism for attenuating BCR signaling (Brown and Song, 2001; Stoddart et al., 2005). Hence, we also investigated BCR signaling to clarify the interaction between BCR internalization and BCR

signaling of the BCR/Ig $\alpha$ /Ig $\beta$  mutant B cells. Because we cannot get a sufficient number of cells from the Ig $\alpha_{\Delta c}$ , Ig $\beta_{\Delta c}$  and Ig $\beta_{\Delta c}$ IgG1i mice to perform Western blot, we were only able to compare the BCR-triggered tyrosine phosphorylation among B cells from WT, IgG1 and Ig $\alpha_{\Delta c}$ IgG1i mice.

In the first two minutes, WT and IgG1i B cells displayed a similar level of total phosphorylation (judged by anti-PY99 antibody). However, total phosphorylation in IgG1i B cells faded away faster than WT B cells (Fig.18A). The rapid and transient process of protein phosphorylation in IgG1i B cells was consistent with the fast internalization of the IgG1 BCR (Fig.17B). On the other hand, resulting from the absence of the cytoplasmic tail of Ig $\alpha$ , a reduced level of total phosphorylation was observed in the Ig $\alpha_{\Delta c}$ IgG1i B cells in response to BCR engagement compared to IgG1i B cells (Fig.14A).

Phospholipase C gamma 2 (PLC $\gamma$ 2) relays information from the activated B cell receptor to downstream signal cascades by production of second-messenger, IP3 and DAG, which serve to activate Ca<sup>2+</sup> mobilization (Kurosaki et al., 2000). The downstream effectors of PLC $\gamma$ 2 in the B cell receptor pathway include MAP Kinase and NF- $\kappa$ B transcript factors, which determine the signals for B cell proliferation and survival, respectively (Dal Porto et al., 2004).

When paralleled with total phosphorylation, phosphorylation of PLC $\gamma$ 2 faded away more quickly in the IgG1i and Ig $\alpha_{\Delta c}$ IgG1i B cells compared to WT, which can explain the shortened period of calcium flux in those IgG1 cells (Fig.18B). On the other hand, only IgG1i B cells did not display an altered level of IKB $\alpha$  phosphorylation when compared to WT B cells, as we were able to show a weaker IKB $\alpha$  phosphorylation in Ig $\alpha_{\Delta c}$ IgG1i B cells (Fig. 18B). Taken together with the reduced survival of Ig $\alpha_{\Delta c}$  and Ig $\alpha_{\Delta c}$ IgG1i B cells, these data indicated that Ig $\alpha$  mutation might result in a lower level of activation in the NF- $\kappa$ B pathway and may consequently lead to a decreased transcription of Bcl-X<sub>L</sub>. In contrast, in the MAP kinase pathway, WT, IgG1i and Ig $\alpha_{\Delta c}$ IgG1i B cells exhibited comparable kinetics in the phosphorylation of ERK. The unaltered ERK phosphorylation suggested that whereas an Ig $\alpha$  mediated signal is critical for the NF- $\kappa$ B pathway, it is not required for the MAP kinase pathway. This divergent effect of an Ig $\alpha$ -derived signal could strongly explain our previous observation that Ig $\alpha_{\Delta c}$ IgG1i B cells proliferate as well as IgG1i B cells but survive less adequately than IgG1i B cells.

Interestingly, IgG1i B cells display a sustained phosphorylation of Lyn compared to WT B cells (Fig. 18C). Correlating with the notion that Lyn plays an essential role in negative

regulation of signaling (Xu et al., 2005), this sustained Lyn phosphorylation in the IgG1i B cells may account for its rapid PLC $\gamma$ 2 phosphorylation.

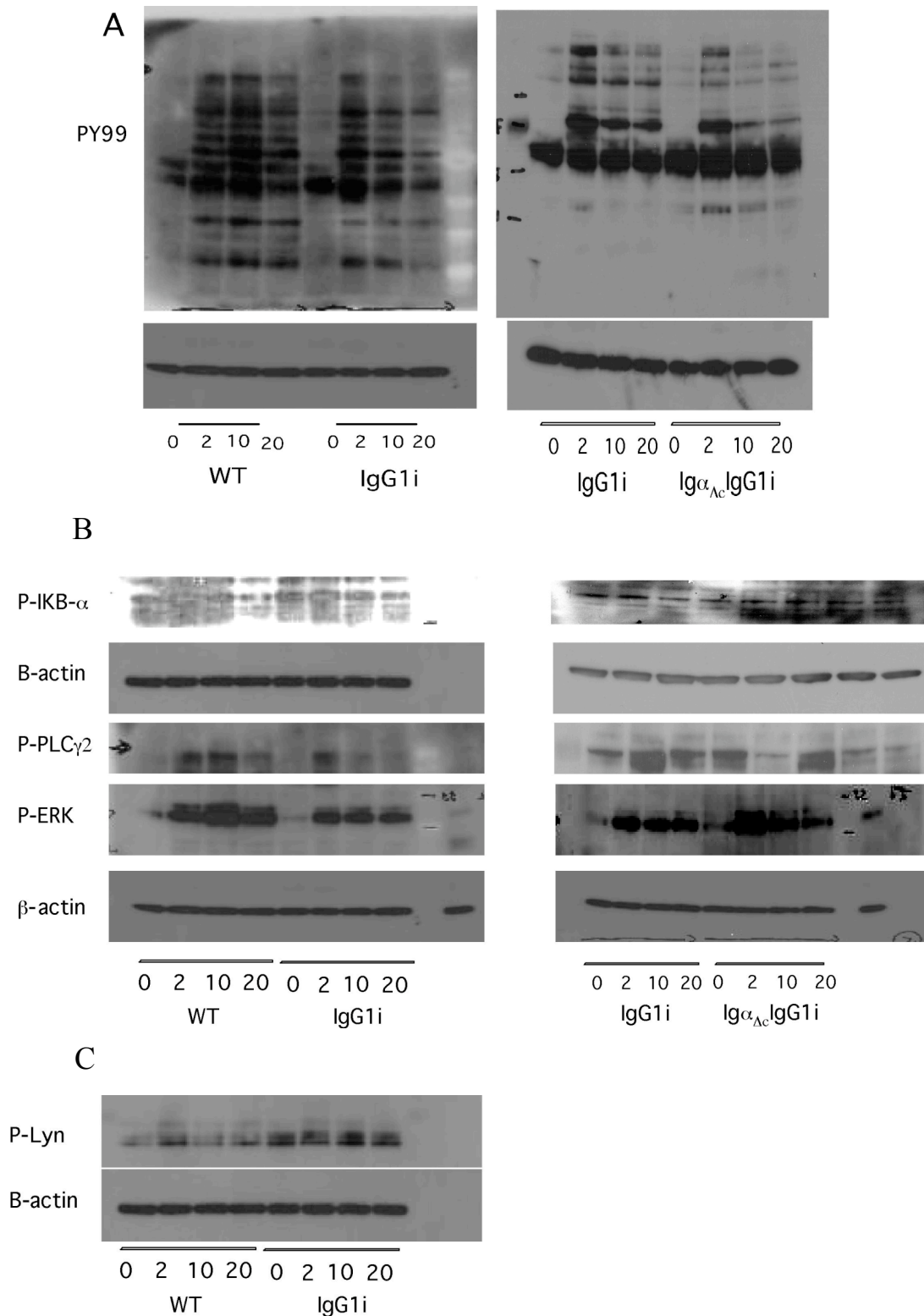


**Fig.18 Western blot analysis of BCR cross-linking induced protein phosphorylation**

Before prepared for protein, B cells were stimulated with anti-kappa antibody for the indicated time. The lysates were loaded for western blot and detected with indicated phosphorylation antibodies.  $\beta$ -actin antibody functioned as loading control.

### 3.5 IgG1 expression promotes the B cell maturation

Immature B cells that passed negative selection circulate to the spleen and develop into mature B cells, marked by the loss of AA4.1 surface expression. We observed an increase in the mature B cell population (AA4.1<sup>-</sup>) in the IgG1i mice compared to WT mice (Fig.19A). This increased maturation was also detected in all the IgG1 expressing B cells in spite of Ig $\alpha$  or Ig $\beta$  mutation compared to the non-IgG1 B cells (IgG1i>WT, Ig $\alpha_{\Delta C}$ IgG1i>Ig $\alpha_{\Delta C}$ , Ig $\beta_{\Delta C}$ IgG1i>Ig $\beta_{\Delta C}$ ), which suggested that IgG1 expression promotes the differentiation of immature B cells into mature B cells (Fig.19A).

As a result of maturation, the majority of B cells enter the follicular regions (FO) in the spleen and LNs. In the IgG1i mice, we detected an increased marginal zone (MZ) compartment compared to WT mice. Likewise, Ig $\alpha$  mutant mice in combination with IgG1i allele (Ig $\alpha_{\Delta C}$ IgG1i) exhibit an increased MZ fraction and elevated level of CD21 expression in the FO fraction compared to Ig $\alpha$  mutant mice (Ig $\alpha_{\Delta C}$ ). Moreover, an increased FO B cell compartment was also observed in the Ig $\beta$  mutant mice in combination with the IgG1i allele (Ig $\beta_{\Delta C}$ IgG1i) compared to the Ig $\beta$  mutant mice (Ig $\beta_{\Delta C}$ ), though MZ cells are completely absent (Fig.19B). Taken together, these results indicate that IgG1 expression increases the B cell population entering the FO and MZ, which further supports the notion that IgG1 enhanced the maturation of B cells (IgG1i, Ig $\alpha_{\Delta C}$ IgG1i and Ig $\beta_{\Delta C}$ IgG1i) compared to non-IgG1 B cells (WT, Ig $\alpha_{\Delta C}$  and Ig $\beta_{\Delta C}$ ) (Fig.19B)

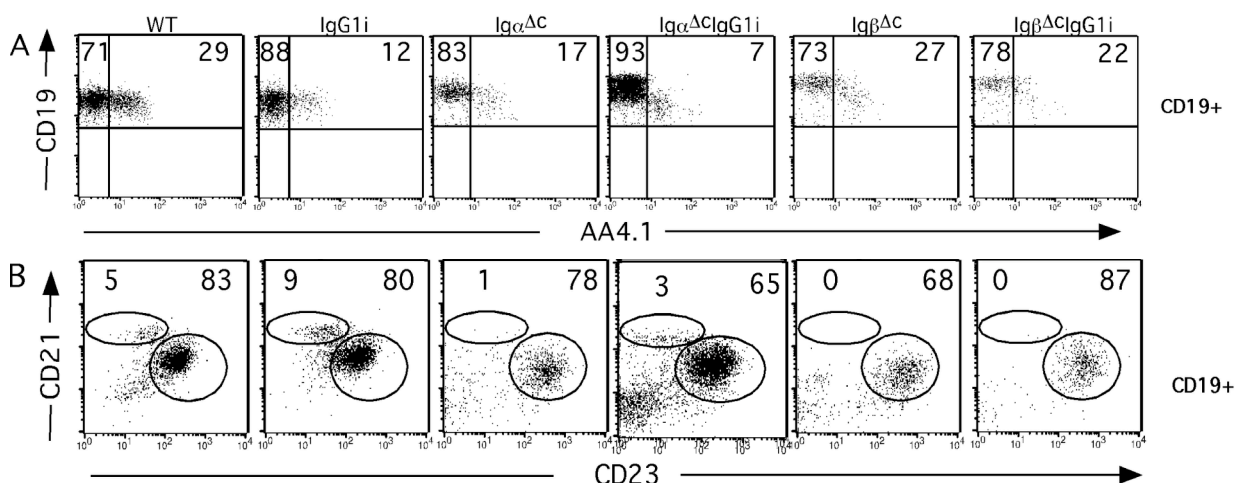


**Fig. 19 FACS analysis of B cell subsets**

**(A) Mature and immature B cells in the spleen of IgG1 expressing mice.** Splenic cells were gated on CD19<sup>+</sup> cells and stained with the indicated surface marker. CD19<sup>+</sup>AA4.1<sup>+</sup> indicates transitional immature B cells. CD19<sup>+</sup>AA4.1<sup>-</sup> indicates mature B cells. **(B) FO and MZ in the spleen of IgG1 expressing mice**

CD19<sup>+</sup>CD21<sup>high</sup>CD23<sup>low</sup> indicates MZ B cells. CD19<sup>+</sup>CD21<sup>low</sup>CD23<sup>high</sup> indicates FO B cells.

\*The numbers refer to the percentages of the specific cells population gated on live lymphocytes.

### 3.6 B-1 B cells in the peritoneal cavity of IgG1 expressing mice

The surface antigen CD5 typically expressed on T cells is also found on B-lymphocytes called B-1 cells (Hardy and Hayakawa, 1986; Herzenberg et al., 1986). B-1 B cells mainly reside in the peritoneal cavity (PC) and differ from conventional B-2 B cells in a number of characteristics (Tarakhovsky, 1997). In particular, their ability to produce multi-reactive IgM, IgG3 and IgA in large amounts has led to the consideration that B-1 B cells might have some innate immune function (Hardy, 1992).

As seen in Fig.20, we observed that the B-1 B cell fractions ( $CD19^{\text{high}}CD5^+$ ) in the PC are distinctly reduced in IgG1i and  $Ig\beta_{\Delta c}IgG1i$  mice (5% and 10%) compared to WT and  $Ig\beta_{\Delta c}$  mice (57% and 31%) respectively. In contrast, B-1 B cells account for 48% of the PC B cells in mice with combined IgG1i and  $Ig\alpha_{\Delta c}$  mutation ( $Ig\alpha_{\Delta c}IgG1i$ ) whereas it displays only 27% with  $Ig\alpha_{\Delta c}$  mutation ( $Ig\alpha_{\Delta c}$ ) (Fig.20). These results indicated that the B-1 B cell compartment is compromised with IgG1 alone or IgG1 in combination with the  $Ig\beta$  mutation, but not by IgG1 in combination with  $Ig\alpha$  mutation where the opposite tendency is observed.

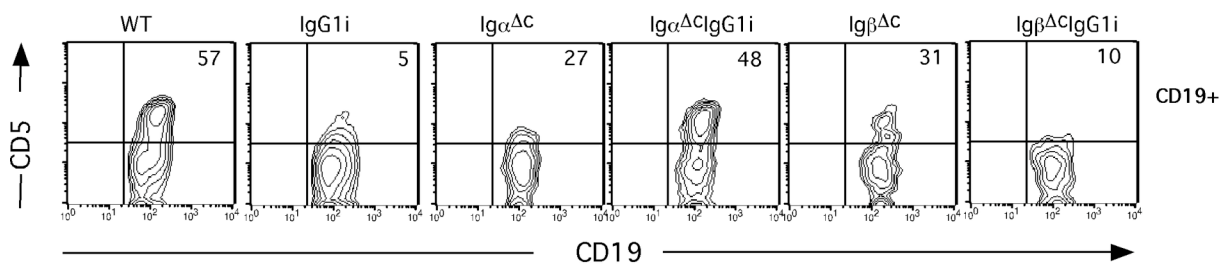


**Fig. 20 FACS analysis of B cell compartment in the peritoneal cavity**

Lymphocytes were prepared from PC of the indicated mice. Cells were gated on  $CD19^+$  cells and stained with CD5.  $CD19^+CD5^+$  cells indicate the B1 B cells. The numbers in the quadrants refer to the percentages of the specific cells population gated on live lymphocytes.

### 3.7 Serum IgG1 level in the IgG1 expressing mice

Sera immunoglobulins in the mice were evaluated in order to determine whether the IgG1 expression of B cells in the IgG1i,  $Ig\alpha_{\Delta c}IgG1i$  and  $Ig\beta_{\Delta c}IgG1i$  mice contribute to basic antibody secretion. Determination of total IgM and IgG1 by ELISA showed that basal levels of immunoglobulin titers in the sera of the WT mice contained significantly higher IgM antibody titers compared to IgG1 expressing mice (Fig.21A). We also detected higher titers of IgG1 in the IgG1i mice compared to WT mice (Fig.21B). These are the consequence of the mutation that constant region of  $\mu H$  was replaced by  $\gamma 1H$  in the IgG1i mice. In addition, there are hardly any IgG1 antibodies detectable in the serum of  $Ig\alpha_{\Delta c}$ ,  $Ig\beta_{\Delta c}$  and  $Ig\beta_{\Delta c}IgG1i$  mice,



which mirrors the small amount of B cells in those mice (Fig.21B). However, despite the ten fold decreased B cell numbers,  $Ig\alpha_{\Delta c}IgG1i$  mice surprisingly exhibited an increased level of serum IgG1 compared to WT mice (Fig.21B).

The source of basal serum immunoglobulin could be plasma cells and B-1 B cells, the natural Ig secreting cells (Hayakawa et al., 2000). To assess whether the elevated serum IgG1 from  $Ig\alpha_{\Delta c}IgG1i$  mice results from increased numbers of IgG1 expressing plasma cells or B-1 B cells, we prepared cytopspin slides of BM cells and stained them with anti-IgG1 antibody to count the plasma cells as plasma cells usually reside in the BM. Counting results show us approximately ten times less plasma cells in the  $Ig\alpha_{\Delta c}IgG1i$  mice than in the WT mice, which is correlated with their total B cells number. These data indicate that plasma cells were not the source of the increased titers of serum IgG1 in the  $Ig\alpha_{\Delta c}IgG1i$  mice. This enhanced titer of IgG1 must result from the increased amount of auto-secreting B-1 B cells.

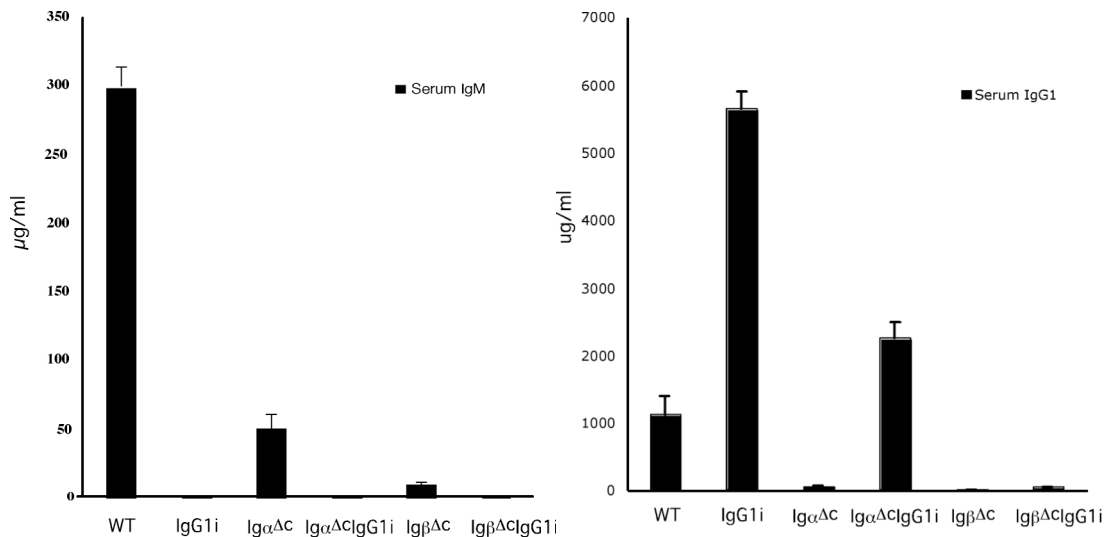


**Fig. 21 Serum IgG1 level in the BCR/  $Ig\alpha$ / $Ig\beta$  mutant mice**

Sera were prepared as described from indicated mice. Titers of antibodies were evaluated by ELISA.

### 3.8 IgG1 B cells in $Ig\alpha$ / $Ig\beta$ double mutant mice

As the  $\gamma 1$  insertion increased the B cell compartment in the  $Ig\alpha$  mutant mice ( $Ig\alpha_{\Delta c}IgG1i$ ) but not in the  $Ig\beta$  mutant mice ( $Ig\beta_{\Delta c}IgG1i$ ), it could be conceived that the combination of  $\gamma 1$  and  $Ig\alpha$  mutation rather than  $\gamma 1$  alone caused the increased B cell compartment. Subsequently, we assessed whether this combination could also contribute to the B cells compartment in the  $Ig\beta_{\Delta c}$  mice.

We generated  $Ig\alpha_{\Delta c}Ig\beta_{\Delta c}IgG1i$  mice, in which IgG1 BCR is associated with cytoplasmic tail-truncated  $Ig\alpha$ / $Ig\beta$  (Fig.7). All the  $Ig\alpha_{\Delta c}Ig\beta_{\Delta c}IgG1i$  mice did not demonstrate any differences in survival capacity compared to WT mice. However, our data show no detectable

B cells in the  $Ig\alpha_{\Delta c}Ig\beta_{\Delta c}IgG1i$  mice, neither in the lymph nodes nor in the spleen (Fig.22A, B). We could not detect any B cells in the peritoneal cavity either (Fig. 22C). This suggests a very severe block exists during BM B cell development in these mice.

Indeed, in the BM of  $Ig\alpha_{\Delta c}Ig\beta_{\Delta c}IgG1i$  mice there were only pro-B cells ( $B220^{+}CD43^{+}$ ) and no immature and recirculation B cells ( $B220^{+}Ig^{+}$ ) detectable (Fig. 22D). Analysis of pre-B cells ( $B220^{+}CD25^{+}$ ) ensured that B cells development of  $Ig\alpha_{\Delta c}Ig\beta_{\Delta c}IgG1i$  mice cannot proceed beyond pre-B cells stage (Fig.22D). Similar to the published data of mice with the double truncation of  $Ig\alpha$  and  $Ig\beta$ ,  $\gamma 1$  expression in combination with double mutation of  $Ig\alpha$  and  $Ig\beta$  ( $Ig\alpha_{\Delta c}Ig\beta_{\Delta c}IgG1i$ ) results in a complete developmental arrest preceding the pre-B cell stage.

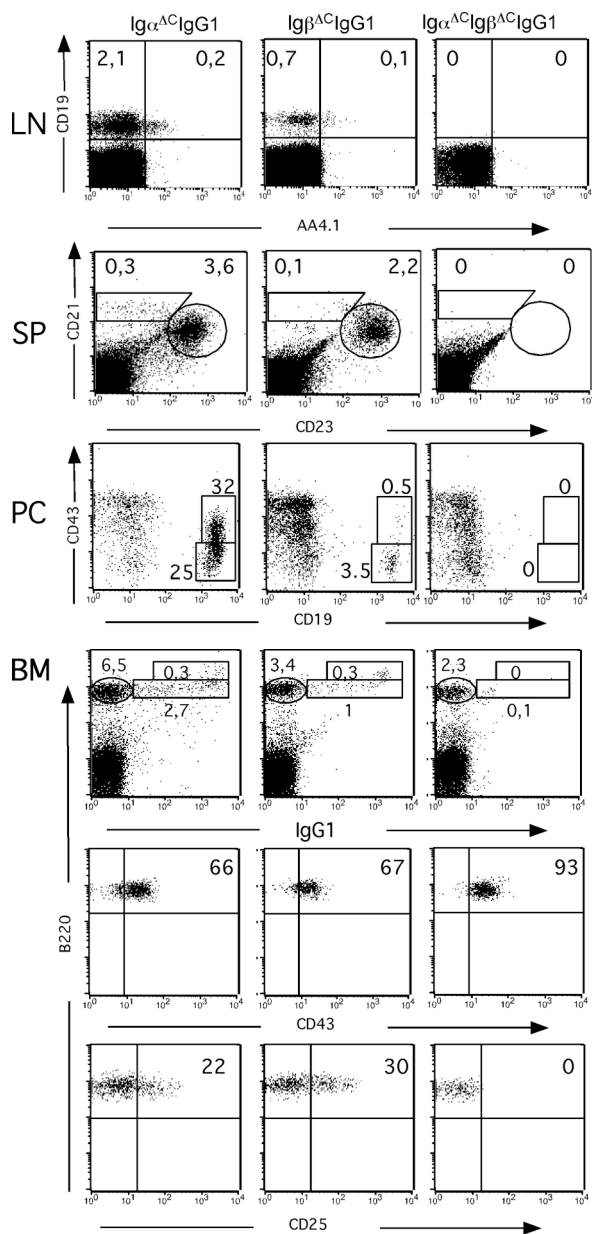


**Fig. 22 FACS analysis of B cell development in the BM of  $IgG1i$ /mutant mice**

(A) Lymphocytes from lymph nodes were gated on  $CD19^{+}$  cells and stained with the surface marker of AA4.1.  $CD19^{+}AA4.1^{-}$  indicates mature B cells.  $CD19^{+}AA4.1^{+}$  indicates immature B cells.

(B) Splenic cells were gated on  $CD19^{+}$  cells and stained with the surface marker of CD21 and CD23.  $CD19^{+}CD21^{high}CD23^{low}$  indicates marginal zone B cells.

(C) Lymphocytes were prepared from peritoneal cavity of the indicated mice. Cells were gated on  $CD19^{+}$  cells and stained with CD5.  $CD19^{+}CD5^{+}$  indicates the B1 B cells.  $CD19^{+}CD5^{-}$  indicates the B2 B cells.

(D) BM lymphocytes were prepared from the indicated mice. Cells were gated on  $B220^{+}$  cells and stained with pro B cells marker CD43 and Ig surface marker.  $B220^{+}Ig^{-}CD43^{+}$  cells are pro-B cells.  $B220^{+}Ig^{low}$  cells are immature B cells and  $B220^{+}Ig^{hi}$  are recirculation mature B cells.  $B220^{+}CD25^{+}$  are pre-B cells.

The numbers in the quadrants or gates refer to the percentages of the specific cell population, gated on live lymphocytes.

B220+

### 3.9 Deficiency of *Smad7* in B cells enhanced IgA class switch

*Smad7* expression is induced by signaling of TGF- $\beta$  superfamily members. After induction, *Smad7* negatively regulates TGF- $\beta$  signaling by two distinct mechanisms. While TGF- $\beta$  receptor I (ALK5) is critical for TGF- $\beta$  signal transduction, *Smad7* can directly compete with *Smad2* and *Smad3* for ALK5 binding or can degrade ALK5 through recruitment of Smurf-containing E3 ubiquitin ligase complexes.

#### 3.9.1 Generation of *Smad7*<sup>FL/FL</sup> mice

To investigate the physiological role of *Smad7* we have generated a conditional *Smad7* knockout mouse model (*Smad7*<sup>flox</sup>). By using this model we are able to check the function of *Smad7* in specific tissues and development stages (Fig.23).

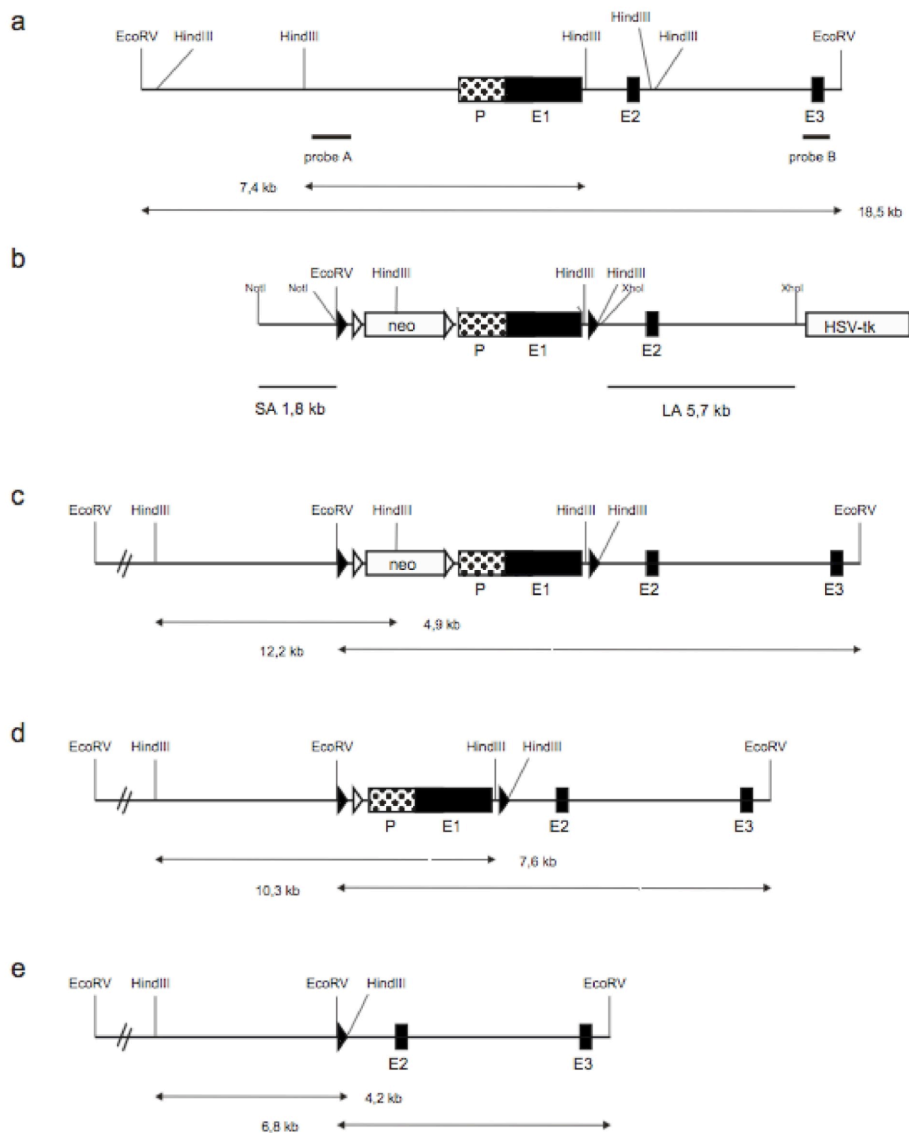


### Fig. 23 Generation of *Smad7<sup>FL/FL</sup>* and *Smad7<sup>del</sup>* mice

The scheme represents the targeting strategy. (Kindly provided by Ingo Kleiter) The targeting vector was constructed based on pRAPIDflirt (a). The structure of the *Smad7* gene from exon 1 to exon 3 is shown on the top (b). Homologous recombination into the *Smad7* gene resulted in the neo<sup>r</sup> containing genotype (*Smad7<sup>neo</sup>*)(c). The following genotypes *Smad7<sup>FL</sup>* and *Smad7<sup>del</sup>* have been generated through Flp- (d) and Cre- (e) mediated recombination (see methods).

### 3.9.2 Generation of CD19Cre *Smad7<sup>FL/FL</sup>* mice

TGF- $\beta$  receptor II is required for the initial binding of TGF- $\beta$ . The absence of TGF- $\beta$  receptor II in B cells leads to a reduced life span of conventional B cells, expansion of peritoneal B-1 cells and elevated serum immunoglobulin with the exception of IgA (Cazac and Roes, 2000). In order to assess whether deficiency of *Smad7* in B cells results in the opposite phenotype, we generated the CD19Cre/*Smad7<sup>fllox</sup>* mice, in which the deletion of *Smad7* takes place solely in B cells.

To generate mice with B cell specific deletion of *Smad7*, *Smad7<sup>fllox</sup>* mice were intercrossed with the *CD19-Cre* mouse strain. The *CD19-Cre* mouse has been shown to delete *loxP* flanked alleles specifically in the B cell lineage (Rickert et al., 1997). The deletion efficiency was shown to be 75- 80% in the BM and over 95% in splenic B cells (Inui et al., 2002) (Cazac and Roes, 2000; Rickert et al., 1997).

To evaluate the efficiency of *Smad7* deletion in the CD19Cre/*Smad7<sup>fllox</sup>* mice, we analyzed the gene transcript of *Smad7* in B and T cells by real time PCR. Compared to the WT control, transcript of *Smad7* in B cells from CD19Cre/*Smad7<sup>fllox</sup>* mice was 20-fold decreased, whereas its expression level remained unchanged in a control T cell population (Fig.24).

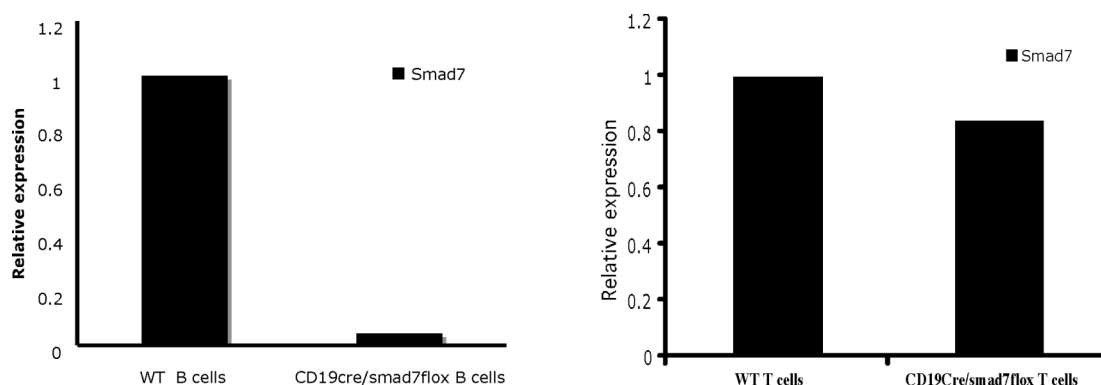


### Fig. 24 Identification of specific deletion in the B cells of CD19Cre/*Smad7<sup>fllox</sup>* (*Smad7-B*) mice

Total RNA was isolated from the B cells of WT and CD19Cre/*Smad7<sup>fllox</sup>* mice. Using these RNAs as templates, cDNA was synthesized according to the Invitrogen protocol and real time PCR was performed with the *Smad7* specific primers from Qiagen.

### 3.9.3 B cell homeostasis in the BM and Spleen of CD19Cre *Smad7<sup>FL/FL</sup>* mice

Former data demonstrate that TGF- $\beta$  inhibits proliferation of B lymphocyte progenitors and also induces apoptosis in B lymphocyte progenitors, immature B cells and resting B cells (Lomo et al., 1995) (Kee et al., 2001). However, the inactivation of TGF- $\beta$ -inhibitor Smad7 did not affect B cell development in the bone marrow, as indicated by normal frequencies of pre-B, immature B, and mature B cells (Fig. 25A). Also, normal proportion of immature, mature, FO and MZ B cells in the spleen indicated efficient B cell generation and establishment of the peripheral B cell pool (Fig. 25B).

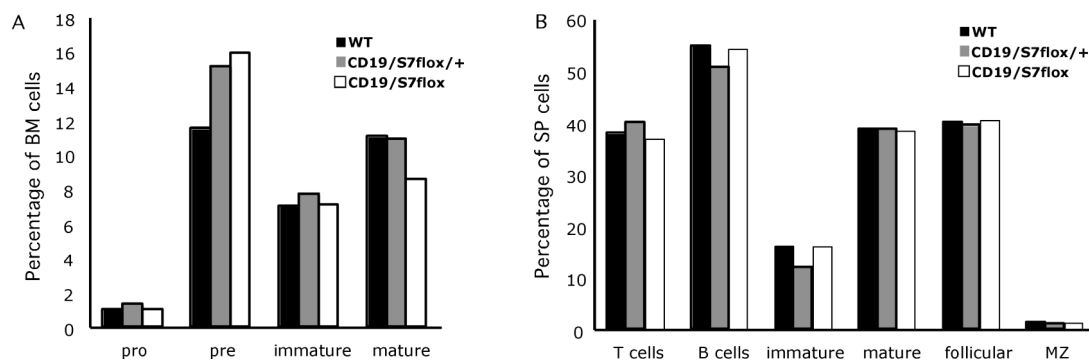


**Fig. 25 B cell homeostasis in the BM and Spleen of CD19Cre *Smad7<sup>FL/FL</sup>* mice**

(A) Percentage of B cells of indicated developmental stages in the bone marrow of CD19Cre/*Smad7<sup>flx</sup>* mice  
 (B) Percentage of indicated subsets of lymphocytes in the spleen of CD19Cre/*Smad7<sup>flx</sup>* mice

In the PC, we detected a 2-fold decrease of B-2 B cells in the *Smad7* mutant mice compared to controls, which is shown by the cell proportions (Fig.26A and B). Nevertheless, we did not observed any decrease of B cell population in the spleen and LN.

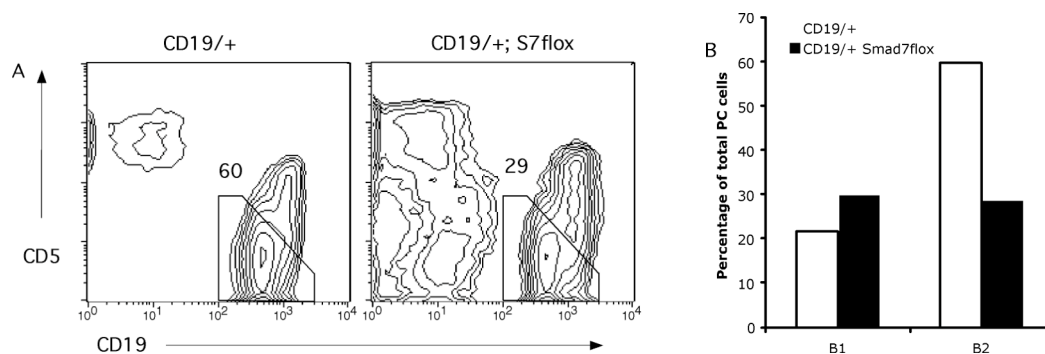


**Fig. 26 FACS analysis of B cell populations in the PC**

(A) Lymphocytes were prepared from peritoneal cavity of the indicated mice. Cells were gated on CD19<sup>+</sup> cells and stained with CD5. CD19<sup>+</sup>CD5<sup>+</sup> cells indicate the B1 B cells. The numbers in the quadrants refer to the percentages of the specific cell population, gated on live lymphocytes.

(B) Bar graph shows the percentage of B-1 and B-2 B cells in the total PC cells.

To assess whether this decrease is attributed to defective survival of the B cells in the Smad7 mutant mice, we cultured B cells from Smad7 deficient or control mice in the presence or absence of TGF- $\beta$  for three days and monitored the viable cell percentage by 7AAD staining. Consistent with the decrease of PC B-2 cells, the Smad7 deficient B cells died much faster compared to control cells when treated with or without TGF- $\beta$  (Fig.27). These *in vitro* data suggested that the decrease of B-2 B cell populations in the Smad7 deficient B cells results from the increased B cell apoptosis.

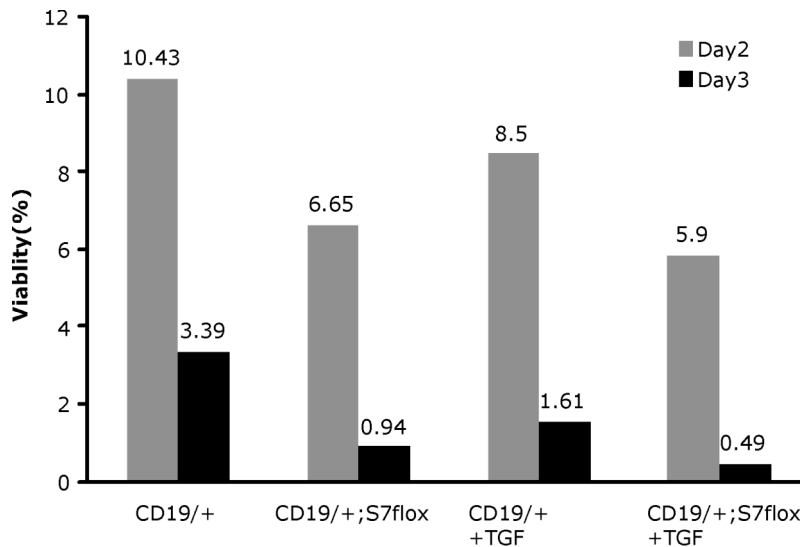


**Fig. 27 Viabilities of peripheral B cells *in vitro* and BAFFR surface level of BCR/ Ig $\alpha$ /Ig $\beta$  mutant**

Mature B cells were cultured in the absence or presence of TGF- $\beta$  (10ng/ml) for 3 days. Viable cells were determined by 7AAD staining. Bars indicate the live cells proportion.

### 3.9.4 *Smad7* mediates TGF- $\beta$ -controlled class switch

TGF-beta signaling is known to direct the class switch toward IgA (Klein et al., 2006). B cell specific Smad7-deficient mice exhibit a clear enhancement in IgA production in the total serum level, consistent with the previously published data. On the other hand, the titer level of serum IgG1 was reduced in the Smad7 mutant mice (Fig. 28).

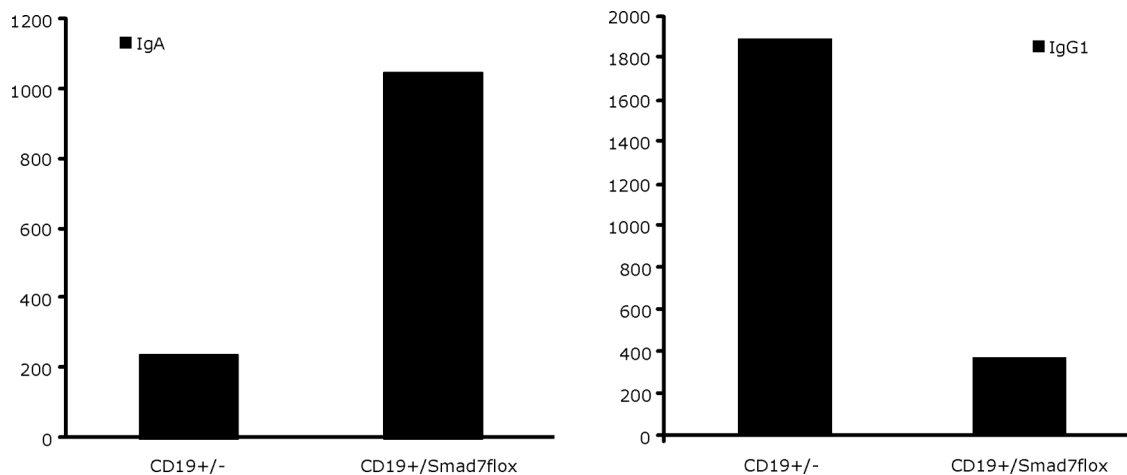


**Fig. 28 Serum IgA level in the CD19Cre/Smad7<sup>fllox</sup> mice**

Serum IgA (A) and IgG1 (B) level were evaluated with ELISA. Bar graph shows the titers of serum Ig from indicated mice.

To investigate whether the enhanced serum IgA of Smad7 deficient mice results from an increase in IgA class switch, we dissected B cell population in the Peyer's patches (PP). PP is one of the gut-associated lymphoid tissues. The activated or switched status of B cells in this compartment is reflected in the numbers of B cells engaged in germinal center reactions, as indicated by their positive staining for peanut agglutinin. Increased numbers of germinal center B cells were observed in CD19Cre/Smad7<sup>fllox</sup> mice compared to WT mice (Fig.29). Accordingly, we detected a 3-fold increase of IgA<sup>+</sup> B cells in the PP of Smad7 mutant mice compared to controls (Fig.29). Since majority of the switched B cells are located in the germinal center, the increase of IgA cells may account for the enlargement of the germinal center in the Smad7 mutant mice. In addition, a reduced population of IgG1<sup>+</sup> B cells was observed in the mutant mice (Fig.29), which is consistent with the decreased titer of total serum IgG1 (Fig.29). These results indicate that the enhanced serum IgA and reduced serum IgG1 in Smad7 mutant mice results from the increase in class switch to IgA and the decrease in class switch to IgG1.

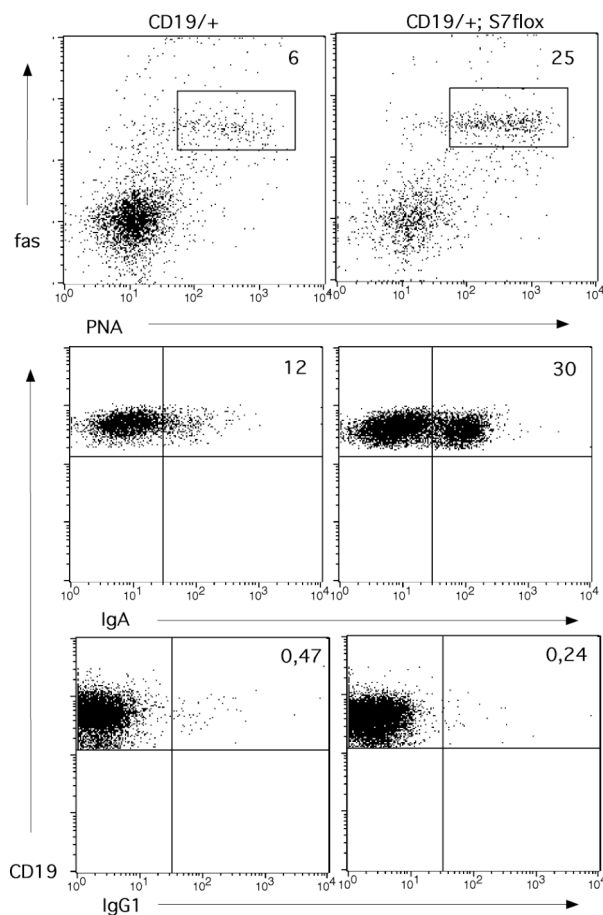


**Fig. 29 FACS analysis of Peyer's patch lymphocytes of control and Smad7 deficient mice**

(A) Fas and PNA staining of Peyer's patch leukocytes.

(B) CD19 and IgA staining identifies IgA<sup>+</sup> B cells in the Peyer's patch.

(C) CD19 and IgG1 staining identifies IgG1<sup>+</sup> B cells in the Peyer's patch.

To assess whether the class switch of increased IgA and decreased IgG1 was due to the altered B cell response to TGF- $\beta$  in the Smad7 mutant mice, we determined IgA expression at the cellular level by inducing class switch *in vitro*. In LPS/TGF- $\beta$  cultures, the frequency of IgA<sup>+</sup> Smad7 mutant B cells increased to 7.2%, whereas IgA class switching in the control B cell cultures increased to 5.5% (Fig.30A). On the other hand, in either LPS/IL4 or LPS/IL4/TGF- $\beta$  cultures, Smad7 mutant B cells exhibited a two-fold reduction in IgG1-directed class switch compared to controls (Fig.30B). This *in vitro* class switch implied that the altered titers of serum antibodies in Smad7- deficient mice result from derangement of TFG-beta signaling in B cells.

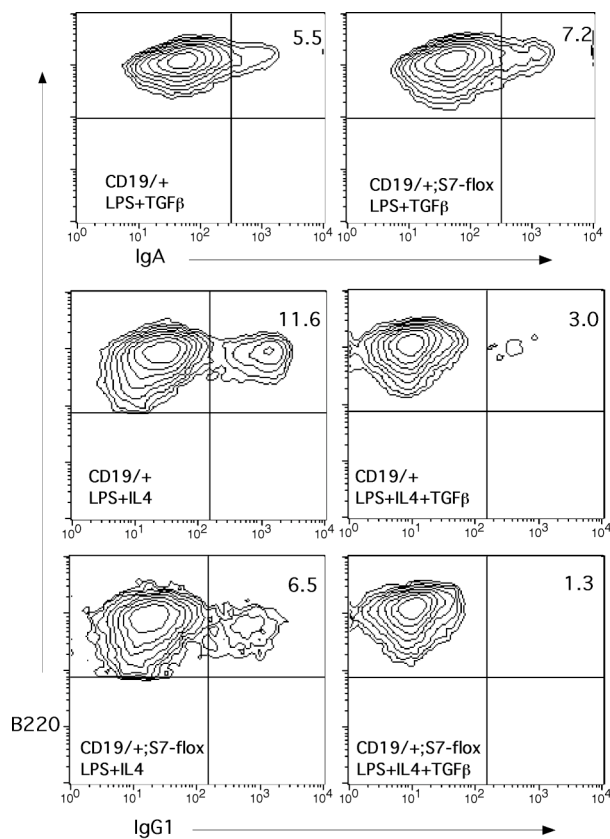


**Fig. 30. IgA class switching in splenic B cell cultures**

CD43-depleted spleen cells from control and Smad7 mutant mice were cultured as indicated for 4 days. Shown is the percentage of IgA<sup>+</sup> (A) or IgG1<sup>+</sup> (B) cells.



### 3.10 Targeting NIK gene by BAC strategy

In the non-canonical NF- $\kappa$ B pathway, stimulation of receptors belonging to the TNFR super-family leads to the recruitment of TRAF proteins like TRAF2, TRAF3 and TRAF6 which activates the protein kinase *NIK* through a currently unknown mechanism. *NIK* then selectively phosphorylates and activates the IKK $\alpha$  catalytic subunit. This pathway is important for secondary lymphoid organogenesis, maturation of B cells, adaptive humoral immunity and optimal promotion of cell survival (Zarnegar *et al.*, 2004).

Although abnormalities in both lymphoid tissue development and antibody responses were shown in both aly mice and *NIK*<sup>-/-</sup> mice (Garceau *et al.*, 2000; Yin *et al.*, 2001), the importance of *NIK* are not clear in the specific cellular lineage and development stage. To identify the physiological functions of *NIK*, we conditionally targeted the *NIK* locus. Interaction of *NIK* in different cell lineages can then be studied by crossing the *NIK**fllox* mice with specific Cre mice.

#### 3.10.1 Gene targeting of *NIK*

The *NIK* gene consists of 14 exons. Exon 2 harbors an ATP binding site. Upon Cre-mediated recombination, excision of exon2 should result in an out-of-frame transcript of *NIK*. Therefore, we decided to flank exon2 with *loxP* sites in order to ablate the gene transcript of *NIK*. Standard gene targeting techniques were employed to generate *NIK*<sup>FL/FL</sup> mice using the strategy shown in Fig.31. To insert the *loxP* sites flanking exon2, the conventional targeting vector was generated by inserting the short arm of homology (SA), exon2 (FA), and the long arm of homology (LA) into the pRAPIDflirt vector (A. Bruehl and A. Waisman; unpublished data). The pRAPIDflirt vector already contained the *loxP* sites, the FRT flanked neomycin resistance gene and the *thymidine kinase (TK)* gene from *Herpes simplex* as a negative selection marker.

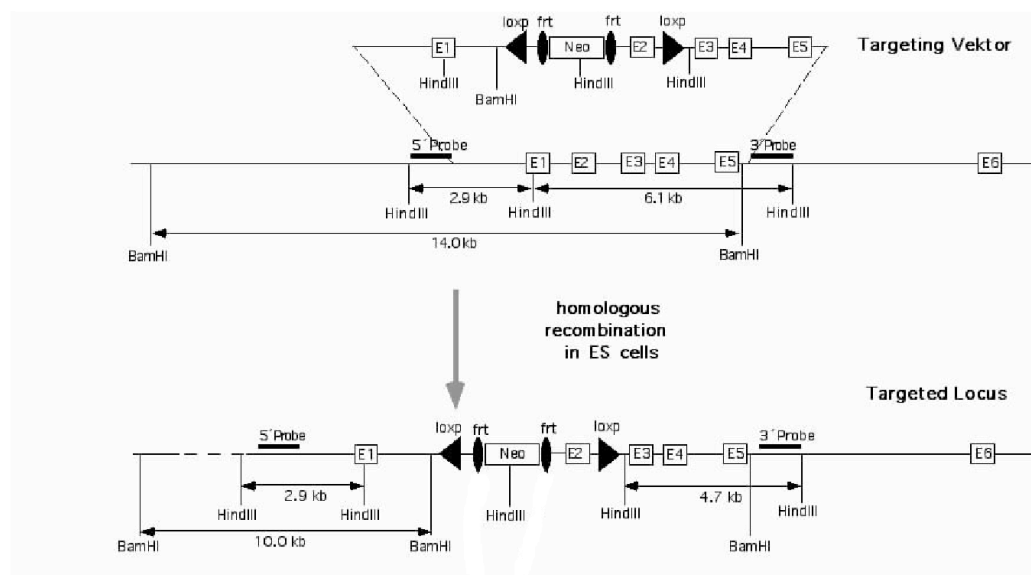


**Fig. 31 Schematic representation of the NIK targeting strategy**

The structure of the NIK gene from exon 1 to exon 6 is shown on top row. Homologous recombination into the NIK gene resulted in the  $neo^f$  containing genotype (NIK<sup>neo</sup>) (Kindly provided by Max v. Hollen). The following step will be Flp- and Cre- mediated gene recombination (see methods). The closed triangles represent *loxP* sites, the closed ovals *FRT* sites. Arrows indicate transcriptional orientations of genes.

This project was done by Max von Holleben. The efficiency of targeting ES cells was very low and the injection of positive clones has so far failed to give rise to chimeric mice. Therefore, we decided to use BAC strategy. BAC targeting works very efficiently because it can provide long homologous recombination arms and avoid mutation derived from unfaithful PCR amplification (Fig.32). In order to modify the BAC, we adopted a novel cassette, in which the kanamycin/neomycin resistance cassette and the neo resistance gene are under the control of a prokaryotic and a eukaryotic promoter, respectively. After insertion of neo cassette into pGEM-T-easy vector by TA cloning, the short arm with one loxP site was amplified from former target vector and inserted with Aat II and Sac I. Finally, the construct was finished by cloning the Exon2 with the other loxP site into Asc I cutting sites. Using this construct as template, we amplified a PCR product including all the inserts from this construct and co-transfected it with the pRed/ET into *NIK*BAC (Fig.32).

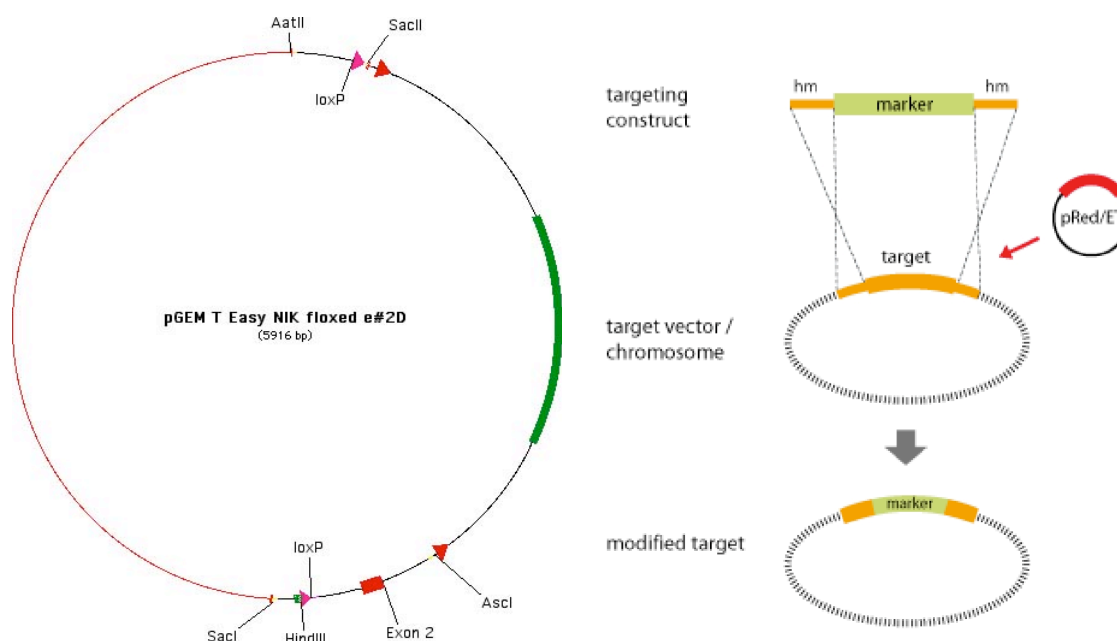


**Fig. 32 Targeting of the Neo-flox Construct into the NIK BAC**

(A) The short arm with one loxP site, the neo cassette and exon2 loxP region were cloned into pGEM-T-easy vector.

(B) The PCR product including neo and loxP sites was recombined into the NIK locus on the BAC by Red/ET cloning. The procedure is described in the methods.

### 3.10.2 Generation of the Modified NIKBAC

To ensure the homology arms and loxP region are free of mutations, they were sequenced by use of the primers for the 5' end and for the 3' end of the exon2. Since the Neo-flox cassette was PCR amplified, it was also sequenced. No mutations were detected.

The PCR product was introduced into *E. coli* cells carrying the NIK BAC and the Red/ET recombination plasmid pSC101-BAD-gbaA-tetra. Expression of the recombinases was induced by administration of L-Arabinose on 37°C. Recombination between the PCR product and the NIK gene on the BAC results in a BAC with a modified NIK gene, as shown in Fig. 33. *E. coli* cells were screened for the recombination event by selection with chloramphenicol to screen for the presence of the BAC and kanamycin to screen for the integration of the PCR product.

Surviving colonies had to be further characterized for proper integration of the *Neo-loxP* construct in the NIK locus. A Southern blot strategy was designed to screen the *HindIII* digested targeted BAC DNA. BAC DNA was prepared and digested with *HindIII* and after Southern blotting screened with the 5' probe SA and the 3' probe LA (Fig.33). We expected a wild-type band of 14 kb and a targeted band of 10 kb with the 5' probe, a wild-type band of 6,1 kb and a targeted band of 4,7 kb with the 3' probe (see also Figure 31).

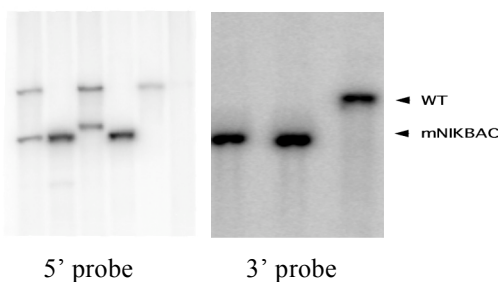


**Fig.33 Analysis of the Targeted NIK BAC with Southern Blot**

*Hind*III digested DNA was transferred onto a nylon membrane and screened with the  $^{32}$ P-radiolabeled 5' probe and 3' probe and evaluated by phosphoimaging. Digested DNA of a wild type NIK BAC was run as a control (upper bands). Arrows indicate modified BAC Clones.

### 3.10.3 Generation of the ES Cell Line NIK<sup>lox</sup>

200 ml of modified BAC were grown overnight and DNA was prepared as described in *methods*. Roughly 100  $\mu$ g of linear DNA were used per transfection. The DNA was linearized with the endonuclease *PI-Sce*I, an enzyme that cuts in the BAC backbone. The transfected cells were plated on ten gelatinized feeder covered 10 cm plates. ES cells were screened for *Neo* integration by positive selection with G418. 40 surviving colonies were picked. Screening for homologous recombinants was performed with Southern blot after *Hind*III digest of the ES cell derived genomic DNA (Fig.34).

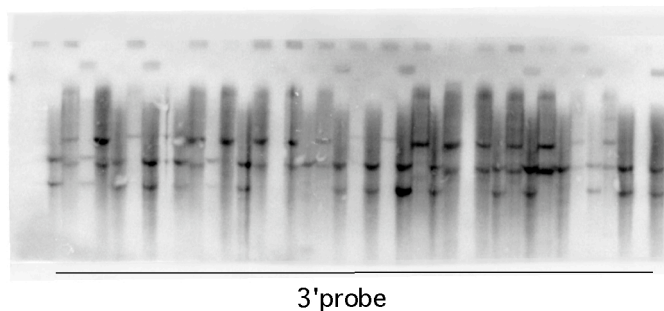


**Fig. 34 Analysis of the Targeted NIK ES cell clones with Southern Blot**

Southern blot analysis of *Hind*III digested ES cell DNA using the  $^{32}$ P-radiolabeled 3' probe to screen homologous recombinants.

It is difficult to screen for homologous recombinants by Southern blot since designing external probes is impossible due to the size of the BAC. Therefore we had to optimize and quantify the signal of the targeted and the wt band. The homologous recombinants should have equal density of these two bands (Fig.34).

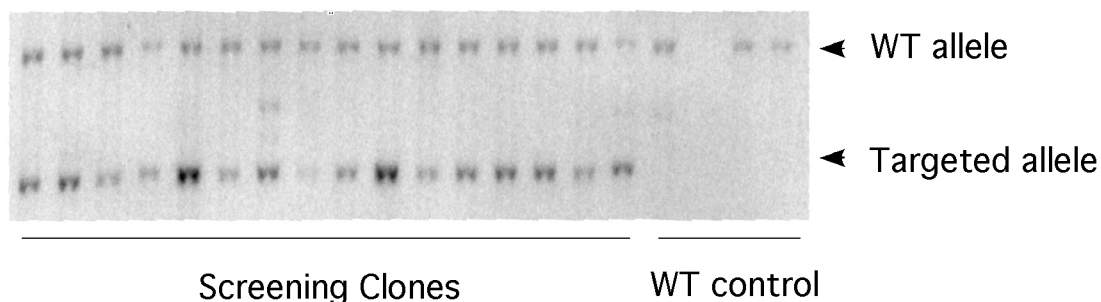


**Fig. 34 Reanalysis and quantification of the targeted NIK ES cell clones with Southern Blot**

Genomic DNA from confluent wells (96 well plate) of cells was digested with *HindIII*. In order to confirm homologous recombinants we performed southern blot analysis using 3' probe to quantify the intensity of WT band and targeted band, in which DNA from WT clones were loaded as control,

Random integration normally leads to insertion of the backbone into random locus. To exclude the double random integration that could also give rise to equal intensity of southern blot bands, a PCR strategy was designed to detect the backbone in which the DNA from promising clones was used as templates (Fig.35). Such a concept was used to adopt TK or DTA as negative selection gene in the traditional strategy (Yu et al., 2000). Two pairs of PCR primers were optimized by using obvious random integration as positive control. Each of them locates on the end of backbone of BAC.

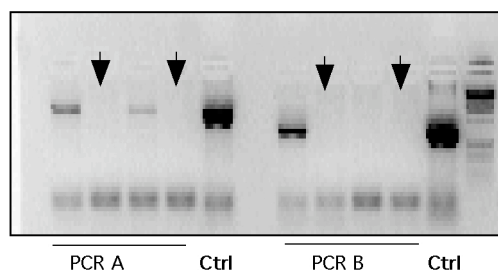


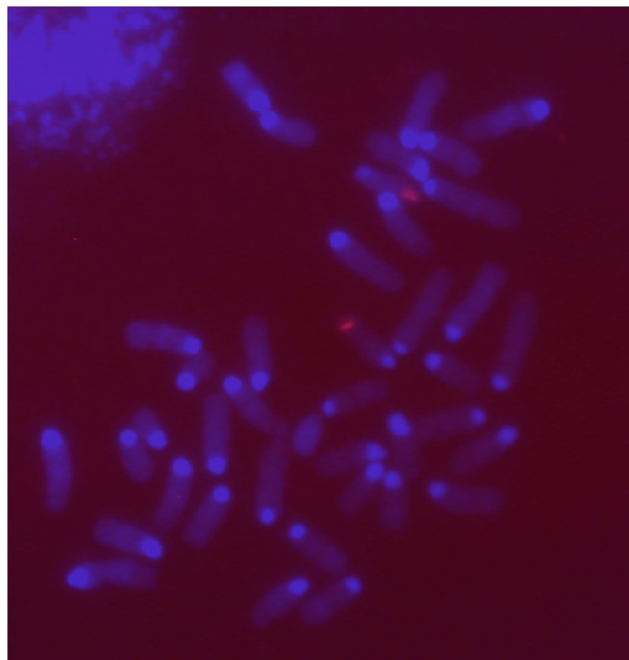
**Fig. 35 BAC backbone PCR to detect random integration**

DNA from promising candidates of southern blot analysis was used as templates. PCR was done with two pairs of primers that located on the both end of the BAC backbone. Arrows indicate the homologous recombination clones.

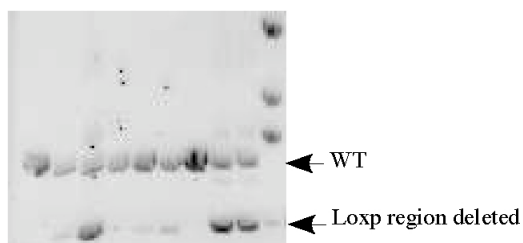
The procedure from injection to homozygous mice is time-consuming. Thus FISH (Fluorescence in situ hybrid) was performed to confirm the copies of NIK gene inside the clone with equal density of WT and targeted band in the quantitative Southern blot and negative in the PCR for detecting random integration. As shown in Fig.36 only two copies of NIK gene were observed which located in the end of chromosome11. The result ensured that the quantitative southern blot and the PCR detecting random integration was efficient tool to select homologous recombination clones.

**Fig. 36 FISH analysis of copies of *NIK***

FISH was performed to identify the copies, location of the allele of interest and the number of chromosomes. Red points indicate binding of the *NIK*-specific probe.



To evaluate the function of *loxP* induced deletion, *in vitro* deletion of the *loxP* flanked exon 2 and the *neomycin resistance* gene by Cre-mediated recombination were performed on the recombinant clones (Fig.37). Cre activity was achieved by transducing with various amounts of a soluble and cell permeable Cre (Peitz et al., 2002).

**Fig. 37 In vitro Cre induced gene recombination**

Homologous recombinant clones were treated with indicated concentrations of a cell permeable Cre (HTNC). PCR was performed with the primers binding outside of the *loxP* region.

## 4 DISCUSSION

### 4.1 IgG1 B cell receptors play distinct roles when in combination with Ig $\alpha$ /Ig $\beta$ mutation

IgG1 ( $\gamma$ 1), known as a surface marker of memory B cells, is characterized by a conserved cytoplasmic tail that is lacking in IgM ( $\mu$ ) and IgD ( $\delta$ ) chains (Geisberger et al., 2003; Neuberger et al., 1989; Reth, 1994). To investigate the physiological role of this cytoplasmic tail, a novel mouse strain (IgG1i) was established in which C $\gamma$ 1 replaces all the other C<sub>H</sub> gene segments. IgG1i mice exclusively express membrane-bound IgG1 in the B lineage. Two major advantages exist in this mouse model compared to previous systems. Firstly, the known limitations involved in using transgenic expression of B cell receptors, namely uncontrolled copy number and position-dependent variations of expression, can be circumvented. Secondly, IgH expression is controlled by the very same V<sub>H</sub> promoters which are used in normal B cell development. In these mice, we observed that B cells of all subsets are generated and the overall size of the peripheral B cell compartment is similar to the one for WT mice. However, B cell development in the BM of IgG1i mice is clearly compromised, with a partial developmental block at the pro- to pre-B cell transition.

Furthermore, it is known that signal transduction through  $\mu$  and  $\delta$  chains relies entirely on the cytoplasmic tails of the BCR-associated Ig $\alpha$ / $\beta$  heterodimer. It was of interest to investigate whether signal-transduction through  $\gamma$ 1 is also Ig $\alpha$ / $\beta$ -dependent. Thus, we generated the Ig $\alpha_{\Delta c}$ IgG1i mice, which carry the IgG1 BCR in combination with Ig $\alpha$  truncation and the Ig $\beta_{\Delta c}$ IgG1i mice, which carry the IgG1 BCR in combination with Ig $\beta$  truncation. Similar to previous reports from Ig $\alpha$  or Ig $\beta$  truncated BCR, the transition from immature to mature B cells is strikingly reduced in both Ig $\alpha_{\Delta c}$ IgG1i and Ig $\beta_{\Delta c}$ IgG1i mice, with most immature B cells undergoing apoptotic cell death. However, signaling through  $\gamma$ 1 affects the peripheral B cell compartment distinctly when combining Ig $\beta$  truncation or Ig $\alpha$  truncation. B cell numbers in Ig $\alpha_{\Delta c}$ IgG1i mice is over ten times the number in Ig $\alpha_{\Delta c}$  mice. In contrast, Ig $\beta_{\Delta c}$ IgG1i mice did not increase the number of B cells when compared with Ig $\beta_{\Delta c}$  mice. There are two possibilities that account for the increased number of B cells in the Ig $\alpha_{\Delta c}$ IgG1i mice. One is that the combination of IgG1 with Ig $\beta$  truncation ablates the B cell development more severely than with Ig $\alpha$  truncation, which could reduce of the number of progenitors that migrate from the BM to differentiate into mature B cells in the spleen. The other possibility could be that a signal through IgG1-linked Ig $\alpha$  (Ig $\beta_{\Delta c}$ IgG1i) is less capable of

supporting peripheral B cell survival or proliferation compared to the signal through Ig $\beta$  (Ig $\alpha_{\Delta c}$ IgG1i).

Compared to the BM B cell development of non-IgG1 expression mice (WT, Ig $\alpha_{\Delta c}$  and Ig $\beta_{\Delta c}$ ), we observed an accumulated pro-B cell population and a reduced pre-B cell population in the IgG1 expressing mice (IgG1i, Ig $\alpha_{\Delta c}$ IgG1i and Ig $\beta_{\Delta c}$ IgG1i). This indicates that  $\gamma 1$  expression results in an impaired transition from pro- to pre-B cells. In pre-BCR-deficient mice, B cell development is largely blocked at the pro- to pre- B cell transition, during which the cells go through a pre-BCR dependent phase of rapid proliferation (Martensson et al., 2002). This reveals that pre-BCR plays a crucial role at the transition from pro- to pre- B cells in development. Although a developmental block was observed at the same stage of the IgG1i mice, it is clearly much milder than pre-BCR-deficient mice in that many more pre-B cells were detected. We therefore speculate that a  $\gamma 1$  chain-containing pre-BCR-like molecular complex is assembled in the IgG1i mice but it is functionally compromised. On the other hand, immature B cell numbers from IgG1 and non-IgG1 expressing mice are comparable. Ig $\alpha_{\Delta c}$ IgG1i mice contained a similar amount of immature B cells to Ig $\alpha_{\Delta c}$ , which disproved the possibility that the increased number of B cells in Ig $\alpha_{\Delta c}$ IgG1i mice stems from its advantage in BM B cell development. Nonetheless, considering the developmental impairment in the pre-B stage of IgG1 expressing mice, their WT-comparable immature B cell population suggested that rather than pre-BCR, BCR are more compatible with the signals through IgG1.

In line with the decreased number of pre-B cells, the IgG1 expressing cells compete poorly in development with their WT counterparts in heterozygous IgG1i and IgG1iIg $\beta_{\Delta c}$  mice. This effect is more dramatic at the level of immature B cells in the BM than that of mature splenic B cells. On the other hand, in consistent with the increased number of B cells in the Ig $\alpha_{\Delta c}$ IgG1i compared to Ig $\alpha_{\Delta c}$  mice, the dominant population of IgG1<sup>+</sup> cells were detected in the Ig $\alpha_{\Delta c}$ :IgG1i/WT heterozygous mice. However, this advantage of IgG1 expression did not exist in immature B cells in the BM. These data further support that the survival or proliferation factors in the periphery other than BM development account for the increased peripheral B cells in the Ig $\alpha_{\Delta c}$ IgG1i mice compared to Ig $\alpha_{\Delta c}$  mice.

#### 4.1.1 $\gamma 1$ signals support the B cells survival

The survival of mature resting B cells in the periphery depends on signaling from the B-cell receptor (BCR) and the B-cell activating factor of the TNF family receptor (BAFF-R) (Mecklenbrauker et al., 2004; Schneider and Tschopp, 2003). Our *in vitro* data show that all



of Ig $\alpha$  and Ig $\beta$  mutant B cells except for the Ig $\alpha_{Ac}$ IgG1i B cells survive less adequately compared to WT and IgG1i B cells. However, when those B cells were cultured with medium with supplementary BAFF, Ig $\alpha$  or Ig $\beta$  mutant B cells, including Ig $\alpha_{Ac}$ IgG1i B cells, survive much less compared to WT B cells, indicating those cells hardly react to BAFF. Furthermore, The decreased expression level of BAFFR is associated with the reduced BAFF response in the Ig $\alpha$  and Ig $\beta$  mutant B cells. This down-regulation of BAFF-R could explain the impaired survival capacity in those B cells, which was previously reported in the mouse model lack of the RhoGTPases Rac1 and Rac2 (Walmsley et al., 2003).

Although signals through either the BCR or BAFF-R are individually capable of promoting B-cell survival, the simultaneous stimulation of both pathways has a synergistic effect on proliferation and maintenance (Rolink et al., 2002). This is evidenced by a previous study showing that BAFF-R expression is up-regulated in response to IgM stimulation in mature B cells (Patke et al., 2004). One mechanism to account for this could be the sequential induction of one pathway by the other in a positive feedback loop. As BAFF-R expression is induced by BCR signaling, it is conceivable that disruption of BCR would impair BAFF-R expression. Thus, the insufficient expression of BAFF receptor could be a consequence of the mutation of Ig $\alpha$  or Ig $\beta$  and subsequently results in the inability of B cells to respond to BAFF survival signals.

The anti-apoptotic Bcl-2 family proteins Bcl-2 and Bcl-X<sub>L</sub> play important roles in inhibiting mitochondria-dependent extrinsic and intrinsic cell death pathways. In our data, consistent with the increased cell death, Bcl-X<sub>L</sub> expression is down-regulated in both Ig $\alpha$  or Ig $\beta$  truncated B cells compared to WT B cells. It was observed that NF- $\kappa$ B activation and expression of Bcl-X<sub>L</sub> were severely blocked in both PIK3 and Btk deficient mice. Transgenic expression of Bcl-X<sub>L</sub> restored the B cell compartment in the PIK3 deficient mice (Suzuki et al., 2003). Therefore, the truncation of Ig $\alpha$  or Ig $\beta$  might impair the signal through PIK3 and Btk, thereby leading to down-regulated Bcl-X<sub>L</sub> expression. On the other hand, whereas Bcl-2 expression is dramatically down regulated in the Ig $\beta$ -truncated B cells, Ig $\alpha$ -truncated B cells exhibit a similar level of Bcl-2 expression compared to WT B cells. The difference in the Bcl-2 expression level between Ig $\alpha$  and Ig $\beta$  truncated B cells shows that the signal through Ig $\beta$  rather than Ig $\alpha$  is essential for the expression of Bcl-2. Also, these data addressed that the distinct signals regulate Bcl-2 and Bcl-X<sub>L</sub> in the inhibition of cell death, which was observed in a previous study showing that Bcr-Abl induced a dramatic down-regulation of Bcl-2 and increased the levels of Bcl-X<sub>L</sub> in HL-60 cells (Amarante-Mendes et al., 1998).

#### 4.1.2 $\gamma 1$ signals in the BCR signaling

Compared to WT B cells, BCR expression levels on Ig $\alpha$  or Ig $\beta$  truncated B cells are enhanced while IgG1i B cells exhibit a decreased expression. An enhanced BCR level was reported to be attributable to a decrease in the BCR internalization (Gazumyan et al., 2006). In line with the increased BCR levels, either Ig $\alpha_{\Delta c}$  or Ig $\beta_{\Delta c}$  BCR internalized slower than WT BCR. Nonetheless, both Ig $\alpha_{\Delta c}$ IgG1i and Ig $\beta_{\Delta c}$ IgG1i BCR showed a similar kinetic of internalization when compared to IgG1i BCR, which was in contrast to their enhanced surface levels. Therefore, other than altered BCR internalization, there might be some reasons remaining for the down-regulated surface levels of BCR in Ig $\alpha_{\Delta c}$ IgG1i or Ig $\beta_{\Delta c}$ IgG1i B cells.

Experiments with inhibitors of tyrosine kinases and phosphatases have implicated ligand-induced tyrosine phosphorylation in regulating BCR internalization (Pure and Tardelli, 1992; Salamero et al., 1995). On the other hand, blocking BCR endocytosis with pharmacologic agents or by deletion of the clathrin heavy chain in chicken B cell lines leads to enhanced signaling, suggesting that receptor internalization is an important mechanism for attenuating BCR signaling (Brown and Song, 2001; Stoddart et al., 2005). Supporting the interaction between BCR internalization and the subsequent dynamic changes of phosphorylation, our data showed that BCR induced general tyrosine phosphorylation disappeared faster in the IgG1 expressing B cells than in the WT B cells, which is consistent with the fast ligand-mediated internalization of BCR on these cells. Paralleled with general phosphorylation, phosphorylation of PLC $\gamma 2$  faded away more rapidly in the IgG1i and Ig $\alpha_{\Delta c}$ IgG1i B cells compared to WT B cells. As PLC $\gamma 2$  is the molecule responsible for the activation of BCR mediated calcium mobilization (Alberola-Ila et al., 1997), we have observed the shortened process of calcium flux in those IgG1 cells. Due to the small number of B cells, we do not have the data of PLC $\gamma 2$  phosphorylation of Ig $\beta_{\Delta c}$ IgG1i B cells. Thus it is hard to explain the prolonged calcium flux in Ig $\beta_{\Delta c}$ IgG1i cells while BCR internalization in these cells was as fast as in IgG1i B cells. However, it is clear that one of the calcium release pathways is ablated in the BCR signaling mediated by IgG1 in absence of Ig $\beta$ .

Calcium influx can regulate a large number of downstream molecules including transcription factors such as NF- $\kappa$ B and NFAT in lymphocytes (Antony et al., 2003). However, while the magnitude of the calcium response controls NF- $\kappa$ B activity, it is the duration of elevated Calcium influx that influences NF-AT activation (Dolmetsch et al., 1997). Since the dynamic changes of calcium in Ig $\alpha_{\Delta c}$ IgG1i and Ig $\beta_{\Delta c}$ IgG1i B cells is time-dependent, it would be interesting to analyze the signaling of NFAT pathway in the future.

PLC $\gamma 2$  activity and the subsequent generation of IP3 and DAG potentially influence the

MAP Kinase and NF- $\kappa$ B pathway, which determine the signals of B cell proliferation and survival, respectively (Patterson et al., 2005). We have observed a distinct role of PLC $\gamma$ 2 in the promotion of MAP Kinase and NF- $\kappa$ B pathways. Whereas Ig $\alpha_{\Delta c}$ IgG1i B cells share a similar kinetic of ERK phosphorylation with IgG1i B cells, a weaker I $\kappa$ B $\alpha$  phosphorylation was detected in the Ig $\alpha_{\Delta c}$ IgG1i B cells compared to IgG1i B cells. This result suggests that Ig $\alpha$  is critical for the signal transduction of IgG1 BCR by regulating PLC $\gamma$ 2 phosphorylation and subsequently the activation of NF- $\kappa$ B pathway, which could account for the altered expression of basal Bcl-X $_L$ . However, MAP Kinase ERK is not directly influenced by IgG1 BCR mediated PLC $\gamma$ 2 phosphorylation. This might explain that no apparent ablation was observed in the proliferation of the Ig $\alpha_{\Delta c}$ IgG1i B cells.

Lyn, one of the Src-family kinases, was assigned a role in signal initiation from BCR (Gauld and Cambier, 2004). Interestingly, phosphorylation of Lyn shows distinct kinetics in the WT and IgG1 B cells in which Lyn was phosphorylated more slowly in the IgG1 B cells than in the WT B cells. Hence, it is reasonable to conceive that unlike WT BCR, activation of IgG1 BCR induced a sustained phosphorylation of Lyn, which subsequently regulated the downstream signal transduction such as PLC $\gamma$ 2, which exhibited a quickly diminished phosphorylation. This correlated with the notion that Lyn can also play an essential role in negative regulation of signaling through its unique ability to phosphorylate ITIMs in inhibitory cell surface receptors (Xu et al., 2005).

#### **4.1.3 $\gamma$ 1 in combination with mutation of both Ig $\alpha$ and Ig $\beta$**

Similar to the previous report of Ig $\alpha_{\Delta c}$ Ig $\beta_{\Delta c}$  mice, our data showed no detectable B cells in the Ig $\alpha_{\Delta c}$ Ig $\beta_{\Delta c}$ IgG1i mice, neither in the spleen nor in the peritoneal cavity. We could not detect immature B cells in the periphery of those mice either. By different BM staining, we were able to explain the complete lack of B cells in those mice since B cell development is completely blocked before pre-BII stage. This is identical with the published data of mice with a double truncation of Ig $\alpha$  and Ig $\beta$ , in which only pro-B cells are detectable (Reichlin et al., 2001). B cell development cannot proceed beyond the pre-BI stage in the absence of the cytoplasmic domains of both Ig $\alpha$  and Ig $\beta$ . Our data suggested that signaling through IgG1 only contributes to the peripheral B cells and IgG1, instead of IgM, is less efficient in the BM B cell development.

## **4.2 Signals of Smad7 in the B cells immunity**

TGF- $\beta$  is a central regulator of immune system. It maintains tolerance via the regulation

of lymphocyte proliferation, differentiation, and survival (Li et al., 2006a). *In vitro* studies showed that Smad7 is induced by the TGF- $\beta$  superfamily members and negatively modulates TGF- $\beta$  signaling, thus acting in a negative, autocrine feedback manner (Yoshimura et al., 2003). To clarify the biological role of Smad7 in lymphocytes *in vivo*, we have generated a B cell-specific Smad7-deficient mouse line (CD19Cre/Smad7flox) and have demonstrated the efficient and B cell-specific deletion of Smad7 in CD19Cre/Smad7flox mice. Loss of Smad7 was also shown in the Smad7 <sup>$\Delta$ ex1</sup> mice, in which the Smad7 gene was inactivated by replacing exon I of Smad7 with the *neo* resistance cassette (Li et al., 2006b). However, the remaining Smad7 5-leader sequence and the inserted *neo* cassette results in expression of three spliced variants that do not exist in wild type mice. The function of the proteins derived from these spliced variants remains unclear. Hence, it is hard to determine whether the phenotypes of this mouse strain result from deficiency of Smad7 or expression of the spliced variants. In our mouse model, the *neo* cassette was deleted by FRT-induced deletion and the *loxP*-flanked region is based on the whole Smad7 promoter and first exon. Therefore there should be no *neo* cassette and spliced variant left. Moreover, B cell-specific deficiency also avoids the effects of Smad7 deletion in other cell types that could mask the phenotype or complicate data interpretation.

Our analysis of CD19Cre/Smad7flox mice reveals several distinct roles of Smad7 in B cells. Smad7 was shown to be important for the induction of an IgA response. Also it regulates the maintenance of peripheral B cells, because there was a decreased number of B2-B cells in the peritoneal cavity (PC) and an increased population of germinal center B cells in the Peyer's patches (PP) of the Smad7 mutant mice.

TGF- $\beta$  is also a crucial factor for induction of IgA response. It has been shown that TGF- $\beta$  synergizes with other cytokines such as IL-5 or IL-2 for IgA class switch from murine LPS-stimulation B cells *in vitro*. Moreover, TGF- $\beta$  receptor type II deficient mice (T $\beta$ PII-B) had almost absent IgA levels in the serum, and IgA was not inducible by T cell-dependent Ags (Cazac and Roes, 2000). IgA production was also partially blocked in TGF- $\beta$ 1-deficient mice (van Ginkel et al., 1999). Because the intracellular TGF- $\beta$  signal is mainly inhibited by Smad7, an increase of IgA would also be expected in Smad7-deficient mice. Indeed, the Smad7 deficient mice showed a clear enhancement in IgA level of total serum. *Ex vivo*, we found a 3-fold increase of surface IgA<sup>+</sup> B cells in the PP of Smad7-deficient mice compared to controls. The increased surface IgA<sup>+</sup> B cells suggest that the enhanced serum IgA of Smad7 deficient mice results from an increase in class switch to IgA in response to TGF- $\beta$ . This was evidenced by the increased *in vitro* TGF- $\beta$ /LPS-induced IgA class switch in Smad7-

deficient B cells. Therefore, Smad7 has a clear role as an inhibitor in TGF- $\beta$  induced IgA class switch recombination, thereby leading to the regulation of serum IgA secretion. In addition, the increased surface IgA<sup>+</sup> B cells were detected in the PP but not in the spleen of Smad7 mutant mice. PP of the GALT are distinct compartments in which specialized epithelial M cells deliver antigen from the intestinal lumen, through transcytosis, into direct contact with lymphocytes and macrophages (Brandtzaeg and Johansen, 2005). Our finding reflects that TGF- $\beta$  plays a major role in the control of B cell responsiveness in GALT (Cazac and Roes, 2000).

TGF- $\beta$  directs an LPS-triggered B cell switch to IgA, but inhibits LPS/IL4-triggered IgG1 class switch. The increased *in vitro* IgA class switch is associated with decreased IgG1 class switch in the TGF- $\beta$  treated Smad7-deficient B cells compared to controls. *Ex vivo*, a reduced population of surface IgG1<sup>+</sup> B cells was also detected in the PP of Smad7-deficient mice compared to controls. This is in line with low IgG1 serum levels in the mutant mice. On the other hand, we observed an enlarged population of germinal center B cells in the PP of Smad7 mutant mice. The reduced population of IgG1<sup>+</sup> B cells in the PP of mutant mice indicates that this enlargement is not due to the inflammation condition of the individual mouse. Since surface IgA<sup>+</sup> and IgG1<sup>+</sup> B cells locate in the germinal center, the enlarged germinal center must be mainly attributed to the increased population of IgA<sup>+</sup> B cells in the PP of Smad7-deficient mice.

*In vitro* data demonstrate that TGF- $\beta$  inhibits proliferation of B lymphocyte progenitors and also induces apoptosis in B lymphocyte progenitors, immature B cells and resting B cells (Lomo et al., 1995) (Kee et al., 2001). Thus, a developmental impairment would be expected in the TGF- $\beta$  receptor or inhibitor (Smad7) deficient mice. In contrast, T $\beta$ PII-B mice exhibit a non-impaired B cell development in the BM and periphery except for increased IgA<sup>+</sup> B cells and B1-B cells in the GALT (Cazac and Roes, 2000). Consistent with the T $\beta$ PII-B mice, we did not detect any impairment of B cell development in the BM and spleen of Smad7-deficient mice. However, apart from PP B cells, a 2-fold decrease of B-2 B cells was noted in the PC of Smad7-deficient mice compared to control mice. Our analysis of *in vitro* B cell survival revealed that this decrease results from the increased TGF- $\beta$ -induced B cell apoptosis in the Smad7-deficient B cells. Thus, Smad7 is also critical for inhibiting the signaling of TGF- $\beta$ -induced apoptosis in B cells.

In summary, the B cell-specific Smad7 knock-out mouse generally exhibits an opposite phenotype as T $\beta$ PII-B mice. This indicates that Smad7 is a crucial downstream inhibitor in TGF- $\beta$  receptor signaling in B cells. In particular, Smad7 plays an important role in TGF-

$\beta$ -dependent regulation of IgA switching. Secretory IgA is known to be important for the prevention of microbial infection in the mucosa (Sun et al., 2004). Therefore, it is of interest to further investigate in the future how Smad7 functions during a B cell response to exogenous infection, especially the secretory manner of IgA and the disease process related to IgA level, by inducing inflammation in the mucosa of our mouse model.

### **4.3 BAC strategy for the gene targeting**

The NIK gene targeting project was started from Max von Holleben's work in which he used traditional targeting vector. But the efficiency of targeting ES cells was very low and the injection of positive clone fails to give rise to chimeric mice. Therefore, a BAC strategy was devised to enhance the targeting efficiency.

In our experiment, the transfection of ES cells with linearised BAC resulted in more than 80% of the picked clones screening positively using an internal probe southern blot. But it is hard to make an external probe strategy since the BAC is too long to find suitable cutting sites. Semi-quantitative southern blot was performed to resolve this issue. Because homologous recombination will give rise to one additional band with the same intensity as WT band, the method will determine homologous recombinants based on band intensity. The DNA from promising clones was used as a template for PCR that was designed to detect the backbone of BAC. The concept is based on the phenomenon that random integration normally leads to insertion of the backbone into a random location in the genome. The TK gene and DTA gene in the conventional targeting vector are based on the same principle (Yu et al., 2000). Finally, the result of FISH (fluorescence in situ hybridization) confirmed that the quantitative southern blot and the PCR detecting random integration were efficient in finding homologously recombined clones. In addition to these two methods, real time PCR is believed to be alternative approach that is able to detect the copies of the gene of interest. The design of primers for real time PCR should base on the target exon.

Comparing the BAC targeting strategy with conventional strategy, it becomes clear that neither one is free of disadvantages. The major advantage of the conventional targeting approach is that it is possible to screen for homologous recombination with standard techniques like Southern blotting. Disadvantages are the tedious cloning of the targeting vector and the possibility of very low targeting frequencies. On the other hand, the BAC Red/ET cloning strategy has several advantages. Once it is established in a lab, it is very fast. If the Southern blot strategy has been tested before, a targeting vector can be generated in less than three weeks. A second major advantage is that the targeting efficiency is very high, which reduces the amount of colonies that have to be screened to less than 100. Third,

multiple integration of the BAC into the genome can be of interest because this leads to higher expression levels of the construct. Multiple integrations should be detectable in a Southern blot screen indicated by a stronger signal for the targeted band than the wt band. Therefore BAC strategy provides a very efficient and reliable way to generate knock-in mouse model, especially Cre mice. The modified BAC could be directly injected into stem cells and transfer to mouse, which save a lot of time from cell culture work and also decrease the possibility of harmful stem cells.

One has to thoroughly balance the advantages and disadvantages of the two approaches. Once the BAC Red/ET approach is set-up in the laboratory, it can be a fast and efficient approach alternative to the conventional targeting.

## 5 Summary

IgG1 ( $\gamma$ 1), known as surface marker of memory B cells, is characterized with a conserved cytoplasmic tail that is lacking in IgM ( $\mu$ ) and IgD ( $\delta$ ) chains (Geisberger et al., 2003; Neuberger et al., 1989; Reth, 1994). To investigate the physiological role of this cytoplasmic tail, a novel mouse strain (IgG1i) was established in which C $\gamma$ 1 takes place all the other C<sub>H</sub> gene segments. IgG1i mice exclusively express membrane-bound IgG1 in the B lineage. On the other hand, it is known that signal transduction through  $\mu$  and  $\delta$  chains relies entirely on the cytoplasmic tails of the BCR-associated Ig $\alpha$ / $\beta$  heterodimer. To assess whether signal-transduction through  $\gamma$ 1 is also Ig $\alpha$ / $\beta$ -dependent, we generated the Ig $\alpha_{\Delta c}$ IgG1i mice which carry the IgG1 BCR in combination with Ig $\alpha$  truncation and the Ig $\beta_{\Delta c}$ IgG1i mice which carry the IgG1 BCR in combination with Ig $\beta$  truncation. We found that signal of  $\gamma$ 1 affects peripheral B cell compartment distinctly when combining Ig $\beta$  truncation or Ig $\alpha$  truncation. B cells number in Ig $\alpha_{\Delta c}$ IgG1i mice is over ten times as the number in Ig $\alpha_{\Delta c}$  mice. In contrast, Ig $\beta_{\Delta c}$ IgG1i mice did not increase the number of B cells in compared with Ig $\beta_{\Delta c}$  mice. Our data suggested that the increased number of peripheral B cells in the Ig $\alpha_{\Delta c}$ IgG1i mice compared to Ig $\beta_{\Delta c}$ IgG1i mice did not come from an advantage in the BM B cell development, but rather from a peripheral influence. Due to the insufficient receptor expression, Ig $\alpha$  or Ig $\beta$  mutant B cells were unable to respond to the survival signal of BAFF and exhibit down-regulated expression of basal Bcl-X<sub>L</sub> accordingly. This down-regulation of Bcl-X<sub>L</sub> is correlated with the faster faded away phosphorylation of PLC $\gamma$ 2 and reduced level of IKB $\alpha$  phosphorylation. These findings suggested that the B cell survival signal through  $\gamma$ 1 depends on both Ig $\alpha$  and Ig $\beta$  but mainly on Ig $\beta$  which is required for NF- $\kappa$ B-directed Bcl-X<sub>L</sub> expression.

### **B cell-specific Smad7-deficient mouse**

Previous *in vitro* studies showed Smad7 is induced by the TGF- $\beta$  superfamily members and negatively modulates TGF- $\beta$  signaling. To clarify the biological role of Smad7 in B-lymphocytes, we have generated a B cell-specific Smad7-deficient mouse line (CD19Cre/Smad7flox). Our data indicated that Smad7 plays an important role in TGF- $\beta$ -dependent regulation of IgA switching. Also it regulates the maintenance of B-2 B cells in the peritoneal cavity. In summary, our findings suggest that Smad7 is a crucial downstream inhibitor in TGF- $\beta$  receptor signaling in B cells.



## 6 Zusammenfassung

Der Zelloberflächenmarker IgG1 auf Memory B Zellen ist durch eine konservierte zytoplasmatischen Domäne, die bei den IgM und IgD Ketten fehlt, charakterisiert. Um die Rolle dieser zytoplasmatischen Domäne zu untersuchen, wurde die IgG1i Maus generiert, welche die C $\gamma$ 1 Kette anstatt der restlichen Ch Segmente trägt/exprimiert. Diese Mäuse exprimieren ausschließlich IgG1 in B Zellen. Die Signaltransduktion der B Zell Rezeptoren (BCR) erfolgt über die  $\mu$  bzw.  $\gamma$  Kette in Kombination mit den Heterodimeren Ig $\alpha/\beta$ . Um herauszufinden ob die Signaltransduktion über  $\gamma$ 1 zusätzlich abhängig von Ig $\alpha/\beta$  ist, wurden Ig $\alpha_{\Delta c}$ IgG1i Mäuse generiert, die den IgG1 BCR in Kombination mit Ig $\alpha$  Mutation tragen und Ig $\beta_{\Delta c}$ IgG1i Mäuse, welche den IgG1 BCR in Kombination mit einer Ig $\beta$  Mutation tragen. Mit Hilfe dieser Mausmodelle konnten wir zeigen, dass  $\gamma$ 1 ausschließlich in Kombination mit Ig $\alpha$  oder Ig $\beta$  Einfluss auf das periphere B Zell Kompartiment hat. Die Anzahl der B Zellen in Ig $\alpha_{\Delta c}$ IgG1i Mäusen ist 10 fach erhöht verglichen mit der Anzahl von B Zellen in Ig $\alpha_{\Delta c}$  Mäusen. In Ig $\beta_{\Delta c}$ IgG1i ist die B Zell Zahl im Vergleich mit Ig $\beta_{\Delta c}$  Mäusen unverändert. Diese Daten deuten darauf hin, dass die divergenten Effekte der  $\gamma$ 1 Signal Transduktion im peripheren B Zell Kompartiment der Ig $\alpha_{\Delta c}$ IgG1i und der Ig $\beta_{\Delta c}$ IgG1i Mäuse vom Überleben oder von der Proliferation der B Zellen in der Peripherie abhängig ist. Auf Grund der insuffizienten Expression der Rezeptoren, reagieren Ig $\alpha$  oder Ig $\beta$  mutierte B Zellen nicht auf den Überlebensfaktor BAFF und regulieren die basale Expression von Bcl-X<sub>L</sub> herunter. Die verminderte Expression von Bcl-X<sub>L</sub> korreliert mit der beschleunigten PLC $\gamma$ 2 Phosphorylierung und einer verminderten Phosphorylierung von I $\kappa$ B $\alpha$ . Diese Ergebnisse lassen eine Abhängigkeit des  $\gamma$ 1- B Zell Überlebenssignal von Ig $\alpha$  und Ig $\beta$  vermuten, wobei Ig $\beta$  eine wichtigere Rolle auf Grund des Einflusses auf die NF- $\kappa$ B abhängigen Expression von Bcl-X<sub>L</sub> zuteil wird.

Vorangegangene *in vitro* Versuche haben gezeigt, dass Smad7 von Mitgliedern der TGF- $\beta$  Superfamilie induziert wird und die Signaltransduktion von TGF- $\beta$  negativ reguliert. Um die biologische Funktion von Smad7 in B Lymphozyten zu untersuchen, wurde eine Mauslinie etabliert, (CD19Cre/Smad7flox) in der Smad7 ausschließlich in B Zellen deletiert ist. Unsere Ergebnisse zeigen, dass Smad7 eine wichtige Rolle in der TGF- $\beta$  abhängigen Regulation von IgA hat. Des Weiteren reguliert Smad7 Homöostase des B-2 B Zell Pools im Peritoneum. Zusammenfassend lässt sich aus den in dieser Arbeit präsentierten Daten schließen, dass Smad7 ein wichtiger Inhibitor in B Zellen ist, der unterhalb des TGF- $\beta$  Rezeptors fungiert.

## 7 References

- Achatz, G., Nitschke, L., and Lamers, M.C. (1997). Effect of transmembrane and cytoplasmic domains of IgE on the IgE response. *Science* *276*, 409-411.
- Alberola-Ila, J., Takaki, S., Kerner, J.D., and Perlmutter, R.M. (1997). Differential signaling by lymphocyte antigen receptors. *Annual review of immunology* *15*, 125-154.
- Amarante-Mendes, G.P., McGahon, A.J., Nishioka, W.K., Afar, D.E., Witte, O.N., and Green, D.R. (1998). Bcl-2-independent Bcr-Abl-mediated resistance to apoptosis: protection is correlated with up regulation of Bcl-xL. *Oncogene* *16*, 1383-1390.
- Antony, P., Petro, J.B., Carlesso, G., Shinnars, N.P., Lowe, J., and Khan, W.N. (2003). B cell receptor directs the activation of NFAT and NF-kappaB via distinct molecular mechanisms. *Experimental cell research* *291*, 11-24.
- Arsura, M., Wu, M., and Sonenshein, G.E. (1996). TGF beta 1 inhibits NF-kappa B/Rel activity inducing apoptosis of B cells: transcriptional activation of I kappa B alpha. *Immunity* *5*, 31-40.
- Benschop, R.J., Melamed, D., Nemazee, D., and Cambier, J.C. (1999). Distinct signal thresholds for the unique antigen receptor-linked gene expression programs in mature and immature B cells. *The Journal of experimental medicine* *190*, 749-756.
- Brandtzaeg, P., and Johansen, F.E. (2005). Mucosal B cells: phenotypic characteristics, transcriptional regulation, and homing properties. *Immunological reviews* *206*, 32-63.
- Brown, B.K., and Song, W. (2001). The actin cytoskeleton is required for the trafficking of the B cell antigen receptor to the late endosomes. *Traffic (Copenhagen, Denmark)* *2*, 414-427.
- Cazac, B.B., and Roes, J. (2000). TGF-beta receptor controls B cell responsiveness and induction of IgA in vivo. *Immunity* *13*, 443-451.
- Chu, Y.P., Spatz, L., and Diamond, B. (2004). A second heavy chain permits survival of high affinity autoreactive B cells. *Autoimmunity* *37*, 27-32.
- Cooper, M.D., Mulvaney, D., Coutinho, A., and Cazenave, P.A. (1986). A novel cell surface molecule on early B-lineage cells. *Nature* *321*, 616-618.
- Cumano, A., and Rajewsky, K. (1986). Clonal recruitment and somatic mutation in the generation of immunological memory to the hapten NP. *Embo J* *5*, 2459-2468.
- Dal Porto, J.M., Gauld, S.B., Merrell, K.T., Mills, D., Pugh-Bernard, A.E., and Cambier, J. (2004). B cell antigen receptor signaling 101. *Molecular immunology* *41*, 599-613.
- Dialynas, D.P., Quan, Z.S., Wall, K.A., Pierres, A., Quintans, J., Loken, M.R., Pierres, M., and Fitch, F.W. (1983). Characterization of the murine T cell surface molecule, designated L3T4, identified by monoclonal antibody GK1.5: similarity of L3T4 to the human Leu-3/T4 molecule. *J Immunol* *131*, 2445-2451.

- Edry, E., and Melamed, D. (2004). Receptor editing in positive and negative selection of B lymphopoiesis. *J Immunol* *173*, 4265-4271.
- Espeli, M., Rossi, B., Mancini, S.J., Roche, P., Gauthier, L., and Schiff, C. (2006). Initiation of pre-B cell receptor signaling: common and distinctive features in human and mouse. *Seminars in immunology* *18*, 56-66.
- Fagarasan, S., Shinkura, R., Kamata, T., Nogaki, F., Ikuta, K., Tashiro, K., and Honjo, T. (2000). A lymphoplasia (aly)-type nuclear factor kappaB-inducing kinase (NIK) causes defects in secondary lymphoid tissue chemokine receptor signaling and homing of peritoneal cells to the gut-associated lymphatic tissue system. *The Journal of experimental medicine* *191*, 1477-1486.
- Gallatin, W.M., Weissman, I.L., and Butcher, E.C. (2006). A cell-surface molecule involved in organ-specific homing of lymphocytes. 1983. *J Immunol* *177*, 5-9.
- Garceau, N., Kosaka, Y., Masters, S., Hambor, J., Shinkura, R., Honjo, T., and Noelle, R.J. (2000). Lineage-restricted function of nuclear factor kappaB-inducing kinase (NIK) in transducing signals via CD40. *The Journal of experimental medicine* *191*, 381-386.
- Gauld, S.B., and Cambier, J.C. (2004). Src-family kinases in B-cell development and signaling. *Oncogene* *23*, 8001-8006.
- Gazumyan, A., Reichlin, A., and Nussenzweig, M.C. (2006). Ig beta tyrosine residues contribute to the control of B cell receptor signaling by regulating receptor internalization. *The Journal of experimental medicine* *203*, 1785-1794.
- Geisberger, R., Cramer, R., and Achatz, G. (2003). Models of signal transduction through the B-cell antigen receptor. *Immunology* *110*, 401-410.
- Grawunder, U., Leu, T.M., Schatz, D.G., Werner, A., Rolink, A.G., Melchers, F., and Winkler, T.H. (1995). Down-regulation of RAG1 and RAG2 gene expression in preB cells after functional immunoglobulin heavy chain rearrangement. *Immunity* *3*, 601-608.
- Gulley, M.L., Ogata, L.C., Thorson, J.A., Dailey, M.O., and Kemp, J.D. (1988). Identification of a murine pan-T cell antigen which is also expressed during the terminal phases of B cell differentiation. *J Immunol* *140*, 3751-3757.
- Hardy, R.R. (1992). Variable gene usage, physiology and development of Ly-1+ (CD5+) B cells. *Current opinion in immunology* *4*, 181-185.
- Hardy, R.R., and Hayakawa, K. (1986). Development and physiology of Ly-1 B and its human homolog, Leu-1 B. *Immunological reviews* *93*, 53-79.
- Hardy, R.R., and Hayakawa, K. (2001). B cell development pathways. *Annual review of immunology* *19*, 595-621.
- Hayakawa, K., Shinton, S.A., Asano, M., and Hardy, R.R. (2000). B-1 cell definition. *Current topics in microbiology and immunology* *252*, 15-22.

- Herzenberg, L.A., Black, S.J., and Herzenberg, L.A. (1980). Regulatory circuits and antibody responses. *Eur J Immunol* *10*, 1-11.
- Herzenberg, L.A., Stall, A.M., Lalor, P.A., Sidman, C., Moore, W.A., Parks, D.R., and Herzenberg, L.A. (1986). The Ly-1 B cell lineage. *Immunological reviews* *93*, 81-102.
- Inaba, K., Witmer-Pack, M., Inaba, M., Hathcock, K.S., Sakuta, H., Azuma, M., Yagita, H., Okumura, K., Linsley, P.S., Ikehara, S., *et al.* (1994). The tissue distribution of the B7-2 costimulator in mice: abundant expression on dendritic cells in situ and during maturation in vitro. *J Exp Med* *180*, 1849-1860.
- Inoue, H., Nojima, H., and Okayama, H. (1990). High efficiency transformation of *Escherichia coli* with plasmids. *Gene* *96*, 23-28.
- Inui, S., Maeda, K., Hua, D.R., Yamashita, T., Yamamoto, H., Miyamoto, E., Aizawa, S., and Sakaguchi, N. (2002). BCR signal through alpha 4 is involved in S6 kinase activation and required for B cell maturation including isotype switching and V region somatic hypermutation. *Int Immunol* *14*, 177-187.
- Ishimaru, N., Kishimoto, H., Hayashi, Y., and Sprent, J. (2006). Regulation of naive T cell function by the NF-kappaB2 pathway. *Nature immunology* *7*, 763-772.
- Jung, D., Giallourakis, C., Mostoslavsky, R., and Alt, F.W. (2006). Mechanism and control of V(D)J recombination at the immunoglobulin heavy chain locus. *Annual review of immunology* *24*, 541-570.
- Kaisho, T., Schwenk, F., and Rajewsky, K. (1997). The roles of gamma 1 heavy chain membrane expression and cytoplasmic tail in IgG1 responses. *Science* *276*, 412-415.
- Kee, B.L., Rivera, R.R., and Murre, C. (2001). Id3 inhibits B lymphocyte progenitor growth and survival in response to TGF-beta. *Nature immunology* *2*, 242-247.
- Kim, P.H., and Kagnoff, M.F. (1990). Transforming growth factor beta 1 increases IgA isotype switching at the clonal level. *J Immunol* *145*, 3773-3778.
- Kinoshita, T., Takeda, J., Hong, K., Kozono, H., Sakai, H., and Inoue, K. (1988). Monoclonal antibodies to mouse complement receptor type 1 (CR1). Their use in a distribution study showing that mouse erythrocytes and platelets are CR1-negative. *J Immunol* *140*, 3066-3072.
- Klein, J., Ju, W., Heyer, J., Wittek, B., Haneke, T., Knaus, P., Kucherlapati, R., Bottlinger, E.P., Nitschke, L., and Kneitz, B. (2006). B cell-specific deficiency for Smad2 in vivo leads to defects in TGF-beta-directed IgA switching and changes in B cell fate. *J Immunol* *176*, 2389-2396.
- Kraus, M., Saijo, K., Torres, R.M., and Rajewsky, K. (1999). Ig-alpha cytoplasmic truncation renders immature B cells more sensitive to antigen contact. *Immunity* *11*, 537-545.
- Kurosaki, T., Maeda, A., Ishiai, M., Hashimoto, A., Inabe, K., and Takata, M. (2000). Regulation of the phospholipase C-gamma2 pathway in B cells. *Immunological reviews* *176*, 19-29.

- Lang, J., Jackson, M., Teyton, L., Brunmark, A., Kane, K., and Nemazee, D. (1996). B cells are exquisitely sensitive to central tolerance and receptor editing induced by ultralow affinity, membrane-bound antigen. *The Journal of experimental medicine* *184*, 1685-1697.
- Ledbetter, J.A., and Herzenberg, L.A. (1979). Xenogeneic monoclonal antibodies to mouse lymphoid differentiation antigens. *Immunol Rev* *47*, 63-90.
- Leo, O., Foo, M., Sachs, D.H., Samelson, L.E., and Bluestone, J.A. (1987). Identification of a monoclonal antibody specific for a murine T3 polypeptide. *Proc Natl Acad Sci U S A* *84*, 1374-1378.
- Li, M.O., Wan, Y.Y., Sanjabi, S., Robertson, A.K., and Flavell, R.A. (2006a). Transforming growth factor-beta regulation of immune responses. *Annu Rev Immunol* *24*, 99-146.
- Li, R., Rosendahl, A., Brodin, G., Cheng, A.M., Ahgren, A., Sundquist, C., Kulkarni, S., Pawson, T., Heldin, C.H., and Heuchel, R.L. (2006b). Deletion of exon I of SMAD7 in mice results in altered B cell responses. *J Immunol* *176*, 6777-6784.
- Lomo, J., Blomhoff, H.K., Beiske, K., Stokke, T., and Smeland, E.B. (1995). TGF-beta 1 and cyclic AMP promote apoptosis in resting human B lymphocytes. *J Immunol* *154*, 1634-1643.
- Lutz, C., Ledermann, B., Kosco-Vilbois, M.H., Ochsenbein, A.F., Zinkernagel, R.M., Kohler, G., and Brombacher, F. (1998). IgD can largely substitute for loss of IgM function in B cells. *Nature* *393*, 797-801.
- Lyons, A.B., and Parish, C.R. (1994). Determination of lymphocyte division by flow cytometry. *J Immunol Methods* *171*, 131-137.
- Malek, T.R., Robb, R.J., and Shevach, E.M. (1983). Identification and initial characterization of a rat monoclonal antibody reactive with the murine interleukin 2 receptor-ligand complex. *Proc Natl Acad Sci U S A* *80*, 5694-5698.
- Martensson, I.L., Rolink, A., Melchers, F., Mundt, C., Licence, S., and Shimizu, T. (2002). The pre-B cell receptor and its role in proliferation and Ig heavy chain allelic exclusion. *Seminars in immunology* *14*, 335-342.
- Martin, S.W., and Goodnow, C.C. (2002). Burst-enhancing role of the IgG membrane tail as a molecular determinant of memory. *Nature immunology* *3*, 182-188.
- Massoumi, R., Chmielarska, K., Hennecke, K., Pfeifer, A., and Fassler, R. (2006). Cyld inhibits tumor cell proliferation by blocking Bcl-3-dependent NF-kappaB signaling. *Cell* *125*, 665-677.
- McIntyre, T.M., Klinman, D.R., Rothman, P., Lugo, M., Dasch, J.R., Mond, J.J., and Snapper, C.M. (1993). Transforming growth factor beta 1 selectivity stimulates immunoglobulin G2b secretion by lipopolysaccharide-activated murine B cells. *The Journal of experimental medicine* *177*, 1031-1037.
- Mecklenbrauker, I., Kalled, S.L., Leitges, M., Mackay, F., and Tarakhovsky, A. (2004). Regulation of B-cell survival by BAFF-dependent PKCdelta-mediated nuclear signalling. *Nature* *431*, 456-461.

- Melchers, F. (2005). The pre-B-cell receptor: selector of fitting immunoglobulin heavy chains for the B-cell repertoire. *Nature reviews* 5, 578-584.
- Miltenyi, S., Muller, W., Weichel, W., and Radbruch, A. (1990). High gradient magnetic cell separation with MACS. *Cytometry* 11, 231-238.
- Miyawaki, S., Nakamura, Y., Suzuka, H., Koba, M., Yasumizu, R., Ikehara, S., and Shibata, Y. (1994). A new mutation, *aly*, that induces a generalized lack of lymph nodes accompanied by immunodeficiency in mice. *European journal of immunology* 24, 429-434.
- Neuberger, M.S., Caskey, H.M., Pettersson, S., Williams, G.T., and Surani, M.A. (1989). Isotype exclusion and transgene down-regulation in immunoglobulin-lambda transgenic mice. *Nature* 338, 350-352.
- Ollila, J., and Vihinen, M. (2005). B cells. *The international journal of biochemistry & cell biology* 37, 518-523.
- Opitz, H.G., Opitz, U., Hewlett, G., and Schlumberger, H.D. (1982). A new model for investigations of T-cell functions in mice: differential immunosuppressive effects of two monoclonal anti-Thy-1.2 antibodies. *Immunobiology* 160, 438-453.
- Park, S.H. (2005). Fine tuning and cross-talking of TGF-beta signal by inhibitory Smads. *Journal of biochemistry and molecular biology* 38, 9-16.
- Patil, S., Wildey, G.M., Brown, T.L., Choy, L., Derynck, R., and Howe, P.H. (2000). Smad7 is induced by CD40 and protects WEHI 231 B-lymphocytes from transforming growth factor-beta -induced growth inhibition and apoptosis. *The Journal of biological chemistry* 275, 38363-38370.
- Patke, A., Mecklenbrauker, I., and Tarakhovsky, A. (2004). Survival signaling in resting B cells. *Current opinion in immunology* 16, 251-255.
- Patterson, R.L., van Rossum, D.B., Nikolaidis, N., Gill, D.L., and Snyder, S.H. (2005). Phospholipase C-gamma: diverse roles in receptor-mediated calcium signaling. *Trends in biochemical sciences* 30, 688-697.
- Peitz, M., Pfannkuche, K., Rajewsky, K., and Edenhofer, F. (2002). Ability of the hydrophobic FGF and basic TAT peptides to promote cellular uptake of recombinant Cre recombinase: a tool for efficient genetic engineering of mammalian genomes. *Proc Natl Acad Sci U S A* 99, 4489-4494.
- Pure, E., and Tardelli, L. (1992). Tyrosine phosphorylation is required for ligand-induced internalization of the antigen receptor on B lymphocytes. *Proceedings of the National Academy of Sciences of the United States of America* 89, 114-117.
- Rao, M., Lee, W.T., and Conrad, D.H. (1987). Characterization of a monoclonal antibody directed against the murine B lymphocyte receptor for IgE. *J Immunol* 138, 1845-1851.
- Reichlin, A., Hu, Y., Meffre, E., Nagaoka, H., Gong, S., Kraus, M., Rajewsky, K., and Nussenzweig, M.C. (2001). B cell development is arrested at the immature B cell stage in

mice carrying a mutation in the cytoplasmic domain of immunoglobulin beta. *The Journal of experimental medicine* 193, 13-23.

Reth, M. (1994). B cell antigen receptors. *Current opinion in immunology* 6, 3-8.

Rickert, R.C., Roes, J., and Rajewsky, K. (1997). B lymphocyte-specific, Cre-mediated mutagenesis in mice. *Nucleic Acids Res* 25, 1317-1318.

Rodriguez, C.I., Buchholz, F., Galloway, J., Sequerra, R., Kasper, J., Ayala, R., Stewart, A.F., and Dymecki, S.M. (2000). High-efficiency deleter mice show that FLPe is an alternative to Cre-loxP. *Nat Genet* 25, 139-140.

Roes, J., and Rajewsky, K. (1991). Cell autonomous expression of IgD is not essential for the maturation of conventional B cells. *International immunology* 3, 1367-1371.

Roes, J., and Rajewsky, K. (1993). Immunoglobulin D (IgD)-deficient mice reveal an auxiliary receptor function for IgD in antigen-mediated recruitment of B cells. *J Exp Med* 177, 45-55.

Rolink, A.G., Andersson, J., and Melchers, F. (1998). Characterization of immature B cells by a novel monoclonal antibody, by turnover and by mitogen reactivity. *European journal of immunology* 28, 3738-3748.

Rolink, A.G., Schaniel, C., Andersson, J., and Melchers, F. (2001). Selection events operating at various stages in B cell development. *Current opinion in immunology* 13, 202-207.

Rolink, A.G., Tschopp, J., Schneider, P., and Melchers, F. (2002). BAFF is a survival and maturation factor for mouse B cells. *European journal of immunology* 32, 2004-2010.

Roth, P.E., Kurtz, B., Lo, D., and Storb, U. (1995). lambda 5, but not mu, is required for B cell maturation in a unique gamma 2b transgenic mouse line. *The Journal of experimental medicine* 181, 1059-1070.

Salamero, J., Fougereau, M., and Seckinger, P. (1995). Internalization of B cell and pre-B cell receptors is regulated by tyrosine kinase and phosphatase activities. *European journal of immunology* 25, 2757-2764.

Sambrook, J. (1989). *Molecular cloning. A laboratory manual*, (2nd edition).

Sanger, F., Nicklen, S., and Coulson, A.R. (1977). DNA sequencing with chain-terminating inhibitors. *Proc Natl Acad Sci U S A* 74, 5463-5467.

Schneider, P., and Tschopp, J. (2003). BAFF and the regulation of B cell survival. *Immunol Lett* 88, 57-62.

Seemann, B., Templin, R., Pietruschka, U., John, R., Schmidt, U., and Erdmann, T. (1981). [The dielectric behavior of the isolated kidney during hypothermic preservation]. *Z Urol Nephrol* 74, 690-696.

Springer, T., Galfre, G., Secher, D.S., and Milstein, C. (1979). Mac-1: a macrophage differentiation antigen identified by monoclonal antibody. *Eur J Immunol* 9, 301-306.

Stoddart, A., Jackson, A.P., and Brodsky, F.M. (2005). Plasticity of B cell receptor internalization upon conditional depletion of clathrin. *Molecular biology of the cell* 16, 2339-2348.

Sun, K., Johansen, F.E., Eckmann, L., and Metzger, D.W. (2004). An important role for polymeric Ig receptor-mediated transport of IgA in protection against *Streptococcus pneumoniae* nasopharyngeal carriage. *J Immunol* 173, 4576-4581.

Suzuki, H., Matsuda, S., Terauchi, Y., Fujiwara, M., Ohteki, T., Asano, T., Behrens, T.W., Kouro, T., Takatsu, K., Kadowaki, T., *et al.* (2003). PI3K and Btk differentially regulate B cell antigen receptor-mediated signal transduction. *Nature immunology* 4, 280-286.

Symington, F.W., Subbarao, B., Mosier, D.E., and Sprent, J. (1982). Lyb-8.2: A new B cell antigen defined and characterized with a monoclonal antibody. *Immunogenetics* 16, 381-391.

Tarakhovsky, A. (1997). Bar Mitzvah for B-1 cells: how will they grow up? *The Journal of experimental medicine* 185, 981-984.

Tiegs, S.L., Russell, D.M., and Nemazee, D. (1993). Receptor editing in self-reactive bone marrow B cells. *The Journal of experimental medicine* 177, 1009-1020.

Torres, R.M., Flaswinkel, H., Reth, M., and Rajewsky, K. (1996). Aberrant B cell development and immune response in mice with a compromised BCR complex. *Science* 272, 1804-1808.

van Ginkel, F.W., Wahl, S.M., Kearney, J.F., Kweon, M.N., Fujihashi, K., Burrows, P.D., Kiyono, H., and McGhee, J.R. (1999). Partial IgA-deficiency with increased Th2-type cytokines in TGF-beta 1 knockout mice. *J Immunol* 163, 1951-1957.

Walmsley, M.J., Ooi, S.K., Reynolds, L.F., Smith, S.H., Ruf, S., Mathiot, A., Vanes, L., Williams, D.A., Cancro, M.P., and Tybulewicz, V.L. (2003). Critical roles for Rac1 and Rac2 GTPases in B cell development and signaling. *Science* 302, 459-462.

Wildey, G.M., Patil, S., and Howe, P.H. (2003). Smad3 potentiates transforming growth factor beta (TGFbeta)-induced apoptosis and expression of the BH3-only protein Bim in WEHI 231 B lymphocytes. *The Journal of biological chemistry* 278, 18069-18077.

Xu, Y., Harder, K.W., Huntington, N.D., Hibbs, M.L., and Tarlinton, D.M. (2005). Lyn tyrosine kinase: accentuating the positive and the negative. *Immunity* 22, 9-18.

Yin, L., Wu, L., Wesche, H., Arthur, C.D., White, J.M., Goeddel, D.V., and Schreiber, R.D. (2001). Defective lymphotoxin-beta receptor-induced NF-kappaB transcriptional activity in NIK-deficient mice. *Science* 291, 2162-2165.

Yokoyama, W.M., Koning, F., Kehn, P.J., Pereira, G.M., Stingl, G., Coligan, J.E., and Shevach, E.M. (1988). Characterization of a cell surface-expressed disulfide-linked dimer involved in murine T cell activation. *J Immunol* 141, 369-376.

Yoshimura, A., Mori, H., Ohishi, M., Aki, D., and Hanada, T. (2003). Negative regulation of cytokine signaling influences inflammation. *Current opinion in immunology* 15, 704-708.



Yu, H., Kessler, J., and Shen, J. (2000). Heterogeneous populations of ES cells in the generation of a floxed Presenilin-1 allele. *Genesis* 26, 5-8.

Zhang, M., Srivastava, G., and Lu, L. (2004). The pre-B cell receptor and its function during B cell development. *Cellular & molecular immunology* 1, 89-94.

Zhou, C., Yang, Y., and Jong, A.Y. (1990). Mini-prep in ten minutes. *Biotechniques* 8, 172-173.

## 8 Acknowledgements

My sincere thanks to Prof. Dr. Ari Waisman for his instruction during my Ph.D study.

I want to thank my wife, my son and my parents for their understanding and support.

I want to thank CMMC (Center of Molecular Medicine of Cologne) for giving me the chance to start my Ph.D study and funding me for the first three years. In particular, I would like to thank Prof. Dr. Mats Paulsson and Dr. Debora Grosskopf-Kroiher.

I thank Prof. Hinrich Abken, Prof. Sigrun Korsching and Prof. Monique Aumailley. They agreed to form my thesis committee.

I also appreciate my tutors, Prof. Jens Brüing and Prof. Martina Deckert, for their advices during my studying.

I want to thank my wife and my parents for their understanding and support.

I acknowledge all the former and present members of the Waisman lab for this friendly and scientific environment. In particular, I would like to thank Nadine, Friederike, Carsten, Thomas, Sabine, Max, Saskia, Lennart, Thorsten, Sonjia, Nir, Andy, Chalotte, Markus, Filiz, Jula, Stefan, Marina, Nicole and Susanne. Specially, I have to appreciate Andy, Nadine and Simone for their critical proofreading of the thesis.

Further I would like to thank Ingo for the Smad7 targeting germline.

## **9 VERSICHERUNG**

Ich versichere, daß ich die von mir vorgelegte Dissertation selbständig angefertigt, die benutzten Quellen und Hilfsmittel vollständig angegeben und die Stellen der Arbeit - einschließlich Tabellen, Karten und Abbildungen, die anderen Werken im Wortlaut oder dem Sinn nach entnommen sind, in jedem Einzelfall als Entlehnung kenntlich gemacht habe; daß diese Dissertation noch keiner anderen Fakultät oder Universität zur Prüfung vorgelegen hat; daß sie - abgesehen von unten angegebenen Teilpublikationen - noch nicht veröffentlicht worden ist sowie, daß ich eine solche Veröffentlichung vor Abschluß des Promotionsverfahrens nicht vornehmen werde. Die Bestimmungen dieser Promotionsordnung sind mir bekannt. Die von mir vorgelegte Dissertation ist von Prof. Dr. Ari Waisman betreut worden.

Köln, im Mai

2007 Jian Song

## 10 LEBENS LAUF

### Persönliche Daten

Name	Jian Song
Geburtsdatum	28.01.1976
Geburtsort	Heilongjiang
Adresse	Kaiserstr 36 55116 Mainz <a href="mailto:songj@uni-mainz.de">songj@uni-mainz.de</a>
Familienstand	Verheirated
Nationalität	China

### Schulische Ausbildung

1980- 1986	Wuyun Grundschule, Heilongjiang, China
1986- 1989	Wuyun Mitteschule, Heilongjiang, China
1989- 1992	Jiayin Gymnasium, Heilongjiang, China

### Studium

1992- 1997	Capital University of Medicine Jiamusi University
1998- 2001	Graduate school, Capital University of Medicine

### Abeit

1997- 1998	Praktikum
2001- 2003	Research assistant, Chinese Academy of Sciences

### Promotion

2003	Exploring the influence of B cell receptor signaling components on the development and homeostasis of B cells
------	---

**Publikationen**

Waisman, A., Kraus, M., Seagal, J., Ghosh, S., Melamed, D., Song, J., Sasaki, Y., Classen, S., Lutz, C., Brombacher, F., *et al.* (2007). IgG1 B cell receptor signaling is inhibited by CD22 and promotes the development of B cells whose survival is less dependent on Ig $\alpha$ / $\beta$ . *The Journal of experimental medicine* 204, 747-758.

Meng, S.D., Song, J., Rao, Z., Tien, P., and Gao, G.F. (2002). Three-step purification of gp96 from human liver tumor tissues suitable for isolation of gp96-bound peptides. *Journal of immunological methods* 264, 29-35.